Research on resonant states

郭建友
Jian-You Guo

安徽大学 物理与材料科学学院
School of Physical and Material Science, Anhui University

Outline

1. Significance of resonant states
2. Methods for resonant states
3. Complex scaling method and its application
4. Complex scaled Green's function method
5. Complex momentum representation
6. Summary and perspective

Physical importance of resonant states

As claimed by Taylor in his book on scattering theory, the resonances are the most striking phenomenon in the whole range of scattering experiments. The resonances appear widely in atomic, molecular, nuclear physics and in chemical reactions.

A particle is scattered from a target.

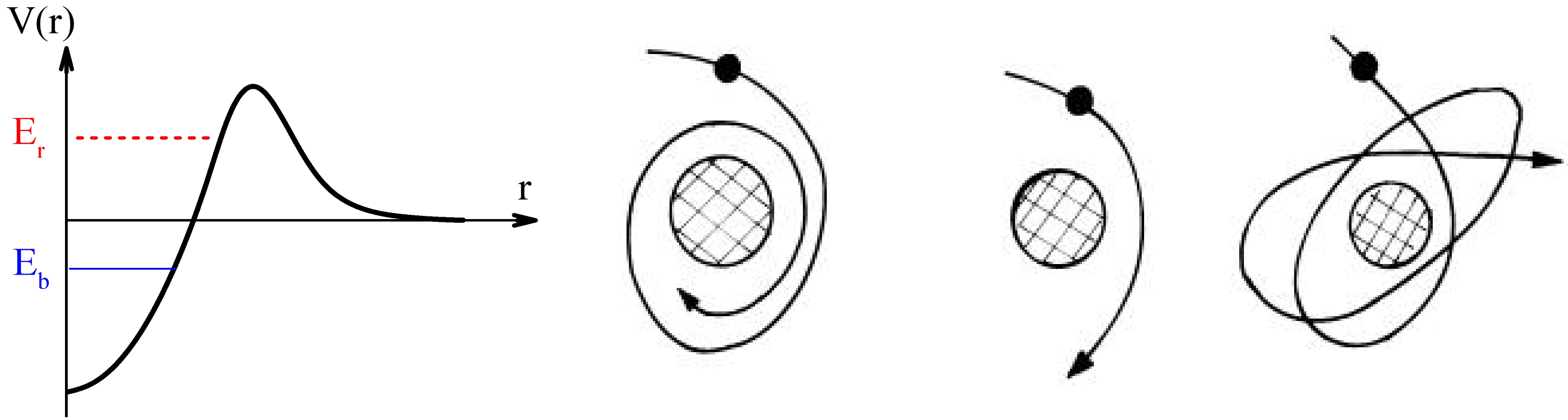

- The particle is trapped by the target
- A direct scattering event
- The particle is temporarily trapped by the target

Resonances play important roles in the formation of exotic nuclei

Explanation on neutron halo

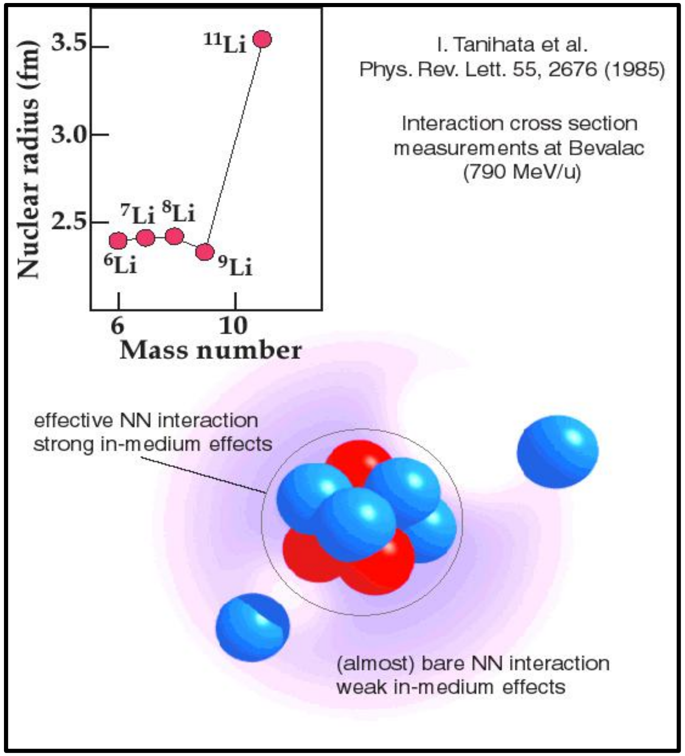

Measurements of Interaction Cross Sections and Nuclear Radii in the Light *p*-Shell Region,
I.Tanihata *etal.*, PRL55, 2676 (1985).

Relativistic Hartree-Bogoliubov Description of the Neutron Halo in ^{11}Li,
J.Meng and P.Ring, PRL77, 3963 (1996);

^{208}Pb

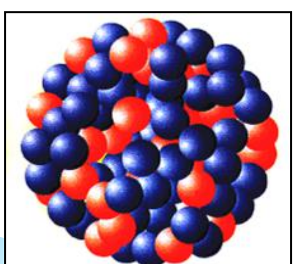

spatial distribution

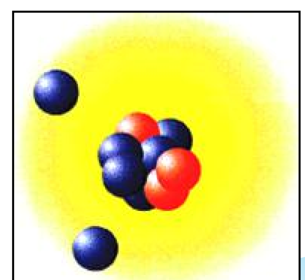

^{11}Li

Prediction on giant halo

Giant Halo at the Neutron Drip Line, J.Meng and P.Ring, PRL80, 460 (1998)

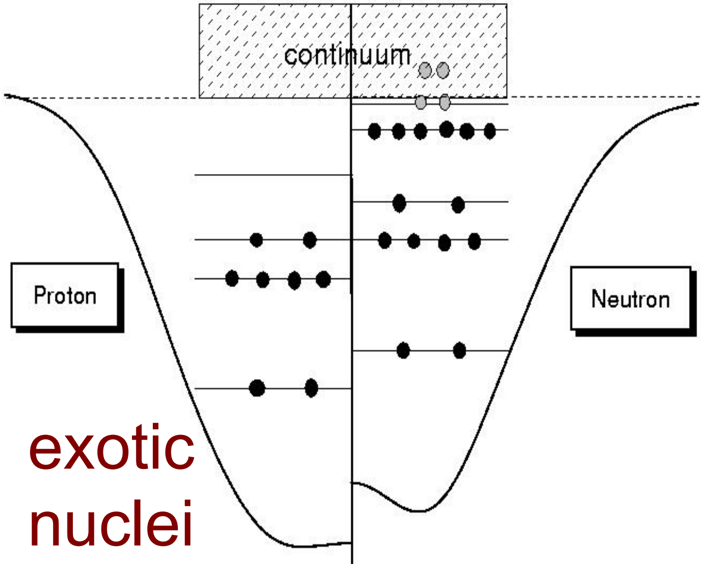

exotic nuclei

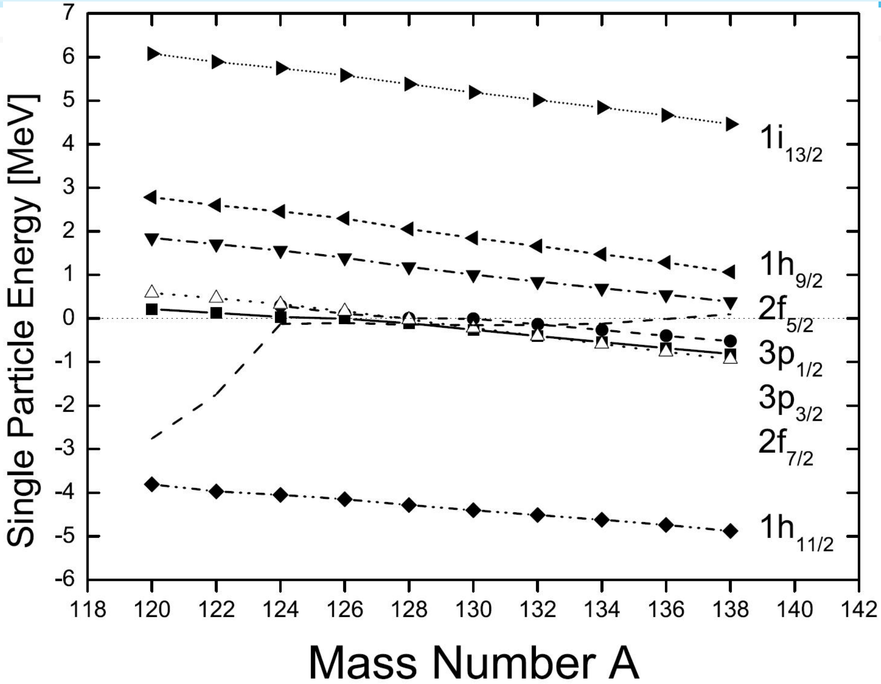

Pairing correlations and resonant states in the relativistic mean field theory, N.Sandulescu, L.S.Geng, etal, PRC2003

PHYSICAL REVIEW C **86**, 054318 (2012)

Pair correlation of giant halo nuclei in continuum Skyrme-Hartree-Fock-Bogoliubov theory

Y. Zhang (张颖),[1,2,*] M. Matsuo (松尾正之),[2,3] and J. Meng (孟杰)[1,4,5]

Understanding of deformation halo

PRL **103,** 262501 (2009) PHYSICAL REVIEW LETTERS week ending 31 DECEMBER 2009

Halo Structure of the Island of Inversion Nucleus ^{31}Ne

T. Nakamura,[1] N. Kobayashi,[1] Y. Kondo,[1] Y. Satou,[1] N. Aoi,[2] H. Baba,[2] S. Deguchi,[1] N. Fukuda,[2] J. Gibelin,[3] N. Inabe,[2] M. Ishihara,[2] D. Kameda,[2] Y. Kawada,[1] T. Kubo,[2] K. Kusaka,[2] A. Mengoni,[4] T. Motobayashi,[2] T. Ohnishi,[2] M. Ohtake,[2] N. A. Orr,[3] H. Otsu,[2] T. Otsuka,[5] A. Saito,[5] H. Sakurai,[2] S. Shimoura,[5] T. Sumikama,[6] H. Takeda,[2] E. Takeshita,[2]

PRL **112,** 142501 (2014) PHYSICAL REVIEW LETTERS week ending 11 APRIL 2014

Deformation-Driven *p*-Wave Halos at the Drip Line: ^{31}Ne

T. Nakamura,[1] N. Kobayashi,[1] Y. Kondo,[1] Y. Satou,[1,2] J. A. Tostevin,[3] Y. Utsuno,[4] N. Aoi,[5] H. Baba,[5]
A. Orr,[6]
hi,[5]

PHYSICAL REVIEW C **81**, 021304(R) (2010)

Interpretation of Coulomb breakup of ^{31}Ne in terms of deformation

Ikuko Hamamoto
Division of Mathematical Physics, Lund Institute of Technology at the University of Lund, Lund, Sweden and The Niels Bohr Institute, Blegdamsvej 17, Copenhagen Ø, DK-2100, Denmark
(Received 12 December 2009; published 23 February 2010)

The observed large Coulomb breakup cross section of ^{31}Ne is interpreted easily and simply in terms of *p*-wave neutron halo together with the deformed core ^{30}Ne.

Zhang, Smith, Kang, Zhao, Microscopic self-consistent study of neon halos with resonant contributions, PLB 730 (2014) 30–35

PRL **112,** 242501 (2014) PHYSICAL REVIEW LETTERS week ending 20 JUNE 2014

Observation of a *p*-Wave One-Neutron Halo Configuration in ^{37}Mg

N. Kobayashi,[1,*] T. Nakamura,[1] Y. Kondo,[1] J. A. Tostevin,[2,1] Y. Utsuno,[3] N. Aoi,[4,†] H. Baba,[4] R. Barthelemy,[5] M. A. Famiano,[5] N. Fukuda,[4] N. Inabe,[4] M. Ishihara,[4] R. Kanungo,[6] S. Kim,[7] T. Kubo,[4] G. S. Lee,[1] H. S. Lee,[7] M. Matsushita,[4,‡] T. Motobayashi,[4] T. Ohnishi,[4] N. A. Orr,[8] H. Otsu,[4] T. Otsuka,[9] T. Sako,[1] H. Sakurai,[4] Y. Satou,[7] T. Sumikama,[10,§] H. Takeda,[4] S. Takeuchi,[4] R. Tanaka,[1] Y. Togano,[4,¶] and K. Yoneda[4]

K. Fossez, J. Rotureau, N. Michel, Quan Liu, and W. Nazarewicz, , Single-particle and collective motion in unbound deformed 39Mg, PRC 94, 054302 (2016)

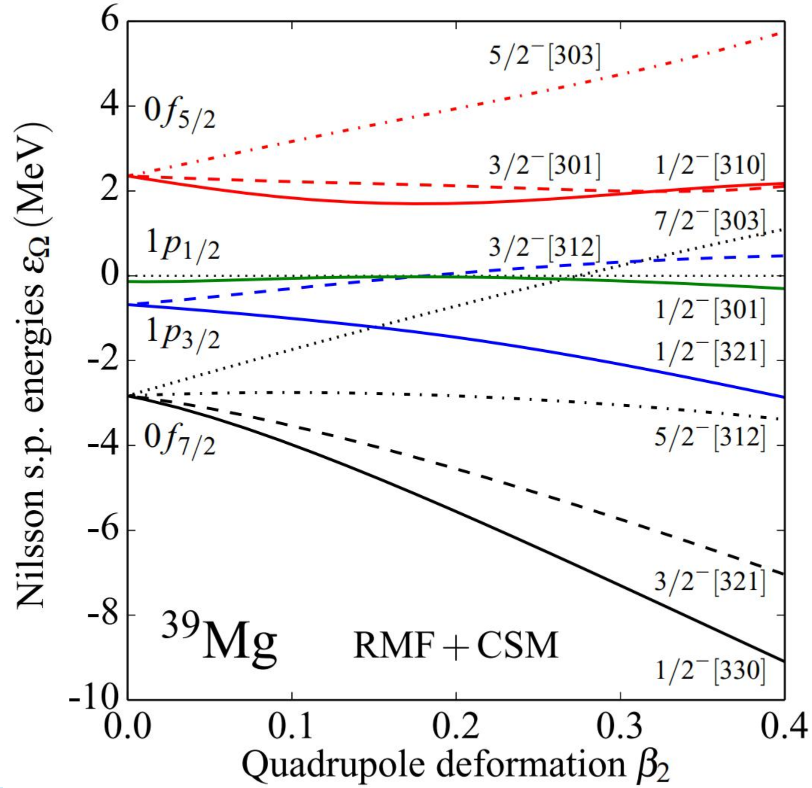

Single-particle neutron Nilsson diagram for 39Mg from the relativistic mean-field approach with the complex-scaling method. The crossing between the deformed levels 7/2⁻[303] and 1/2⁻[321] originating from the 0f7/2 and 1p3/2 shells, respectively, results in a deformed subshell closure at N = 28 and β2 ≈ 0.3.

deformed "Core"

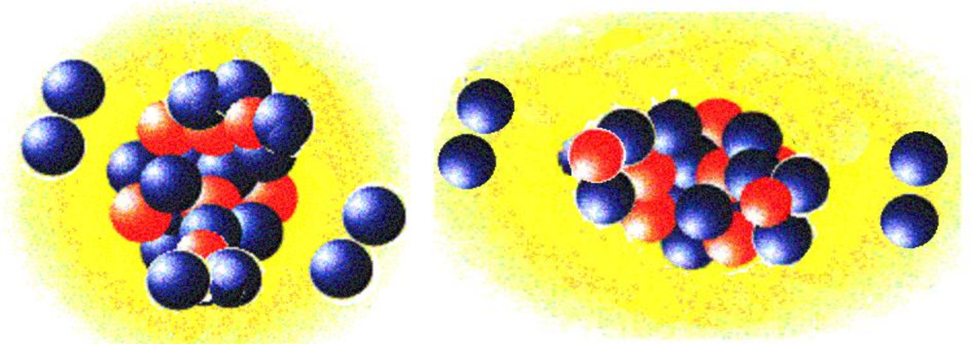

deformed "Core+Halo"

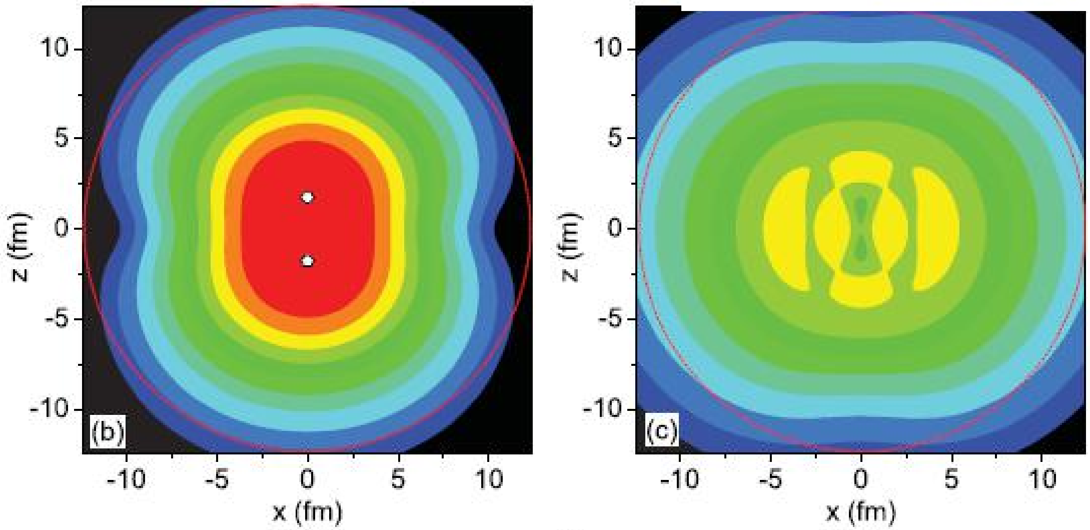

^{44}Mg

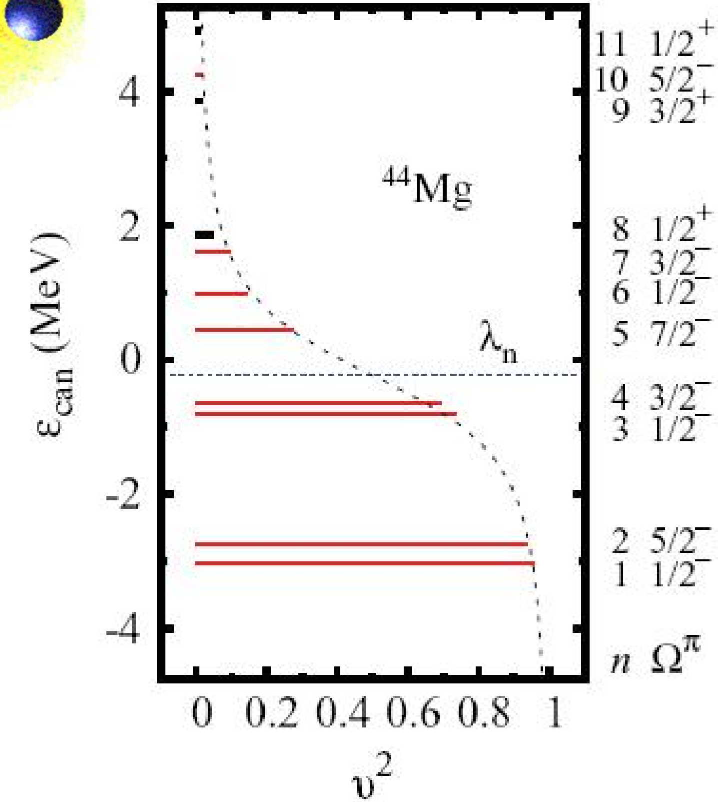

PHYSICAL REVIEW C **82**, 011301(R) (2010)

Neutron halo in deformed nuclei

Shan-Gui Zhou (周善贵),[1,2,3] Jie Meng (孟杰),[1,2,3,4,5,*] P. Ring,[2,4,6] and En-Guang Zhao (赵恩广)[1,2,3,4]

Explanation of the halo phenomena in medium-mass nuclei

PHYSICAL REVIEW C **79**, 054308 (2009)

New analysis method of the halo phenomenon in finite many-fermion systems: First applications to medium-mass atomic nuclei

V. Rotival[1,2,*] and T

[1]*DPTA/Service de Physique Nucléaire, CEA/DAM Île-d*

[2]*National Superconducting Cyclotron Laboratory, 1 Cyclo*

Performing spherical Hartree-Fock-Bogoliubov calculations with state-of-the-art Skyrme plus pairing functionals, a collective halo is predicted in drip-line Cr isotopes.

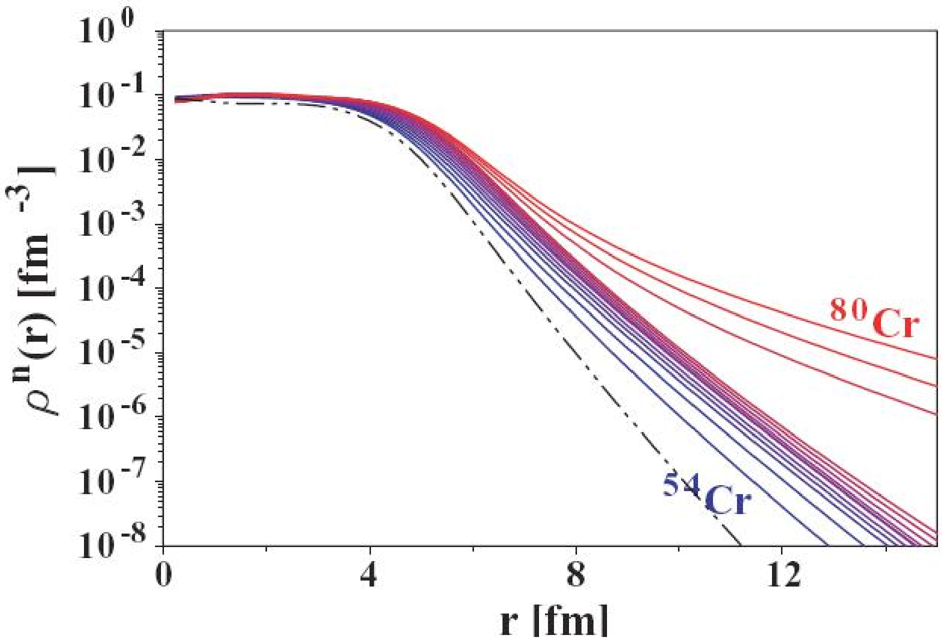

PHYSICAL REVIEW C **79**, 054309 (2009)

Halo phenomenon in finite many-fermion systems: Atom-positron complexes and large-scale study of atomic nuclei

V. Rotival,[1,2,*] K. Bennaceur,[3,4,†] and T. Duguet[2,4,5,‡]

Review

Progress in Particle and Nuclear Physics 68 (2013) 215–313

Recent experimental progress in nuclear halo structure studies

Isao Tanihata[a,b,*], Herve Savajols[c], Rituparna Kanungo[d]

[a] RCNP, Osaka University, 10-1 Mihogaoka, Ibaraki, Osaka 567-0047, Japan

[b] RCNST, Beihang University, Beijing, PR China

[c] GANIL, Boulevard Henri Becquerel, Boite Postale 55027, F-14076 Caen Cedex 05, France

[d] Astronomy and Physics Department, Saint Mary's University, 923 Robie Street, Halifax, NS B3H 3C3, Canada

IOP Publishing Journal of Physics G: Nuclear and Particle Physics

J. Phys. G: Nucl. Part. Phys. **42** (2015) 093101 (52pp) doi:10.1088/0954-3899/42/9/093101

Topical Review

Halos in medium-heavy and heavy nuclei with covariant density functional theory in continuum

J Meng[1,2,3,7] **and S G Zhou**[4,5,6]

Recent progress on halo

PHYSICAL REVIEW LETTERS **124**, 222504 (2020)

^{29}F as the heaviest two-neutron Borromean halo to date. The halo is attributed to neutrons occupying the $2p_{3/2}$ orbital.

Two-Neutron Halo is Unveiled in ^{29}F

S. Bagchi,[1,2,3] R. Kanungo,[1,4,*] Y. K. Tanaka,[1,2,3] H. Geissel,[2,3] P. Doornenbal,[5] W. Horiuchi,[6] G. Hagen,[7,8] T. Suzuki,[9]

PHYSICAL REVIEW C **101**, 031301(R) (2020)

Rapid Communications

Two-neutron halo structure of ^{31}F

N. Michel,[1,2,*] J. G. Li,[3] F. R. Xu,[3] and W. Zuo[1,2,†]
[1] *Institute of Modern Physics, Chinese Academy of Sciences, Lanzhou 730000, China*
[2] *School of Nuclear Science and Technology, University of Chinese Academy of Sciences, Beijing 100049, China*

PHYSICAL REVIEW C **104**, 014307 (2021)

Role of quadrupole deformation and continuum effects in the "island of inversion" nuclei ^{28,29,31}F

Yu-Xuan Luo (罗雨轩),[1] Kévin Fossez,[2,3] Quan Liu (刘泉),[1,*] and Jian-You Guo (郭建友)[1]
[1] *School of physics and materials science, Anhui University, Hefei 230601, People's Republic of China*
[2] *FRIB Laboratory, Michigan State University, East Lansing, Michigan 48824, USA*
[3] *Physics Division, Argonne National Laboratory, Lemont, Illinois 60439, USA*

11Be、19C等单中子晕，11Li、22C等Borromean晕，8B、17F等质子晕，8He等四中子晕

Rep.Prog.Phys.80(056001)2017

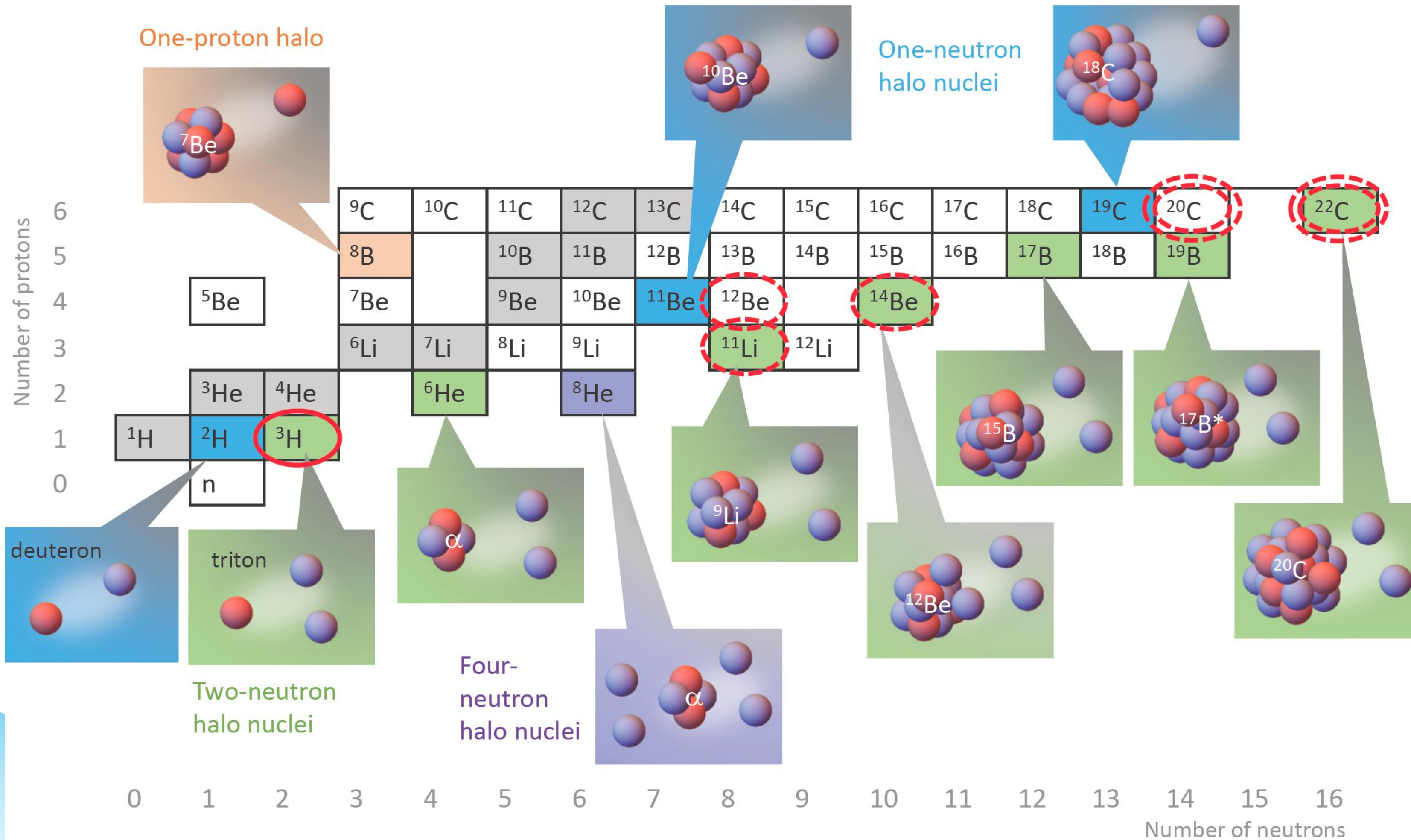

Nuclear chart showing the most neutron-rich isotopes from C to Cl

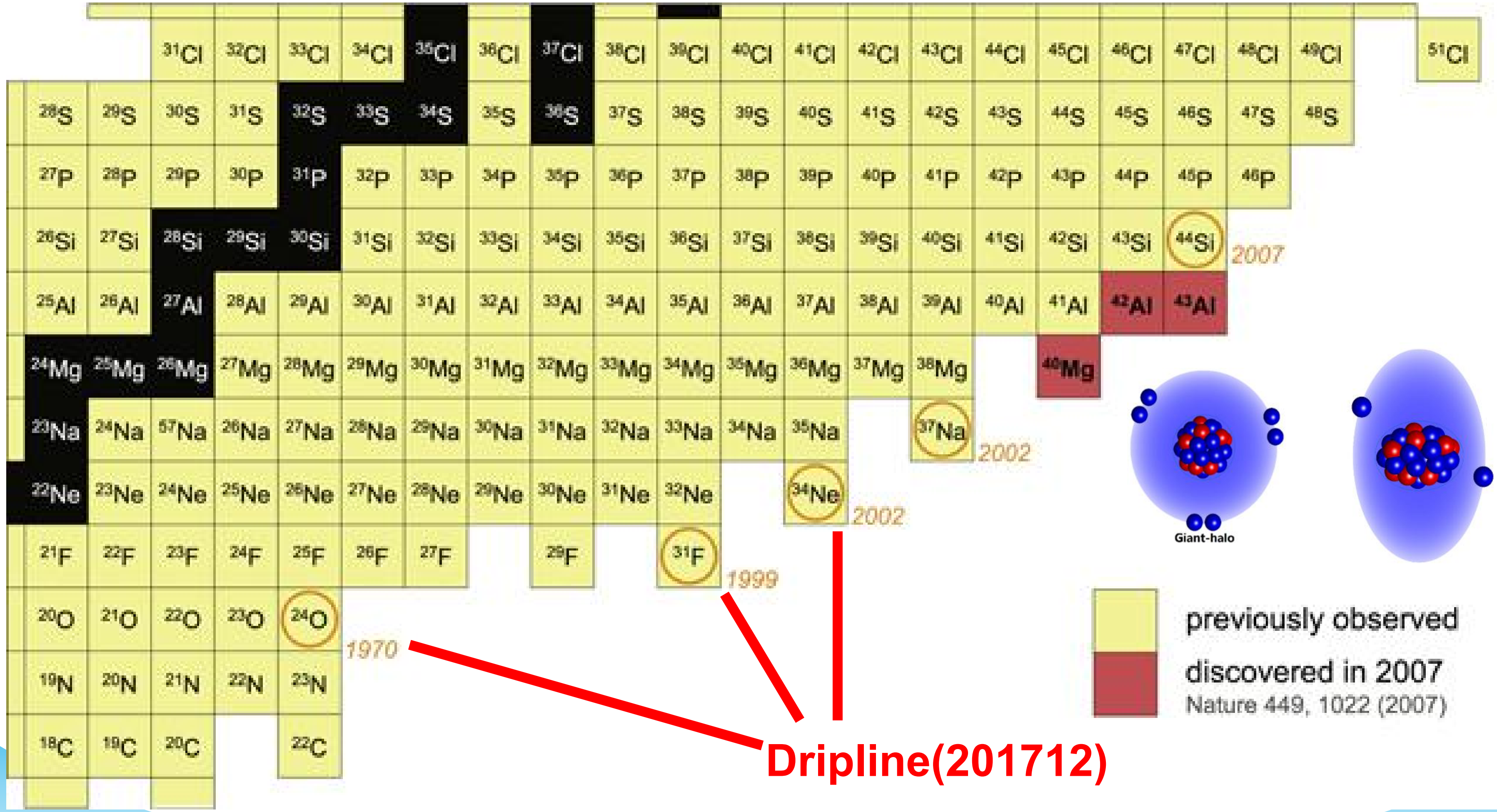

T Baumann et al 2007 Nature 449 1022

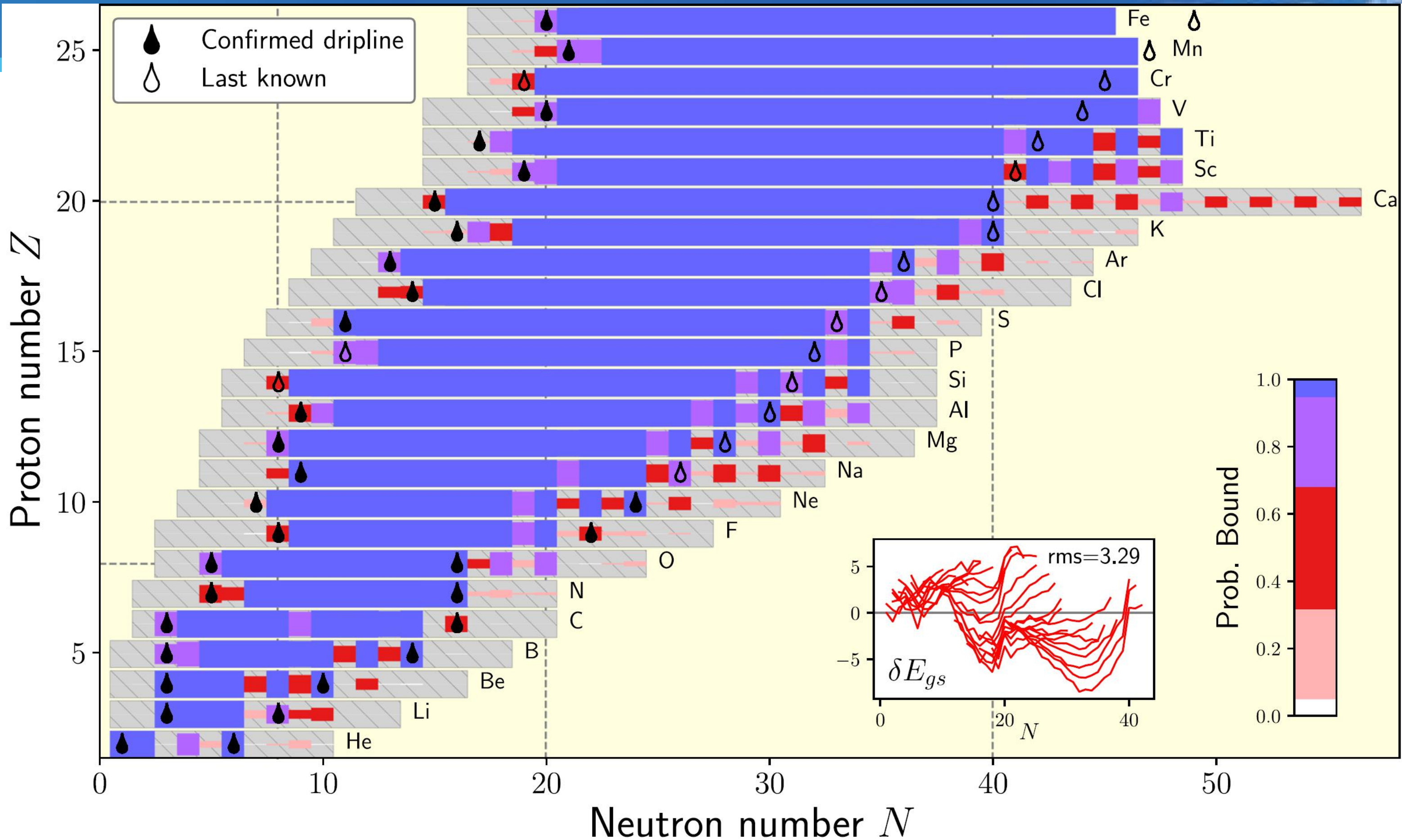

S. R. Stroberg etal., Ab Initio Limits of Atomic Nuclei, PRL 126, 022501 (2021)

Calculated probabilities for given isotopes to be bound with respect to one- or two-neutron (proton) removal. The gray region indicates nuclei that have been calculated, while the height of the boxes corresponds to the estimated probability that a given nucleus is bound with respect to one- or two-neutron (proton) removal in the neutron-rich (deficient) region of the chart. The inset shows the residuals with experimental ground-state energies.

Shell structure near dripline and new magic number

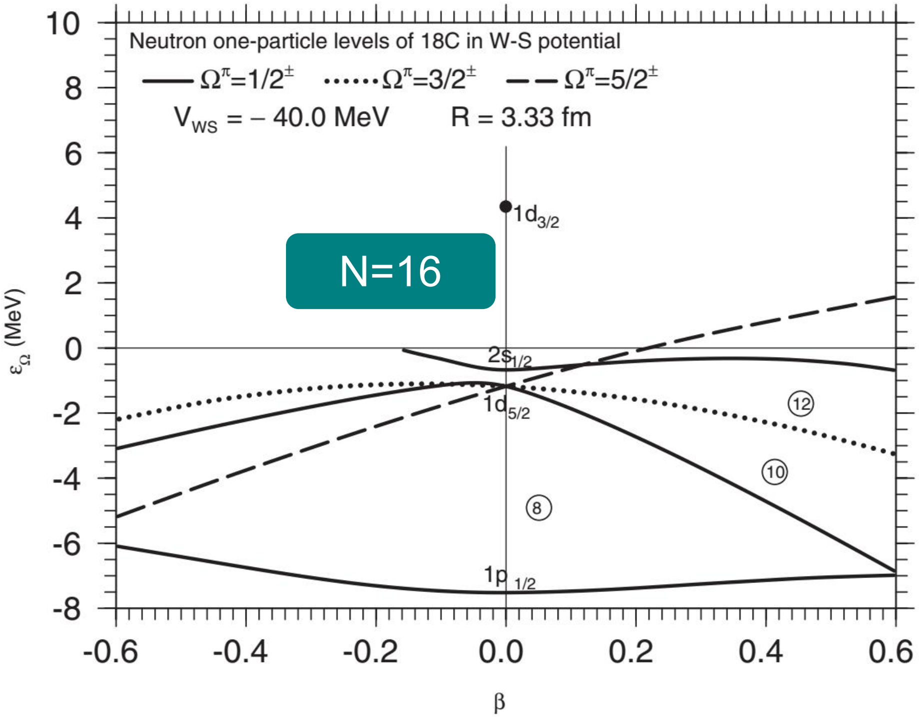

Neutron shell structure and deformation in neutron-drip-line nuclei

Hamamoto, PRC 85, 064329 (2012)

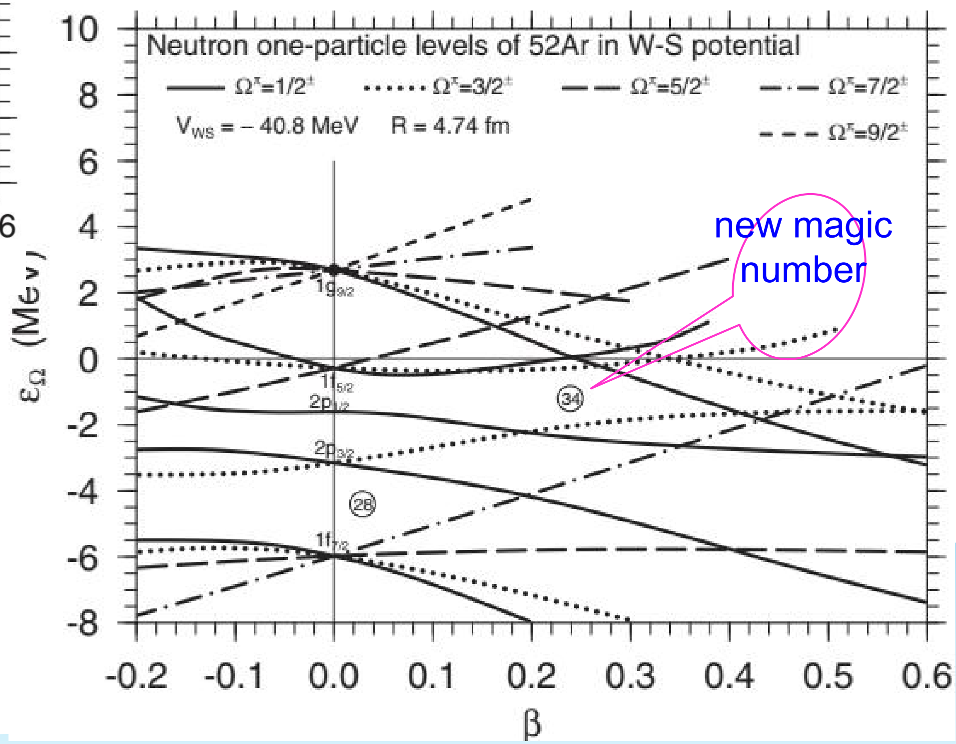

New magic number appears in $N \approx 28$ odd-N nuclei with weakly bound or resonant neutrons.

Hamamoto, PRC95, 044325 (2017)

2p1/2,2p3/2 ?

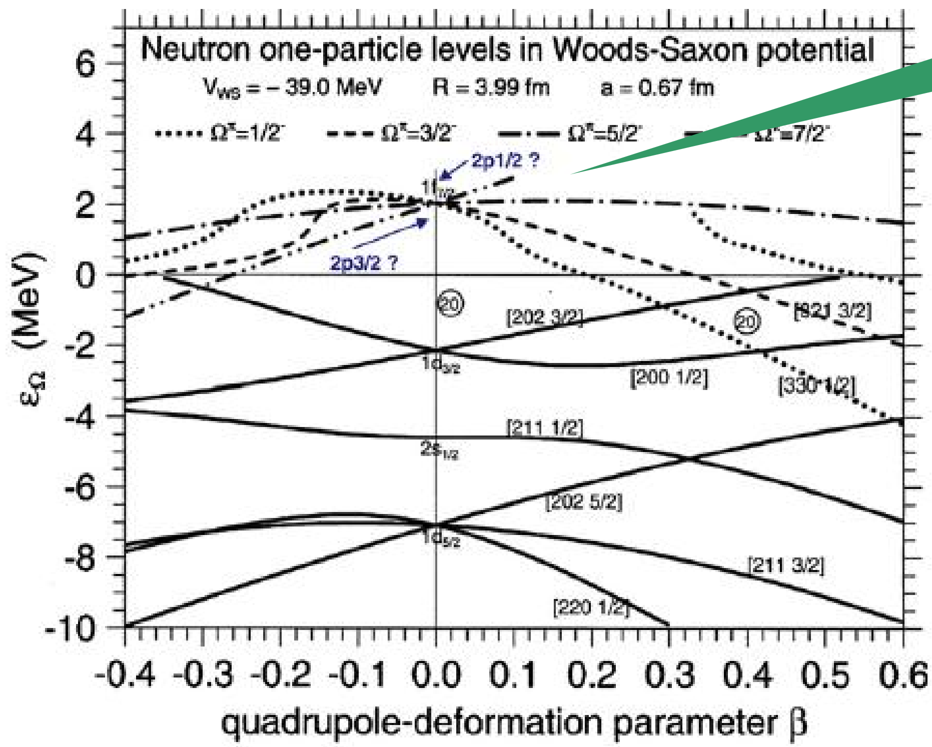

Change of shell structure and magnetic moments of odd-*N* deformed nuclei towards the neutron drip line, I.Hamamoto, J. Phys. G: Nucl. Part. Phys. 37 (2010) 055102

One-particle properties of deformed *N* ≈ 28 odd-*N* nuclei with weakly bound or resonant neutrons, I.Hamamoto, PRC79, 014307 (2009)

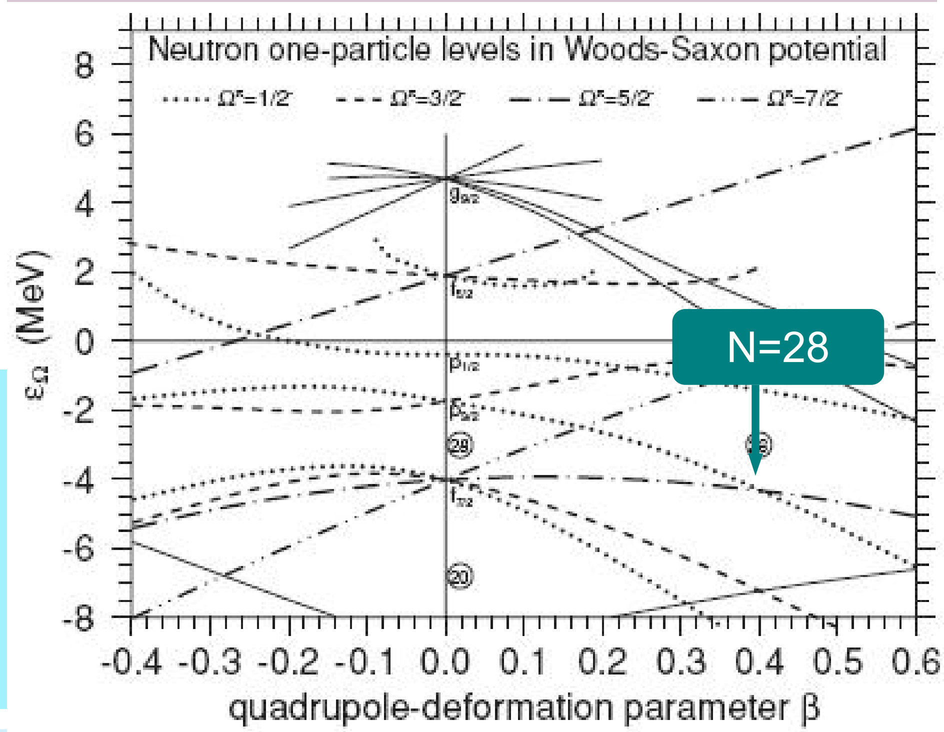

Level inversion and island of inversion

PRL **117,** 272501 (2016) PHYSICAL REVIEW LETTERS week ending 30 DECEMBER 2016

Shape Coexistence in ^{78}Ni as the Portal to the Fifth Island of Inversion

F. Nowacki,[1,2] A. Poves,[3] E. Caurier,[1,2] and B. Bounthong[1,2]
[1]*Université de Strasbourg, IPHC, 23 rue du Loess 67037 Strasbourg, France*
[2]*CNRS, UMR7178, 67037 Strasbourg, France*
[3]*Departamento de Física Teórica e IFT-UAM/CSIC, Universidad Autónoma de Madrid, E-28049 Madrid, Spain and Institute for Advanced Study, Université de Strasbourg, France*

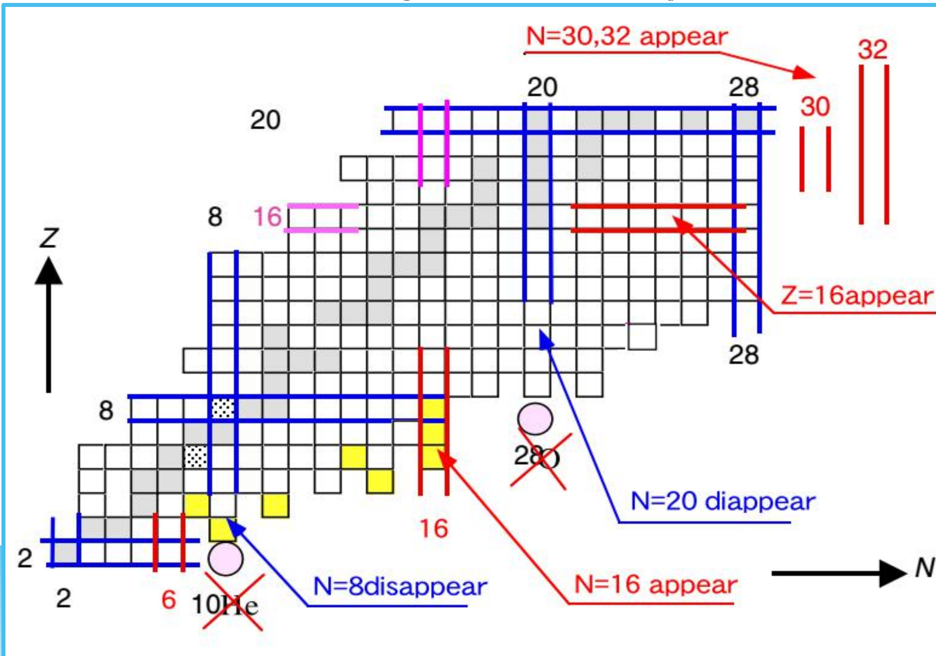

Fig. 7.4. Change of magic numbers from [150,240].

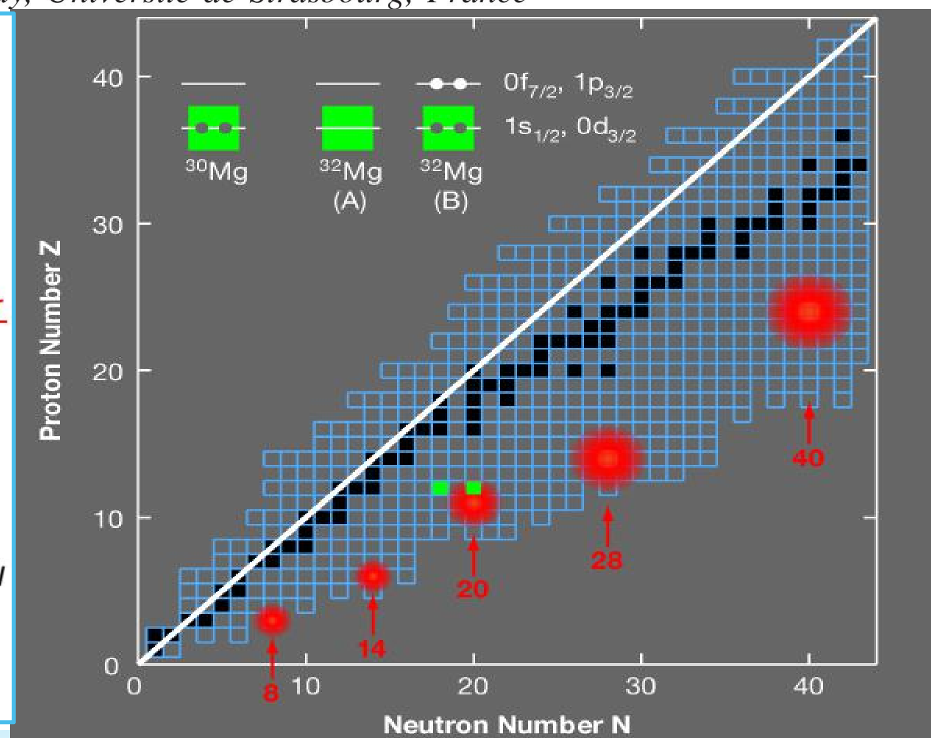

Role in the formation of giant resonance

The single particle resonances in the continuum play an important role in the description of the nuclear dynamical processes, such as the collective giant resonances.

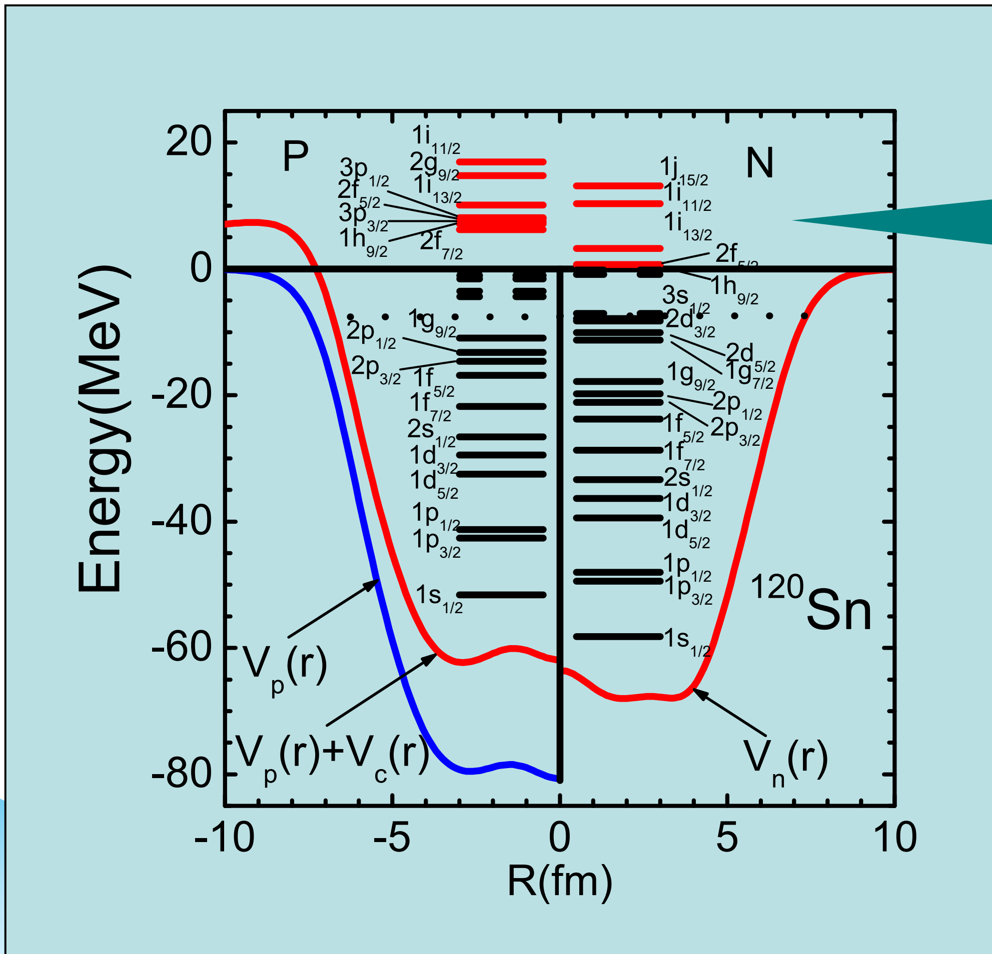

Single-particle resonant levels

Figure: Single-particle levels for ^{120}Sn calculated in the relativistic mean field theory.

L.G.Cao, Z.Y.Ma, PRC60 (2002) 024311

Stellar nucleosynthesis

Properties of the resonant states play a important role in the nucleosynthesis

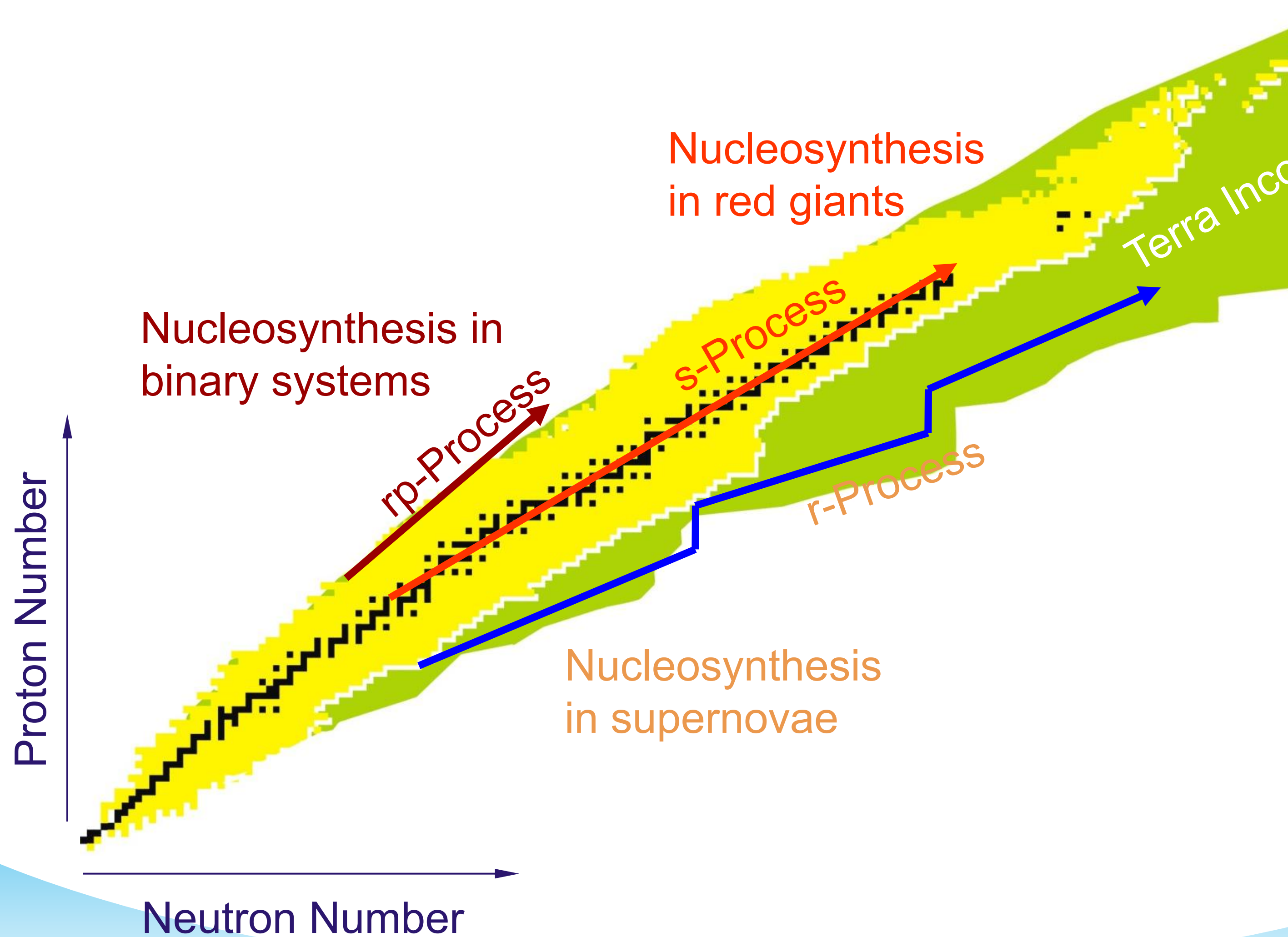

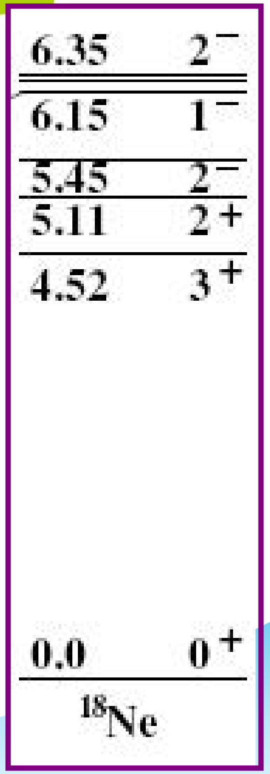

More researches on resonances

- Ikuko Hamamoto, One-particle resonant levels in a deformed potential, PRC72, 024301 (2005)
- Ikuko Hamamoto, Neutron decay width of one-particle resonant levels in deformed nuclei, PRC77, 054311 (2008)
- Chen Xu, etal., Molecular structure of highly excited resonant states in ^{24}Mg and the corresponding ^{8}Be + ^{16}O and ^{12}C + ^{12}C decays, PRC81, 054319 (2010)
- T.N.Leite, etal., ^{12}O resonant structure evaluated by the two-proton emission process, PRC80, 014606 (2009)
- Takayuki Myo, etal., Five-body resonances of ^{8}He using the complex scaling method, PLB 691, 150 (2010)

- **R-Matrix method,** **E.Wigner etal., PR 72, 29 (1947).**
- **K-Matrix method,** **J.Humblet etal., PRC 44, 2530 (1991).**
- **The phase-shift method,** **J.R.Taylor, *Scattering Theory: The Quantum Theory on Nonrelativistic Collisions* (Wiley, New York, 1972).**
- **Theory of continous spectrum,** **NPA 635, 31 (1998); NPA 422, 103 (1984).**
- **J-Matrix method,** **H.A.Yamani etal., J.Math.Phys.16, 410 (1975); A.M.Shirokov, etal., PRC79, 014610 (2009).**
- **Coupled-Channel Approach (CCA),** **I.Hamamoto, PRC 72, 024301 (2005); Z.P.Li etal., PRC 81, 034311 (2010).**

- **Jost function method**

B.N.Lu, E.G.Zhao, and S.G.Zhou, PRL 109, 072501 (2012);
B.N.Lu, E.G.Zhao, and S.G.Zhou, PRC 88, 024323 (2013).

- **Real stabilization method (RSM)**

A.U.Hazi and H.S.Taylor, PRA 1, 1109 (1970);
Y.K.Ho, Phys. Rept. 99, 1 (1983).

$\Longrightarrow$ **RMF-RSM**

L. Zhang, S.G. Zhou etal., PRC 77, 014312(2008).

- **Analytic continuation in the coupling constant (ACCC)**

V.I.Kukulin etal., Theory of Resonances: Principles and Applications (Kluwer Academic, Dordrecht, 1989).

$\Longrightarrow$ **RMF-ACCC**

S.C.Yang, J.Meng, S.G.Zhou, CPL 18, 196 (2001).
S.S.Zhang, J.Meng, S.G.Zhou etal., PRC 70, 034308 (2004).
J.Y.Guo, R.D.Wang, and X.Z.Fang, PRC 72, 054319(2005).
J.Y.Guo and X.Z.Fang, PRC 74, 024320 (2006).

◆ Green's function method

E.N.Economou, Green’s Fucntion in Quantum Physics, Springer-Verlag, Berlin, 2006.

Y. Zhang, M. Matsuo, and J. Meng, Persistent contribution of unbound quasiparticles to the pair correlation in the continuum Skyrme-Hartree-Fock-Bogoliubov approach, Phys Rev C, 2011, 83:054301.

==> RMF-GF

T.T.Sun, S.Q.Zhang, Y.Zhang, J.N.Hu, J.Meng, Green's function method for single-particle resonant states in relativistic mean field theory, Phys.Rev.C 90, 054321(2014). T.T.Sun etal., Phys.Rev.C 95, 054318 (2017).

◆ Complex Scaling Method (CSM)

Kiyoshi Kato, J. Phys.: Conf. Ser. 49, 73 (2006).
A. T. Kruppa, etal., PRC37, 383 (1988).
B. Gyarmati and A. T. Kruppa, PRC34, 95(1986).
A. T. Kruppa, etal , PRL79, 2217 (1997).
K. Arai, PRC74, 064311 (2006).

Our researches on resonant states

- **RMF-CSM**

1. Jian-You Guo etal., Application of the complex scaling method in relativistic mean-field theory, Phys.Rev.C 82, 034318 (2010).
2. Quan Liu, Jian-You Guo etal., Resonant states of deformed nuclei in the complex scaling method, Phys.Rev.C 86, 054312 (2012).
3. Quan Liu, Zhong-Ming Niu, and Jian-You Guo, Resonant states and pseudospin symmetry in the Dirac-Morse potential, Phys.Rev.A 87, 052122 (2013).
4. Zhong-Lai Zhu, Zhong-Ming Niu, Dong-Peng Li, Quan Liu, and Jian-You Guo, Probing single-proton resonances in nuclei by the complex-scaling method, Phys.Rev.C 89, 034307 (2014).
5. Min Shi, Quan Liu, Zhong-Ming Niu, and Jian-You Guo, Relativistic extension of the complex scaling method for resonant states in deformed nuclei, Phys.Rev.C 90, 034319 (2014).

- **RMF-CGF**

1. Min Shi, Jian-You Guo, Quan Liu, Zhong-Ming Niu, and Tai-Hua Heng, Relativistic extension of the complex scaled Green function method, Phys.Rev.C 92, 054313 (2015)
2. Xin-Xing Shi, Min Shi, Zhong-Ming Niu, Tai-Hua Heng, and Jian-You Guo, Probing resonances in deformed nuclei by using the complex-scaled Green's function method, Phys.Rev.C 94, 024302 (2016)
3. Relativistic extension of the complex scaled Green's function method for resonances in deformed nuclei, Min Shi, Xin-Xing Shi, Zhong-Ming Niu, Ting-Ting Sun, and Jian-You Guo, Eur. Phys. J. A 53: 40 (2017)

- **RMF-CMR**

1. Niu Li, Min Shi, Jian-You Guo, Zhong-Ming Niu, and Haozhao Liang, Probing Resonances of the Dirac Equation with Complex Momentum Representation, Phys.Rev.Lett. 117, 062502 (2016)
2. Ya-Juan Tian, Quan Liu, Tai-Hua Heng, and Jian-You Guo, Research on the halo in 31Ne with the complex momentum representation method, Phys.Rev.C 95, 064329 (2017)
3. Zhi Fang, Min Shi, Jian-You Guo, Zhong-Ming Niu, Haozhao Liang, and Shi-Sheng Zhang, Probing resonances in the Dirac equation with quadrupole-deformed potentials with the complex momentum representation method, Phys.Rev.C 95, 024311 (2017)
4. Ke-Meng Ding, Min Shi, Jian-You Guo, Zhong-Ming Niu, and Haozhao Liang, Resonant continuum relativistic mean field plus BCS in complex momentum representation, Phys.Rev.C 98, 014316 (2018).

Complex scaling method (CSM) is an effective method for resonances

- Among the continuum states, resonant states can be considered as an extension of bound states because they result from correlations and interactions.
- As pointed out by Berggren [NPA109, 265(1968)], the properties of resonant states, including the orthogonality and completeness, in many ways quite analogous to those of the ordinary bound states."
- As the physical similarity between the resonant and bound states, the bound method can be used. Especially for many-body system, CSM is more convenient.

Complex scaling method (CSM) has been applied in many fields. In web of science, we search for the paper with key words: Complex scaling method. About **39,865** papers have been found in the recent **five** years. Several reviews are listed in the following:

- N.Moiseyev, Quantum theory of resonances: calculating energies, widths and cross-sections by complex scaling, Phys. Rept. 302, 211 (1998);
- Takayuki Myo etal., Recent development of complex scaling method for many-body resonances and continua in light nuclei, Prog.Part.Nucl.Phys.79, 1 (2014);
- J.Carbonell etal., Bound state techniques to solve the multiparticle scattering problem, Prog.Part.Nucl.Phys.74, 55 (2014).

CSM has gained very success in nuclear physics

- CSM + few-body model

- Takayuki Myo, etal., Analysis of 6He Coulomb breakup in the complex scaling method, PRC63, 054313(2001)
- Kenichi Yoshida, Role of low-l component in deformed wave functions near the continuum threshold, PRC72, 064311 (2005)
- A. T. Kruppa, Scattering amplitude without an explicit enforcement of boundary conditions, PRC75, 044602 (2007)
- Takayuki Myo, etal., Five-body resonances of 8He using the complex scaling method, PLB691, 150 (2010)

➢ CSM + Shell model => Gamow Shell Model

- ⌘ N. Michel, etal., Gamow Shell Model Description of Neutron-Rich Nuclei, PRL89, 042502 (2002).
- ⌘ N. Michel, etal., Gamow shell model description of weakly bound nuclei and unbound nuclear states, PRC67, 054311 (2003).
- ⌘ G. Hagen,etal., Gamow shell model description of weakly bound nuclei and unbound nuclear states, PRC 73, 064307 (2006)
- ⌘ N. Michel, etal., Antibound states and halo formation in the Gamow shell model, PRC74, 054305 (2006).
- ⌘ J. Rotureau, etal., PRL97, 110603 (2006).
- ⌘ N. Michel, Shell Model in the Complex Energy Plane, JPG36,013101(2009)
- ⌘ J. G. Li, N. Michel, W. Zuo, and F. R.Xu, Unbound spectra of neutron-rich oxygen isotopes predicted by the Gamow shell model, PRC 103, 034305 (2021)

- CSM + HFB => Gamow-Hartree-Fock-Method

- A.T.Kruppa, and etal., Particle-Unstable Nuclei in the Hartree-Fock Theory, PRL79, 2217(1997)
- A.T.Kruppa, Resonances in the Hartree-Fock BCS theory, PRC63, 044324(2001)
- N. Michel, etal., Gamow-Hartree-Fock-Bogoliubov method: Representation of quasiparticles with Berggren sets of wave functions, PRC78, 044319 (2008)

Idea of complex scaling method

As is indicated in "Physics Reports 302 (1998) 211"

$$\hat{H}(r)\phi_n^{\mathrm{res}}(r) = E_n\phi_n^{\mathrm{res}}(r), \qquad E_n = \varepsilon_n - (\mathrm{i}/2)\Gamma_n\,, \tag{1.4.12}$$

Most of the computational algorithms in quantum mechanics have been developed for hermitian operators (as discussed above, the physical Hamiltonians are hermitian only when they operate on bounded functions which get finite values as any point in the coordinate space). For example, variational methods which were successfully used to solve many-body problems in physics and chemistry are not applicable and cannot be used to solve Eq. (1.4.12) even for the one-dimensional case. As we will show, here, an extension of the variational principle and of other well-known theorems in quantum mechanics to non-hermitian operators can be made by carrying out similarity transformations $\hat{S}$ which make the resonance functions, ϕ^{res}, square integrable functions. That is,

$$(\hat{S}\hat{H}\hat{S}^{-1})(\hat{S}\phi_n^{\mathrm{res}}) = (\varepsilon_n - (\mathrm{i}/2)\Gamma_n)(\hat{S}\phi_n^{\mathrm{res}}) \tag{1.5.5}$$

such that

$$\hat{S}\phi_n^{\mathrm{res}} \to 0 \quad \text{as } r \to \infty \tag{1.5.6}$$

and $\hat{S}\phi_n^{\mathrm{res}}$ are in the Hilbert space although ϕ^{res} are not. The complex-scaling operator to be defined below is only one example of a possible similarity transformation for which Eq. (1.5.6) is satisfied [13].

Complex scaling method

A many-body system can be described with Schrödinger equation as

$$H\psi(\vec{r}) = E\psi(\vec{r})$$

Spectrum of Hamiltonian

- Bound states $\xrightarrow[r\to\infty]{} e^{-\kappa\cdot r}$
- Continuum st.
  - Resonant states $\xrightarrow[r\to\infty]{} e^{+\gamma\cdot r}$
  - Non-Resonant states

The continuum is structured. The phase shift function δ(E) may show steep rises by nearly π; these phenomena are called resonances. Mathematical considerations reveal that this behavior of the phase shift may be associated with a pole if the scattering amplitude at $E_{res} = E - i\Gamma/2$.

- Y. K. Ho, Phys. Rep. 99, 1 (1983);
- N.Moiseyev, Phys. Rept. 302, 211 (1998);
- N.Michel etal., JPG36,013101(2009)

The starting point of CSM is a coordiante-transformation

$$\vec{r} \rightarrow \vec{r}\,' = g\vec{r} = e^{\Theta}\vec{r}$$

g∈G (space dilation group), and Θ is of complex number.

Usually,Θ is adopted as a pure imaginary parameter iθ (θ is real)

The corresponding transformation operator $U(\theta)$ is defined as

$$\left[U(\theta)\right]\psi(\vec{r}) = e^{Ni\theta/2}\psi\left(\vec{r}e^{i\vartheta}\right) = \psi_\theta(\vec{r})$$

The transformed Hamiltonian

$$H_\theta = U(\theta)HU^{-1}(\theta)$$

The transformed Schrödinger equation

$$H_\theta\psi_\theta(\vec{r}) = E_\theta\psi_\theta(\vec{r})$$

[1] J.Aguilar and J.M.Combes, Commun.Math.Phys.22,269(1971);
[2] E.Balslev and J.M.Combes, ibid.22,280(1971);
[3] B.Simon, ibid.27,1(1972)

The transformation was introduced by Aguilar, Balslev, Combes and Simon.

ABC theorem

Conditions:

- The strongly restrictive sufficient conditions are given with mathematical rigor in the references above.
- loosely speaking they amount to the requirement that all quantities in the Schrödinger equation are dilation analytic.
- This means that there exists a finite region of θ in which their transforms obtained by the application of $U(\theta)$ are analytic.

Results:

- A bound state eigenvalue of H remains also an eigenvalue of H_θ
- A resonance pole $E_{res} = E - i\Gamma/2$ of the Green-operator of H is an eigenvalue of H_θ
- The continuous part of the spectrum of H is rotated down into the complex energy plane by the angle 2θ .
- The important point is that the wavefunctions of resonant states are square integrable.

The integration path for resonances

Complex energy plane

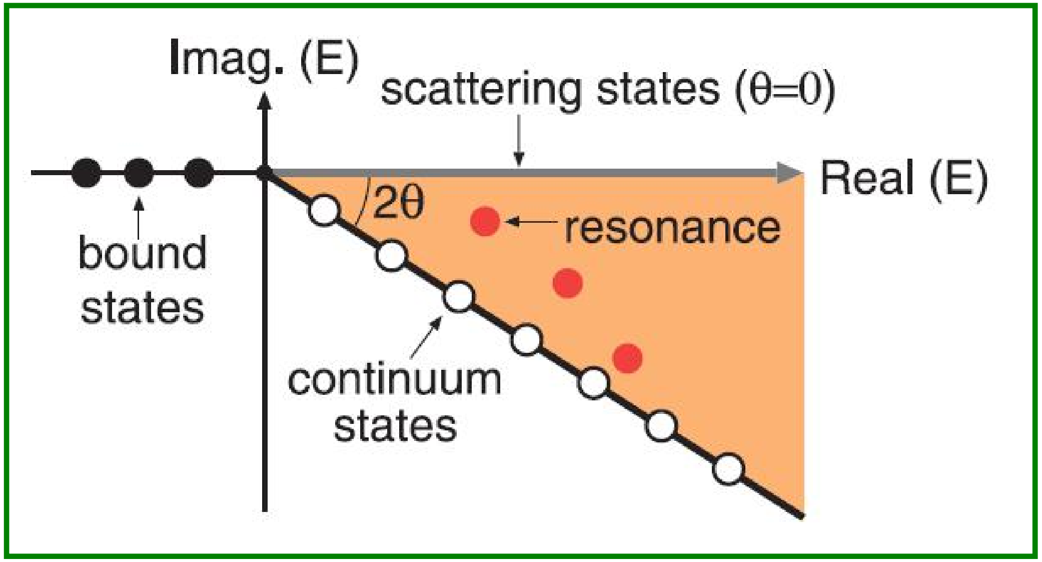

The transformation of coordinate and momentum:

coordinate: $r \rightarrow re^{i\theta}$

momentum: $k \rightarrow ke^{-i\theta}$

The integration path for bound states

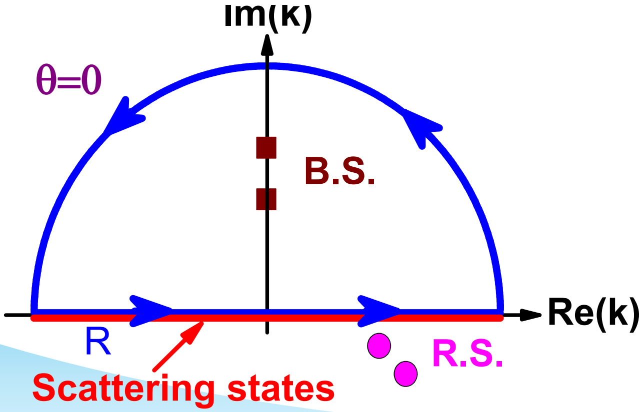

The integration path for bound and resonant states

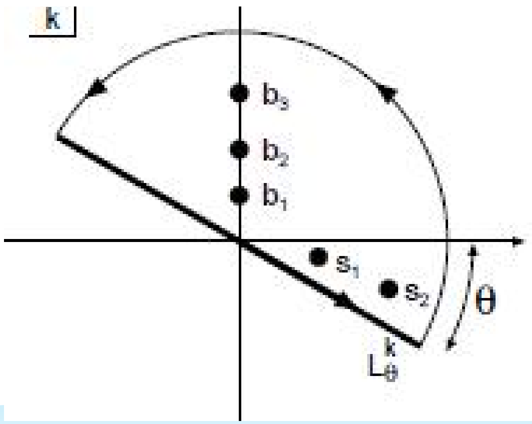

Solution of complex scaled equation

Resonant eigensolutions of $H(r)$ can be transformed into square integral $\psi_\theta(r)$. $\psi_\theta(r)$ can be approximated by an expansion with N linearly independent real square integral functions
$\chi_i(r)$ (i = 1; 2; …… N)

$$\psi_\theta(\vec{r}) = \sum_{i=1}^{N} c_i(\theta)\chi_i(\vec{r})$$

The unknown coefficients $c_i(\theta)$ are determined by a generalized variation principle

$$\delta\left[\int d\vec{r}\tilde{\psi}_\theta(\vec{r})H_\theta(\vec{r})\psi_\theta(\vec{r}) / \int d\vec{r}\tilde{\psi}_\theta(\vec{r})\psi_\theta(\vec{r})\right] = 0$$

And, we obtain a matrix equation

$$\sum_{j=1}^{N}\left[H_{ij}(\theta) - EN_{ij}\right]c_j(\theta) = 0$$

where

$$H_{ij}(\theta) = \left\langle \chi_i(\vec{r}) \middle| H_\theta(\vec{r}) \middle| \chi_j(\vec{r}) \right\rangle$$

$$N_{ij} = \left\langle \chi_i(\vec{r}) \middle| \chi_j(\vec{r}) \right\rangle$$

When the square integral functions $\chi_i(r)$ are chosen, the matrix elements H_{ij} and N_{ij} can be calculated. Then the solution of equation is obtained. The calculated complex energies can be shown in the following figures

Ideal case

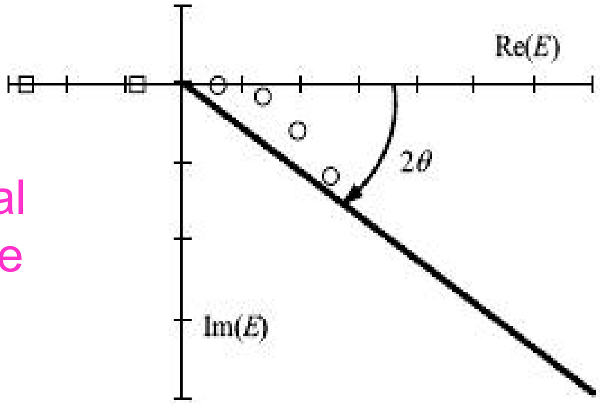

Real case

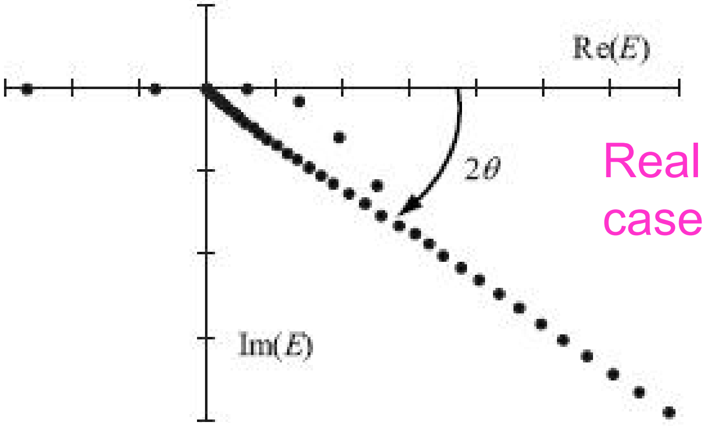

$$(E_\alpha(\theta),\ \Psi_\alpha^\theta) = \begin{cases} (E_b,\ \Psi_b^\theta), & b = 1, \ldots, N_b; \quad \text{bound states,} \\ (E_r,\ \Psi_r^\theta), & r = 1, \ldots, N_r^\theta; \quad \text{resonant states,} \\ (E_c(\theta),\ \Psi_c^\theta), & c = 1, \ldots, N - N_b - N_r^\theta; \quad \text{rotated continuum states,} \end{cases}$$

where N_b and N_r^θ are the numbers of bound and resonant state solutions, the bound solutions E_b with negative real values are independent of θ. The complex energies $E_r = E_r^{\text{res}} - i\Gamma_r/2$ are the resonant state solutions, which locate in the wedge region between the positive energy axis and the 2θ line, are also independent of θ. The discretized energies $Ec(\theta)$ of continuum states, which are obtained on the 2θ lines, are θ dependent and expressed as $E_c(\theta) = \epsilon_c^r - i\epsilon_c^i$

The calculation of matrix elements of operators

The matrix elements of the operator $\hat{O}$ are expressed as

$$\begin{aligned}\langle\widetilde{\Phi}(k)|\hat{O}|\Psi(k')\rangle &= \langle U(\theta)\widetilde{\Phi}(k)|U(\theta)\hat{O}U^{-1}(\theta)|U(\theta)\Psi(k')\rangle \\ &= \langle\widetilde{\Phi}^{\theta}(k)|\hat{O}^{\theta}|\Psi^{\theta}(k')\rangle, \\ \hat{O}^{\theta} &= U(\theta)\hat{O}U^{-1}(\theta).\end{aligned}$$

Using the solutions of the eigenvalue, the matrix elements are calculated:

$$\langle\widetilde{\Psi}^{\theta}_{\alpha}|\hat{O}^{\theta}|\Psi^{\theta}_{\beta}\rangle = \sum_{i,j=1}^{N} c_i^{\alpha}(\theta)\, c_j^{\beta}(\theta)\, \langle\bar{u}_i|\hat{O}^{\theta}|\bar{u}_j\rangle$$

where the biorthogonal state

$$\widetilde{\Psi}^{\theta}(k) = \Psi^{\theta}(-k^*)$$

Extended completeness relation

In standard quantum mechanics without complex scaling, bound and scattering (continuum) states form a complete set that is represented by the completeness relation with real eigenenergies (momenta) of the Hamiltonian H

$$\mathbf{1} = \sum_{b=1}^{N_b} |\Psi_b\rangle\langle\Psi_b| + \int_0^{\infty} dE\, |\Psi_E\rangle\langle\Psi_E|$$

$$= \sum_{b=1}^{N_b} |\Psi_b\rangle\langle\Psi_b| + \int_{-\infty}^{\infty} dk\, |\Psi_k\rangle\langle\Psi_k|,$$

In CSM, the momentum axis is rotated down by θ, and the poles of resonances can enter the semicircle for the Cauchy integration. Then, the resonances are explicitly included in the completeness relation of the complex-scaled Hamiltonian H(θ) as follows:

$$\mathbf{1} = \sum_{b=1}^{N_b} |\Psi_b^\theta\rangle\langle\widetilde{\Psi}_b^\theta| + \sum_{r=1}^{N_r^\theta} |\Psi_r^\theta\rangle\langle\widetilde{\Psi}_r^\theta| + \int_{L_\theta^E} dE\, |\Psi_E^\theta\rangle\langle\widetilde{\Psi}_E^\theta|$$

$$= \sum_{b=1}^{N_b} |\Psi_b^\theta\rangle\langle\widetilde{\Psi}_b^\theta| + \sum_{r=1}^{N_r^\theta} |\Psi_r^\theta\rangle\langle\widetilde{\Psi}_r^\theta| + \int_{L_\theta^k} dk\, |\Psi_k^\theta\rangle\langle\widetilde{\Psi}_k^\theta|,$$

Progress in Particle and Nuclear Physics 79 (2014) 1–56

Contents lists available at ScienceDirect

Progress in Particle and Nuclear Physics

journal homepage: www.elsevier.com/locate/ppnp

Review

Recent development of complex scaling method for many-body resonances and continua in light nuclei

Takayuki Myo [a,b,*], Yuma Kikuchi [c], Hiroshi Masui [d], Kiyoshi Katō [e]

[a] General Education, Faculty of Engineering, Osaka Institute of Technology, Osaka 535-8585, Japan
[b] Research Center for Nuclear Physics (R
[c] Nishina Center for Accelerator-based S
[d] Information Processing Center, Kitami
[e] Nuclear Reaction Data Centre, Faculty

Progress in Particle and Nuclear Physics 74 (2014) 55–80

Contents lists available at ScienceDirect

Progress in Particle and Nuclear Physics

journal homepage: www.elsevier.com/locate/ppnp

Review

Bound state techniques to solve the multiparticle scattering problem

J. Carbonell [a], A. Deltuva [b], A.C. Fonseca [b], R. Lazauskas [c,*]

[a] Institut de Physique Nucléaire Orsay, CNRS/IN2P3, F-91406 Orsay Cedex, France
[b] Centro de Física Nuclear da Universidade de Lisboa, P-1649-003 Lisboa, Portugal
[c] Université de Strasbourg, IPHC, CNRS, 23 rue du Loess, 67037 Strasbourg, France

Relativistic extension of complex scaling method

In 1988, Seba had proved the CSM can be used to the Dirac equation for the relativistic resonances

Petr Seba, LMP16, 51(1988)

The transformed condition is required by ABC theorem

Conditions:

Under the complex scaling transformations $U(\theta)$ with a finite region of θ, all quantities in the Dirac equation is dilation analytic.

Results:

- A bound state eigenvalue of H remains also an eigenvalue of H_θ
- A resonance pole $\varepsilon_{res} = E - i\Gamma/2$ of the Green-operator of H is an eigenvalue of H_θ
- The continuous part of the spectrum of H_θ is rotated down into the complex energy plane by the angle θ

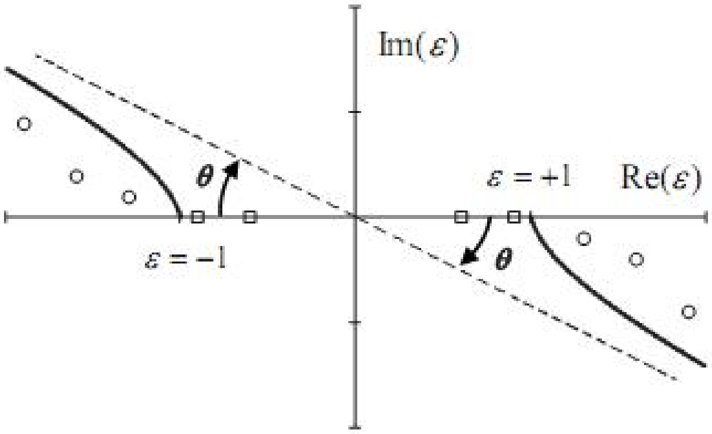

The important point is that the wavefunctions of resonant states are square integrable

Researches on the relativistic resonances

- In 2004, Ivanov etal. had applied the complex scaling method to the Dirac Hamiltonian, and presented the positions and widths of resonance levels for hydrogenlike ions with (Z=1 and Z=10). I.A.Ivanov, Phys.Rev.A 69, 023407 (2004);
- In 2006, Pestka etal. had discussed the relativistic resonances for Dirac-Coulomb with relativistic Hylleraas-CI method, G.Pestka etal., J.Phys.B39 (2006) 2979;
- In 2007, Alhaidari had discussed the relativistic resonances for Dirac-Coulomb problem with Laguerre basis A.D.Alhaidari, Phys.Rev. A75, 042707 (2007);
- In 2007, E.Ackad etal. had researched the supercritical Dirac resonance parameters by complex scaling method, E. Ackad and M.Horbatsch, Phys. Rev. A 76, 022503 (2007);
- In 2008, Bylicki etal. had researched the relativistic models of atoms for the n-electron Dirac-Coulomb DC equation by complex scaling method, M. Bylicki, G. Pestka, and J. Karwowski,, Phys.Rev.A 77, 044501 (2008)

The RMF-CSM formalism

Relativistic mean field theory (RMF)

Jian-You Guo etal., Phy.Rev.C82, 034318 (2010)

Lagrangian density:

$$\mathcal{L}=\bar{\psi}\left(i\gamma^{\mu}\partial_{\mu}-M\right)\psi+\frac{1}{2}\partial^{\mu}\sigma\partial_{\mu}\sigma-U\left(\sigma\right)-g_{\sigma}\bar{\psi}\sigma\psi$$
$$-\frac{1}{4}\Omega^{\mu\nu}\Omega_{\mu\nu}+\frac{1}{2}m_{\omega}^{2}\omega^{\mu}\omega_{\mu}-g_{\omega}\bar{\psi}\gamma^{\mu}\psi\omega_{\mu}$$
$$-\frac{1}{4}\mathbf{R}^{\mu\nu}\mathbf{R}_{\mu\nu}+\frac{1}{2}m_{\rho}^{2}\boldsymbol{\rho}^{\mu}\boldsymbol{\rho}_{\mu}-g_{\rho}\bar{\psi}\gamma^{\mu}\psi\boldsymbol{\rho}_{\mu}$$
$$-\frac{1}{4}F^{\mu\nu}F_{\mu\nu}-e\bar{\psi}\gamma^{\mu}\frac{1-\tau_{3}}{2}\psi A_{\mu}$$

meson	$J\pi$	T
π	0^-	1
σ	0^+	0
ω	1^-	0
ρ	1^-	1

Equations of motion for nucleon:

$$\left[\vec{\alpha}\cdot\vec{\boldsymbol{p}}+V(\vec{r})+\beta\left(M+S(\vec{r})\right)\right]\psi=\varepsilon\psi$$

$$\boxed{U(\sigma)=\frac{1}{2}m_{\sigma}^{2}\sigma^{2}+\frac{g_{2}}{3}\sigma^{3}+\frac{g_{3}}{4}\sigma^{4}}$$

$$\boxed{\begin{cases}\Omega_{\mu\nu}=\partial_{\mu}\omega_{\nu}-\partial_{\nu}\omega_{\mu}\\ \mathbf{R}_{\mu\nu}=\partial_{\mu}\boldsymbol{\rho}_{\nu}-\partial_{\nu}\boldsymbol{\rho}_{\mu}-g_{\rho}\left(\boldsymbol{\rho}_{\mu}\times\boldsymbol{\rho}_{\nu}\right)\\ F_{\mu\nu}=\partial_{\mu}A_{\nu}-\partial_{\nu}A_{\mu}\end{cases}}$$

The vector and scalar potentials

$$\begin{cases}V(\vec{r})=g_{\omega}\omega^{0}(\vec{r})+g_{\rho}\tau_{3}\rho^{0}(\vec{r})+eA^{0}(\vec{r})\left(1-\tau_{3}\right)/2\\ S(\vec{r})=g_{\sigma}\sigma(\vec{r})\end{cases}$$

The Dirac equation for nucleon:

$$[\alpha \bullet p + V(\boldsymbol{r}) + \beta(M + S(\boldsymbol{r}))]\psi_i(\boldsymbol{r}) = \varepsilon_i \psi_i(\boldsymbol{r})$$

The corresponding density

$$\begin{cases} \rho_s(\boldsymbol{r}) = \sum_{i=1}^{A} \overline{\psi}_i(\boldsymbol{r})\psi_i(\boldsymbol{r}) \\ \rho_v(\boldsymbol{r}) = \sum_{i=1}^{A} \psi_i^+(\boldsymbol{r})\psi_i(\boldsymbol{r}) \\ \rho_3(\boldsymbol{r}) = \sum_{i=1}^{A} \psi_i^+(\boldsymbol{r})\tau_3\psi_i(\boldsymbol{r}) \\ \rho_c(\boldsymbol{r}) = \sum_{i=1}^{A} \psi_i^+(\boldsymbol{r})\frac{1-\tau_3}{2}\psi_i(\boldsymbol{r}) \end{cases}$$

the vector and scalar potentials are as following

$$\begin{cases} V(\boldsymbol{r}) = g_\omega \omega^0(\boldsymbol{r}) + g_\rho \tau_3 \rho^0(\boldsymbol{r}) + e\frac{1-\tau_3}{2}A^0(\boldsymbol{r}) \\ S(\boldsymbol{r}) = g_\sigma \sigma(\boldsymbol{r}) \end{cases}$$

The Klein-Gordon equation for mesons and photon:

$$\begin{cases} \left(-\Delta + \partial_\sigma U(\sigma)\right)\sigma(\boldsymbol{r}) = -g_\sigma \rho_s(\boldsymbol{r}) \\ \left(-\Delta + m_\omega^2\right)\omega^0(\boldsymbol{r}) = g_\omega \rho_v(\boldsymbol{r}) \\ \left(-\Delta + m_\rho^2\right)\rho^0(\boldsymbol{r}) = g_\rho \rho_3(\boldsymbol{r}) \\ -\Delta A^0(\boldsymbol{r}) = e\rho_c(\boldsymbol{r}) \end{cases}$$

By solving these coupled equations iteratively with the no-sea and the mean-field approximations, we get self-consistent nuclear potential V(r) and S(r).

The theoretical details for the spherical case

The equation of motion from RMF for nucleon can be written as

$$\{\alpha \cdot \boldsymbol{p} + V(\boldsymbol{r}) + \beta[M + S(\boldsymbol{r})]\}\psi_i = \varepsilon_i \psi_i$$

the radial part of Dirac equation is

$$\begin{pmatrix} V+S+M & -\frac{d}{dr}+\frac{-1+\kappa}{r} \\ \frac{d}{dr}+\frac{1+\kappa}{r} & V-S-M \end{pmatrix}\begin{pmatrix} f(r) \\ g(r) \end{pmatrix} = \varepsilon \begin{pmatrix} f(r) \\ g(r) \end{pmatrix}$$

For complex scaling transformation, we introduce the operator

$$U(\theta) = \begin{pmatrix} e^{i\theta\hat{S}} & 0 \\ 0 & e^{i\theta\hat{S}} \end{pmatrix} \qquad \hat{S} = \frac{1}{2}\left(r\frac{d}{dr} + \frac{d}{dr}r \right)$$

By using the formula

$$e^{A}Be^{-A} = B + [A,B] + \frac{1}{2!}[A,[A,B]] + \frac{1}{3!}[A,[A,[A,B]]] + \cdots$$

The transformed Dirac spinors

$$f_\theta(r) = e^{i\theta\hat{S}} f(r),$$
$$g_\theta(r) = e^{i\theta\hat{S}} g(r)$$

$$\begin{aligned} e^{i\theta\hat{S}}V(r)e^{-i\theta\hat{S}} &= V(r) + \frac{(i\theta)}{1!}V_1(r) + \frac{(i\theta)^2}{2!}V_2(r) + \cdots + \frac{(i\theta)^n}{n!}V_n(r) + \cdots \\ &= V(r) - \frac{\theta^2}{2!}V_2(r) + \cdots + \frac{(-1)^n(\theta)^{2n}}{(2n)!}V_{2n}(r) + \cdots \\ &\quad + i\left[\theta V_1(r) - \frac{\theta^3}{3!}V_3(r) + \cdots + \frac{(-1)^{n-1}(\theta)^{2n-1}}{(2n-1)!}V_{2n-1}(r) + \cdots\right] \\ V_n(r) &= r\frac{d}{dr}V_{n-1}(r), \quad V_0(r) = V(r) \end{aligned}$$

The transformed Hamiltoniar.

$$H_\theta = U(\theta)HU(\theta)^{-1} = \begin{pmatrix} V(re^{i\theta}) + S(re^{i\theta}) + M & e^{-i\theta}\left(-\frac{d}{dr} + \frac{-1+\kappa}{r}\right) \\ e^{i\theta}\left(\frac{d}{dr} + \frac{1+\kappa}{r}\right) & V(re^{i\theta}) - S(re^{i\theta}) - M \end{pmatrix}$$

The transformed Dirac equation

$$\begin{pmatrix} V(re^{i\theta}) + S(re^{i\theta}) + M & e^{-i\theta}\left(-\frac{d}{dr} + \frac{-1+\kappa}{r}\right) \\ e^{i\theta}\left(\frac{d}{dr} + \frac{1+\kappa}{r}\right) & V(re^{i\theta}) - S(re^{i\theta}) - M \end{pmatrix}\begin{pmatrix} f_\theta(r) \\ g_\theta(r) \end{pmatrix} = \varepsilon_\theta \begin{pmatrix} f_\theta(r) \\ g_\theta(r) \end{pmatrix}$$

In order to solve the Dirac equation, the basis expansion method is used. The Dirac spinors f(r) and g(r) are expanded by a set of basis. Such as {Rnl(r), n=1,2,…}

$$f_\theta(r)=\sum_{n=1}^{n_{\max}} f_n(\theta)R_{nl}(r); \quad g_\theta(r)=\sum_{n=1}^{\tilde{n}_{\max}} g_{\tilde{n}}(\theta)R_{\tilde{n}\tilde{l}}(r)$$

The transformed Dirac equation becomes

$$\begin{pmatrix} V^{+}_{n,n'}+M\cdot I_{n,n'} & B_{n,\tilde{n}'} \\ B_{\tilde{n},n'} & V^{-}_{\tilde{n},\tilde{n}'}-M\cdot I_{\tilde{n},\tilde{n}'} \end{pmatrix}\begin{pmatrix} f_{n'} \\ g_{\tilde{n}'} \end{pmatrix}=\varepsilon_\theta\begin{pmatrix} I_{n,n'} & 0 \\ 0 & I_{\tilde{n},\tilde{n}'} \end{pmatrix}\begin{pmatrix} f_{n'} \\ g_{\tilde{n}'} \end{pmatrix}$$

Here

$$I_{n,n'}=\int r^2 dr R_{nl}(r)R_{n'l}(r),$$

$$I_{\tilde{n},\tilde{n}'}=\int r^2 dr R_{\tilde{n}\tilde{l}}(r)R_{\tilde{n}'\tilde{l}}(r).$$

$$B_{\tilde{n},n'}=\int r^2 dr\left[R_{\tilde{n}\tilde{l}}(r)\left(\frac{d}{dr}+\frac{1+\kappa}{r}\right)R_{n'l}(r)\right],$$

$$V^{+}_{n,n'}=\int r^2 dr\, R_{nl}(r)\left[V(r)+S(r)\right]R_{n'l}(r),$$

$$V^{-}_{\tilde{n},\tilde{n}'}=\int r^2 dr\, R_{\tilde{n}\tilde{l}}(r)\left[V(r)-S(r)\right]R_{\tilde{n}'\tilde{l}}(r).$$

- The harmonic oscillator functions are used as the basis set to diagonalize the Hamiltonian

$$R_{nl}(r)=\frac{N_{nl}}{b_0^{3/2}}x^l e^{-x^2/2}L_{n-1}^{l+1/2}(x^2),\quad x=r/b_0 \quad , \qquad N_{nl}=\sqrt{\frac{2\Gamma(n)}{\Gamma(n+l+1/2)}}$$

The matrix elements of unit operator

$$I_{n,n'}=\delta_{n,n'} \quad , \qquad I_{\tilde{n},\tilde{n}'}=\delta_{\tilde{n},\tilde{n}'}$$

The matrix elements of kinetic energy operator

$$B_{\tilde{n},n'}=\int r^2 dr\, R_{\tilde{n}\tilde{l}}(r)\left(\frac{d}{dr}+\frac{1}{r}+\frac{\kappa}{r}\right)R_{n'l}(r)$$

$$=\begin{cases}-\frac{1}{b_0}\left(\sqrt{\tilde{n}+l+1/2}\,\delta_{\tilde{n},n'}+\sqrt{\tilde{n}}\,\delta_{\tilde{n},n'-1}\right), & \kappa<0\\ \frac{1}{b_0}\left(\sqrt{\tilde{n}+l-1/2}\,\delta_{\tilde{n},n'}+\sqrt{\tilde{n}-1}\,\delta_{\tilde{n},n'+1}\right), & \kappa>0\end{cases}$$

The matrix elements of potential energy operator

$$V^{+}_{n,n'} = \int r^2 dr\, R_{nl}(r)\left[V(r)+S(r)\right]R_{n'l}(r)$$

$$= \int r^2 dr \frac{N_{nl}}{b_0^{3/2}} x^l e^{-x^2} L_{n-1}^{l+1/2}(x^2)\left[V(r)+S(r)\right]\frac{N_{n'l}}{b_0^{3/2}} x^l e^{-x^2} L_{n'-1}^{l+1/2}(x^2)$$

$$= \sum_{k=1}^{K} \Lambda_{nk}\Lambda_{n'k}\left[V(b_0\sqrt{\varepsilon_k})+S(b_0\sqrt{\varepsilon_k})\right], \qquad (K \ge n_{\max})$$

$$V^{-}_{\tilde{n},\tilde{n}'} = \sum_{\tilde{k}=1}^{\tilde{K}} \Lambda_{\tilde{n}\tilde{k}}\Lambda_{\tilde{n}'\tilde{k}}\left[V(b_0\sqrt{\varepsilon_{\tilde{k}}})-S(b_0\sqrt{\varepsilon_{\tilde{k}}})\right], \qquad (\tilde{K} \ge \tilde{n}_{\max})$$

Here $\varepsilon_{\mathrm{k}}\left[\varepsilon_{\tilde{k}}\right]$ and $\Lambda_{nk}\left[\Lambda_{\tilde{n}\tilde{k}}\right]$ are the eigenvalues and eigenvectors of the matrix JK with elements $JK_{n,n} = 2n+l-1/2\left[JK_{\tilde{n},\tilde{n}} = 2\tilde{n}+\tilde{l}-1/2\right]$ and $JK_{n,n+1} = -\sqrt{n(n+l+1/2)}\left[JK_{\tilde{n},\tilde{n}+1} = -\sqrt{\tilde{n}(\tilde{n}+\tilde{l}+1/2)}\right]$

More details can be found in the paper:

Jian-You Guo etal., Computer Physics Communications 181, 550 (2010)

- The Laguerre polynomial are used as the basis set to diagonalize the Hamiltonian

$$R_{nl}(r)=\frac{N_{nl}}{b_0^{3/2}}x^l e^{-x/2}L_{n-1}^{2l+1}(x),\quad x=r/b_0,\ n=1,2,3,\cdots \qquad N_{nl}=\sqrt{\frac{\Gamma(n)}{\Gamma(n+2l+1)}}$$

The matrix elements of unit operator

$$N_{n,n'}=\int r^2 dr R_{nl}(r)R_{n'l}(r)=-\sqrt{(n-1)(n+2l)}\,\delta_{n,n'+1}+2(n+l)\,\delta_{n,n'}-\sqrt{n(n+2l+1)}\,\delta_{n,n'-1}$$

The matrix elements of kinetic energy operator

$$B_{\tilde{n},n'}=\int r^2 dr\, R_{\tilde{n}\tilde{l}}(r)\left(\frac{d}{dr}+\frac{1}{r}+\frac{\kappa}{r}\right)R_{n'l}(r)$$

$$=\begin{cases}\frac{1}{2b_0}\left(\sqrt{\tilde{n}(\tilde{n}+1)}\,\delta_{\tilde{n}+2,n'}-\frac{1}{2b_0}\sqrt{(\tilde{n}+2l+1)(\tilde{n}+2l+2)}\,\delta_{\tilde{n},n'}\right), & \kappa<0\\ -\frac{1}{2b_0}\left(\sqrt{(\tilde{n}-1)(\tilde{n}-21)}\,\delta_{\tilde{n}-2,n'}+\frac{1}{2b_0}\sqrt{(\tilde{n}+2l)(\tilde{n}+2l-1)}\,\delta_{\tilde{n},n'}\right), & \kappa>0\end{cases}$$

The matrix elements of potential energy operator

$$V^{+}_{n,n'} = \int r^2 dr\, R_{nl}(r)\left[V(r)+S\left(r\right)\right]R_{n'l}(r)$$

$$= N_{nl}N_{n'l}\int r^2 dr b_0^{-3/2} x^l e^{-x/2} L_{n-1}^{2l+1}(x)\left[V(r)+S\left(r\right)\right]b_0^{-3/2} x^l e^{-x/2} L_{n'-1}^{2l+1}(x)$$

$$= N_{nl}N_{n'l}\int dx\, x^{2l+1} e^{-x} L_{n-1}^{2l+1}(x)x\left[V(b_0 x)+S\left(b_0 x\right)\right]L_{n'-1}^{2l+1}(x)$$

$$= \sum_{k=1}^{K}\Lambda_{nk}\Lambda_{n'k}\left[V\left(b_0\varepsilon_k\right)+S\left(b_0\varepsilon_k\right)\right]\varepsilon_k, \qquad (K \geq n_{\max})$$

$$V^{-}_{\tilde{n},\tilde{n}'} = \int r^2 dr\, R_{\tilde{n}\tilde{l}}(r)\left[V(r)-S\left(r\right)\right]R_{\tilde{n}'\tilde{l}}(r)$$

$$= \sum_{\tilde{k}=1}^{\tilde{K}}\Lambda_{\tilde{n}\tilde{k}}\Lambda_{\tilde{n}'\tilde{k}}\left[V\left(b_0\varepsilon_{\tilde{k}}\right)-S\left(b_0\varepsilon_{\tilde{k}}\right)\right]\varepsilon_{\tilde{k}}, \qquad (\tilde{K} \geq \tilde{n}_{\max})$$

Here $\varepsilon_{\mathrm{k}}\left[\varepsilon_{\tilde{k}}\right]$ and $\Lambda_{nk}\left[\Lambda_{\tilde{n}\tilde{k}}\right]$ are the eigenvalues and eigenvectors of the matrix JK with elements $JK_{n,n} = 2\left(n+l\right)\left[JK_{\tilde{n},\tilde{n}} = 2\left(\tilde{n}+\tilde{l}\right)\right]$ and $JK_{n,n+1} = -\sqrt{n(n+2l+1)}\left[JK_{\tilde{n},\tilde{n}+1} = -\sqrt{\tilde{n}(\tilde{n}+2\tilde{l}+1)}\right]$

Numerical check for the formalism

The exponential model

The adopted potential

$$V(r) = 7.5r^2 e^{-r}, \quad S(r) = 0$$

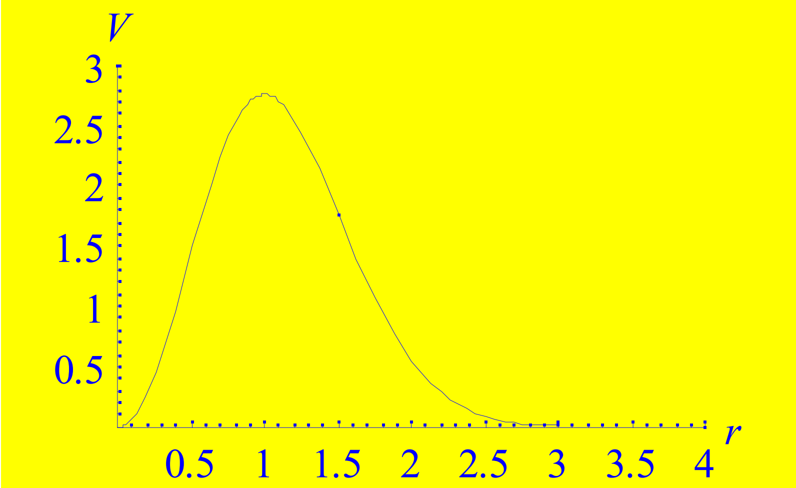

The dependence on the rotated angle θ

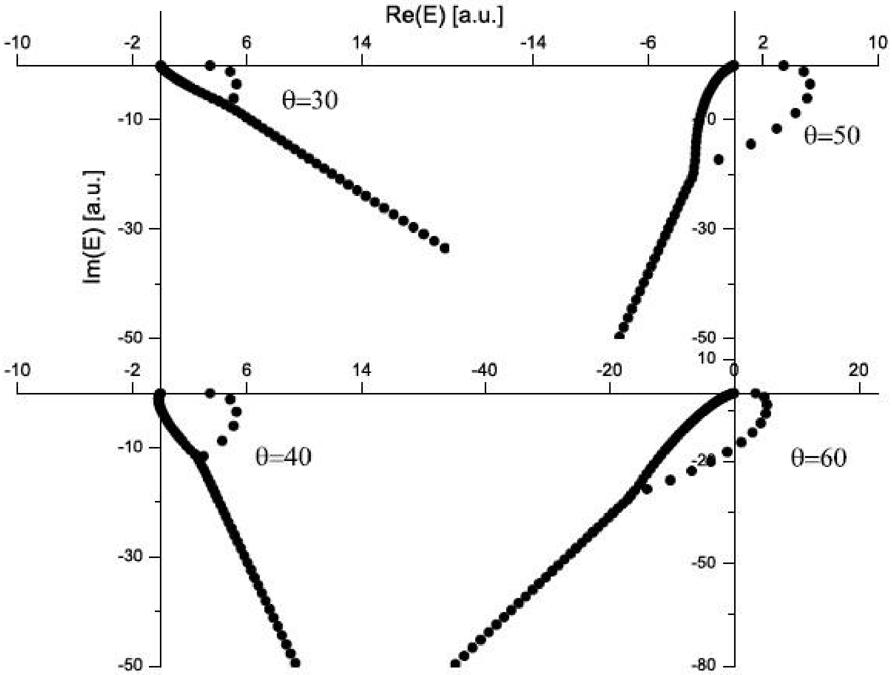

$$\kappa = -1,\ N = 100,\ b_0 = 1.0\,\text{a.u.}$$

Θ	E	Γ
10	3.42637553	0.02554493007
20	3.42637422	0.02554487094
30	3.42637356	0.02554710731
40	3.42637420	0.02554930672
50	3.42637545	0.02554929359
60	3.42637606	0.02554717623
70	3.42637547	0.02554508319
80	3.42637452	0.02555479468

The dependence on the size of basis *N*

N	*E*	*Γ*
30	3.42638378	0.02557000000
40	3.42637992	0.02556000000
50	3.42637800	0.02555757161
60	3.42637694	0.02555421281
70	3.42637631	0.02555215337
80	3.42637590	0.02555082142
90	3.42637563	0.02555000000
100	3.42637545	0.02555000000

N	*E*	*Γ*
30	4.83482424	2.23557000
40	4.83482786	2.23556000
50	4.83482981	2.23555276
60	4.83483095	2.23554986
70	4.83483166	2.23554812
80	4.83483212	2.23554702
90	4.83483243	2.23555000
100	4.83483265	2.23555000

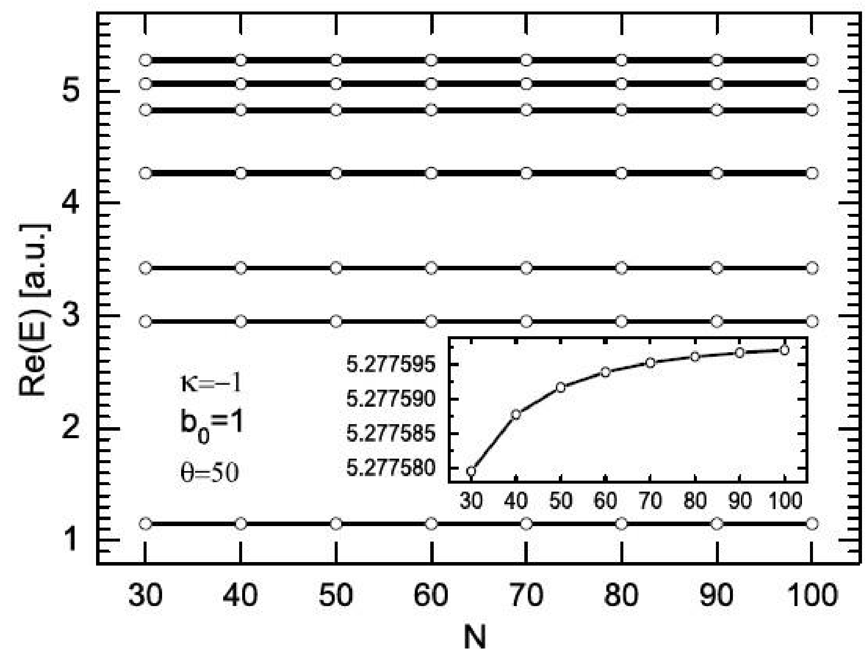

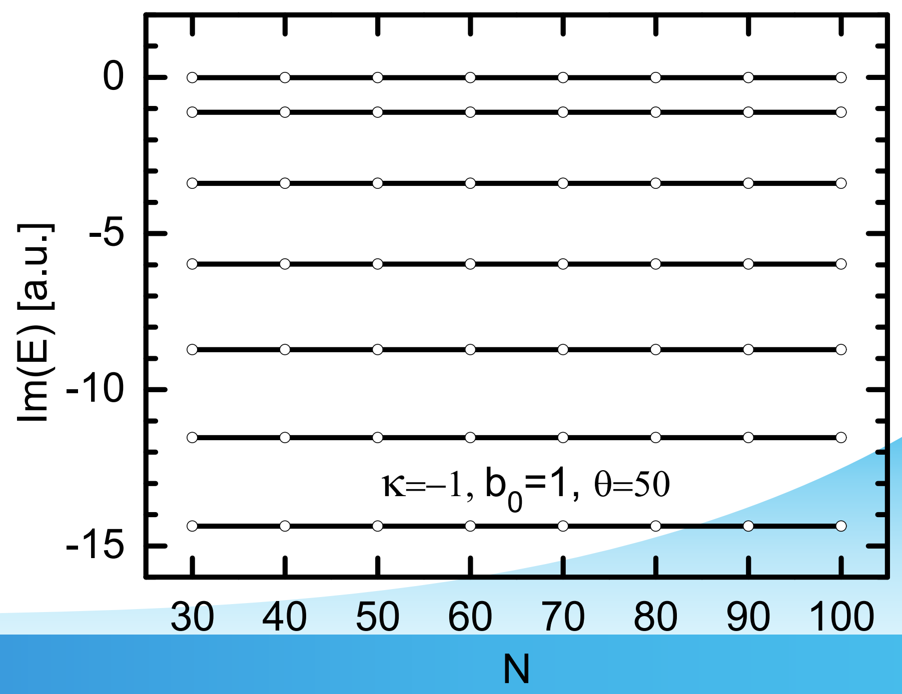

The dependence on the scaling parameter b_0

b_0/b_{00}	E	Γ
1	3.42637484	0.02555000000
2	3.42637487	0.02554724236
3	3.42637516	0.02554829200
4	3.42638000	0.02555000000
5	3.42638000	0.02557000000
6	3.42640000	0.02561000000
7	3.42643000	0.02570000000
8	3.42666000	0.02621000000

b_0/b_{00}	E	Γ
1	4.83483341	2.23554000
2	4.83483337	2.23554418
3	4.83483300	2.23554499
4	4.83483000	2.23555000
5	4.83483000	2.23556000
6	4.83481000	2.23561000
7	4.83480000	2.23568000
8	4.83416000	2.23677000

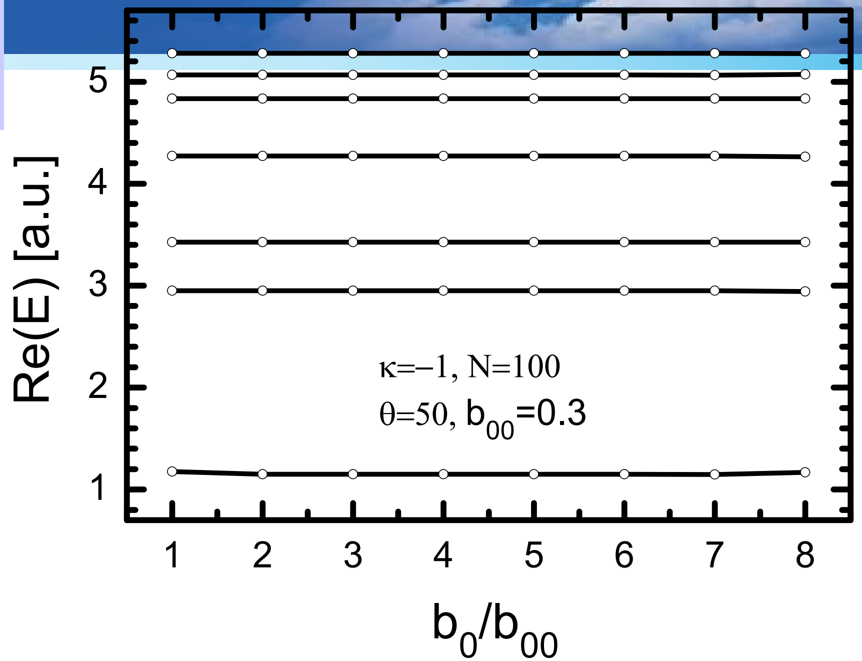

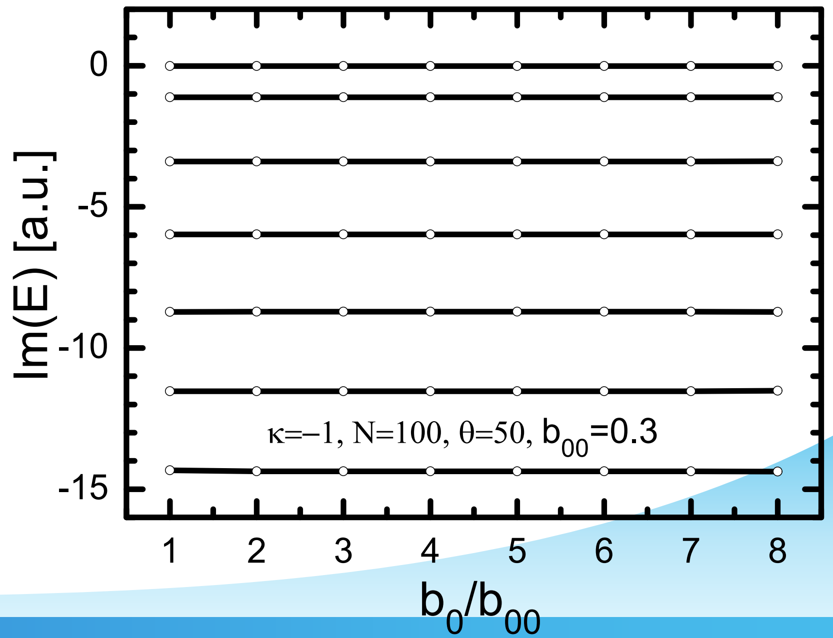

Comparison of energies and widths in this work with Ref. [1] for the resonant states with $\kappa = -1$

This work		Ref.[1]	
E (a.u.)	Γ (a.u.)	E (a.u.)	Γ (a.u.)
2.9498916193	23.064483506	2.9465842	23.06811
3.4263754496	0.0255492936	3.4266874221	0.0255518009
4.2703307927	17.435033899	4.2687950416	17.439000786
4.8348326472	2.2355457803	4.8354225415	2.2361196639
5.0657602535	11.952101919	5.0654945401	11.955326382
5.2775971948	6.7777667228	5.2780344286	6.7796704926

[1] A.D. Alhaidari, PRA75, 042707(2007)

The nonrelativistic limit of our calculations associated with the model potential for $\kappa = -1$ against known nonrelativistic results elsewhere.

E (a.u.)	Γ (a.u.)	References
3.426390331	0.025548962	[2]
3.426390310	0.025548961	[3]
3.4263903	0.025549	[1]
3.426389933	0.025551206	This work
3.426391372	0.025552643	Nonrelativistic
4.834806841	2.235753338	[2]
4.834806841	2.235753338	[3]
4.8348069	2.2357529	[1]
4.834806471	2.235753125	This work
4.834805545	2.235756250	Nonrelativistic

[2] S.A. Sofianos, S.A. Rakityansky, J. Phys. A 30 (1997) 3725.
[3] A.D. Alhaidari, J. Phys. A 37 (2004) 5863.

The Yukawa potential

Few-Body Syst (2014) 55:135–141

Resonances of Dirac Particle in the Yukawa Potential

Min Shi · Quan Liu · Zhong-Ming Niu · Jian-You Guo

Abstract We applied the complex scaling method to study the resonances of a Dirac particle in the Yukawa potential, and obtained the corresponding energies and widths. In the non-relativistic limit, our results are in excellent agreement with those by non-relativistic calculations with *J*-matrix approach. Furthermore, we found that the energies and widths of spin doublets are approximately degenerate, and preserve a good spin symmetry. The quality of spin symmetry is correlated with the parameters of the Yukawa potential.

Resonance energies for the κ=l states in the Yukawa potential in comparison with those in J-matrix calculation. The complex rotation angle θ=1.0 radians and the atomic units ħ = m = 1.

			$E_r + iE_i$	$E_r + iE_i$	$E_r + iE_i$
κ	μ	A	Relativistic	Nonrelativistic limit	J-matrix
5	2	110	2.2834 - i0.0549	2.4208 - i0.0769	2.4209 - i0.0769
			3.0630 - i3.4908	3.0140 - i3.6049	3.0139 - i3.6050
5	2	170	0.4648 - i0.0066	1.0272 - i0.0079	1.0244 - i0.0036
			2.3913 - i2.0708	2.2319 - i2.3825	2.2364 - i2.3818
10	1	200	0.8906 - i0.0000	1.0682 - i0.0168	1.0579 - i0.0000
			1.7214 - i4.7300	1.6440 - i4.8192	1.6518 - i4.7941
			3.0962 - i2.6537	3.0789 - i2.7325	3.0656 - i2.7310
			3.2473 - i0.5827	3.2570 - i0.6332	3.2645 - i0.6393

The Morse potential

The potential

$$V(r) = V_0\left[e^{-2\alpha(x-1)} - 2e^{-\alpha(x-1)}\right]$$

Here $x = r/r_0$

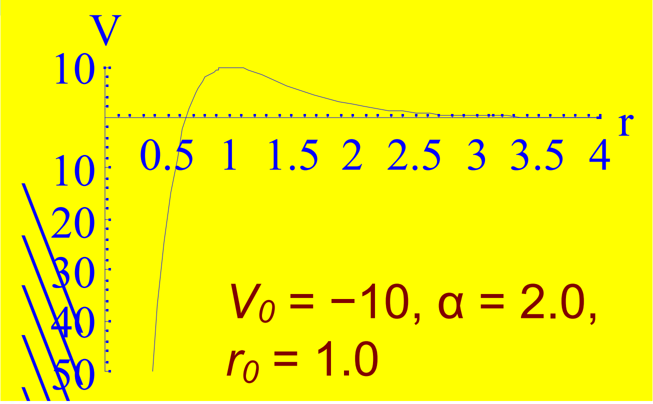

PHYSICAL REVIEW A **87**, 052122 (2013)

Resonant states and pseudospin symmetry in the Dirac-Morse potential

Quan Liu, Zhong-Ming Niu, and Jian-You Guo*

School of Physics and Material Science, Anhui University, Hefei 230039, People's Republic of China

(Received

The complex scaling method is applie
applicability of the method is demonstrat
present calculations in the nonrelativisti
Further, the dependence of the resonant
to the potential parameters analyzed. B
pseudospin symmetry is discovered in t
and the shape of the potential is investig
the equilibrium intermolecular distance,

$E_r + iE_i$ Relativistic	$E_r + iE_i$ Nonrelativistic limit	$E_r + iE_i$ Nasser [38]
−30.7047	−30.4136	−30.4139
10.8020 $-i$ 0.2822	10.9262 $-i$ 0.3026	10.9260 $-i$ 0.3027
17.1419$-i$ 12.3689	17.1244 $-i$ 12.5031	17.1240 $-i$ 12.5027
11.1795 $-i$ 32.0868	11.0511 $-i$32.1914	11.0521 $-i$ 32.1906
−4.8377 $-i$ 52.5443	−5.0383 $-i$ 52.5395	−5.0376 $-i$ 52.5407
−29.3283 $-i$ 72.2381	−29.5208 $-i$ 72.0565	S-matrix

RMF-CSM for neutron resonances in nuclei

PHYSICAL REVIEW C **82**, 034318 (2010)

Application of the complex scaling method in relativistic mean-field theory

Jian-You Guo, Xiang-Zheng Fang, Peng Jiao, .
School of Physics and Material Science, Anhui University, H
(Received 9 October 2009; revised manuscript received 18 J

We develop the complex scaling method within the framewor
With the self-consistent nuclear potentials from the RMF model,
single-particle resonant states in spherical nuclei. As examples,
resonant states in ^{120}Sn are obtained. The results are compared wi

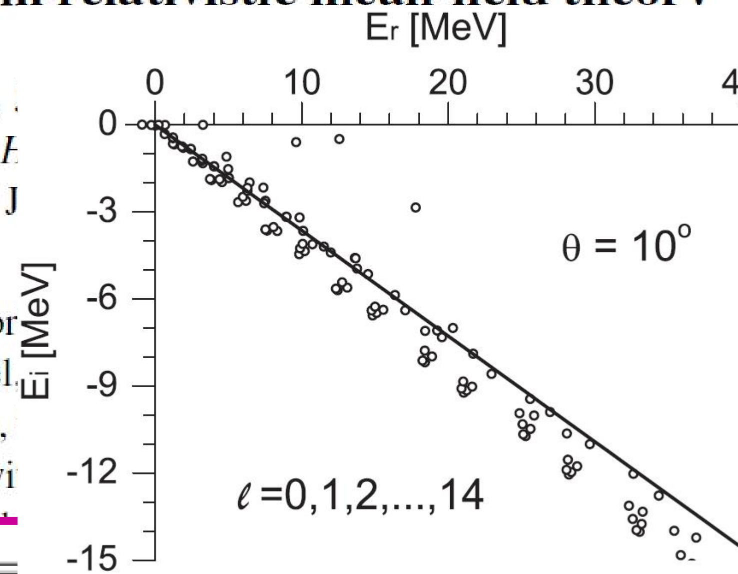

νl_j	RMF-CSM E_γ	RMF-CSM Γ	RMF-RSM E_γ	RMF-RSM Γ	RMF-ACCC E_γ	RMF-ACCC Γ	RMF-S E_γ	RMF-S Γ
$\nu f_{5/2}$	0.68495	0.0172	0.674	0.03	0.685	0.023	0.688	0.032
$\nu i_{13/2}$	3.26501	0.00426	3.266	0.004	3.262	0.004	3.416	0.005
$\nu i_{11/2}$	9.6119	1.20664	9.559	1.205	9.6	1.11	10.01	1.42
$\nu j_{15/2}$	12.55863	0.97994	12.564	0.973	12.6	0.9	12.97	1.1

RMF-CSM for proton resonances in nuclei

PHYSICAL REVIEW C **89**, 034307 (2014)

Probing single-proton resonances in nuclei by the complex-scaling method

Zhong-Lai Zhu, Zhong-Ming Niu,* Dong-Peng Li, Quan Liu, and Jian-You Guo†
School of Physics and Material Science, Anhui University, Hefei 230601, China

(Received 15 January 2014; revised manuscript received 24 February 2014; published 12 March 2014)

By combining the complex scaling method with relativistic mean-field theory, single-proton resonances are probed for spherical nuclei. The energy and width are shown to decrease with the increasing neutron number for the Sn isotopes and increase with the increasing proton number for the $N = 82$ isotones. Furthermore, the influence o ... ^{132}Sn, and ^{208}Pb. It is ... range of 0.4–0.6 Me ... t state.

	RMF-CSM		RMF-ACCC		RMF-S	
nl_j	E_r	Γ	E_r	Γ	E_r	Γ
$2f_{7/2}$	6.207	0.048	6.22	0.073	6.210	0.043
$1h_{9/2}$	7.135	0.003	7.13	0.017	7.132	0.003
$3p_{3/2}$	7.305	0.911	7.32	0.82	7.513	0.924
$3p_{1/2}$	7.663	1.222	7.69	1.13	8.085	1.344
$2f_{5/2}$	7.919	0.283	7.97	0.30	7.934	0.307

CSM for the resonances in deformed nuclei

The non-relativistic case

Liu, Guo etal., Phys.Rev.C 86, 054312 (2012)

Neutron single-particle levels in ^{31}Ne

The interactions are adopted from Hamamoto, Phys.Rev.C 81(R), 021304(R)(2010)

$$H = T + V,$$

$$V_{\rm cent}(r) = V_0 f(r),$$

$$V_{\rm cou}(\vec{r}) = -\beta_2 V_0 k(r) Y_{20}(\vartheta, \varphi),$$

$$V_{\rm so}(r) = -\frac{1}{2} v V_0 g(r)(\vec{s} \cdot \vec{l}).$$

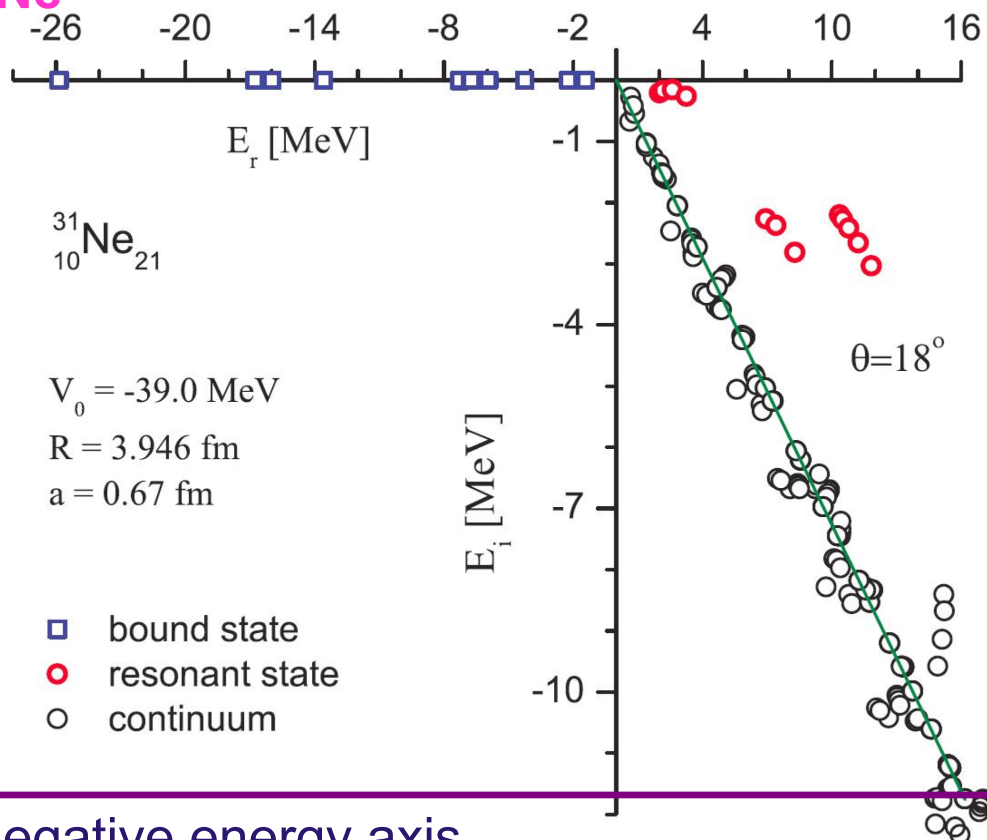

- The bound states remain on the negative energy axis.
- The resonance poles fall on the fourth quadrant
- The continuous spectrum is rotated down into the complex energy plane by the angle 2 θ .

Variation of energy spectrum with θ in the complex energy plane

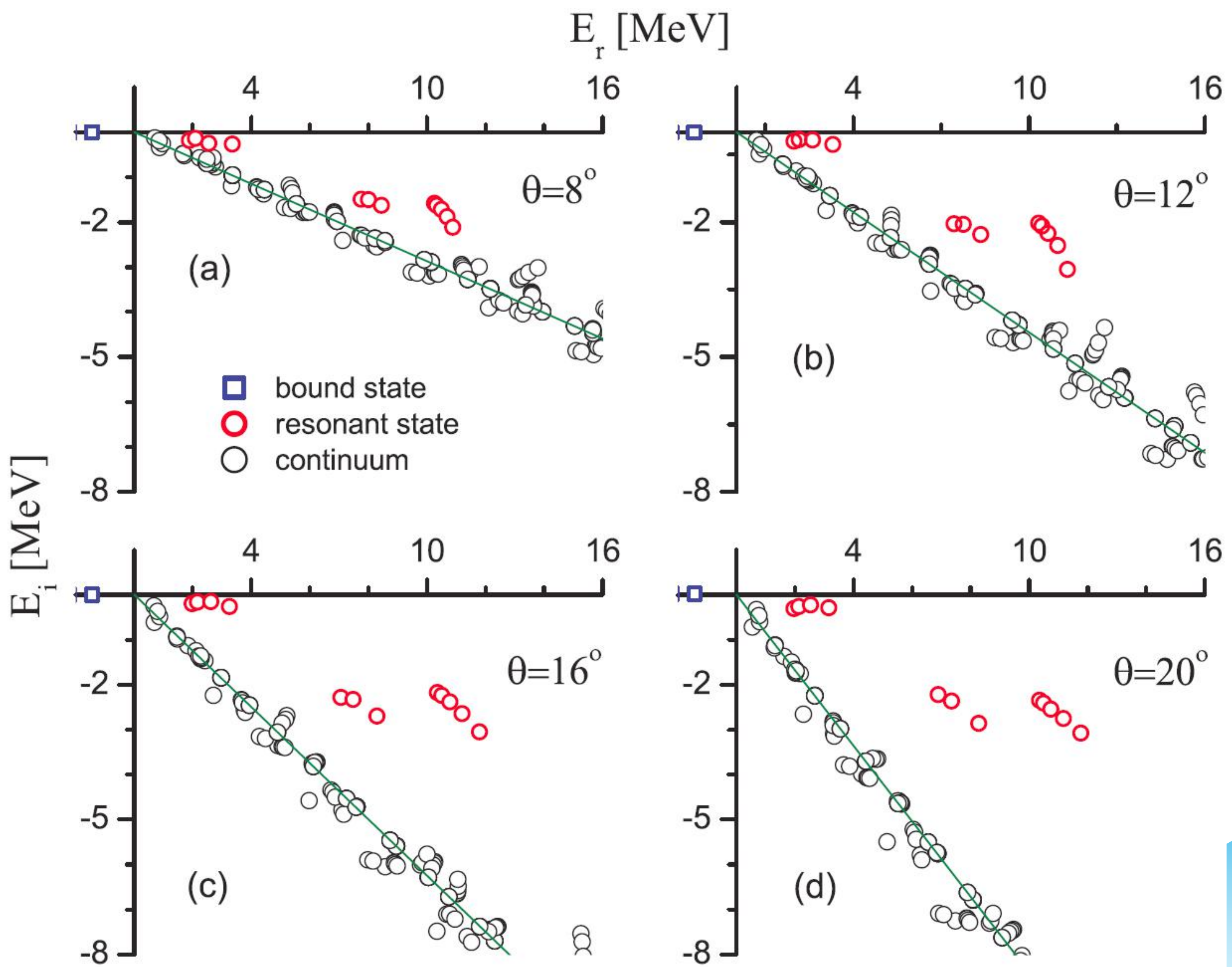

Determination of resonance parameters

Resonance parameters from the θ trajectories

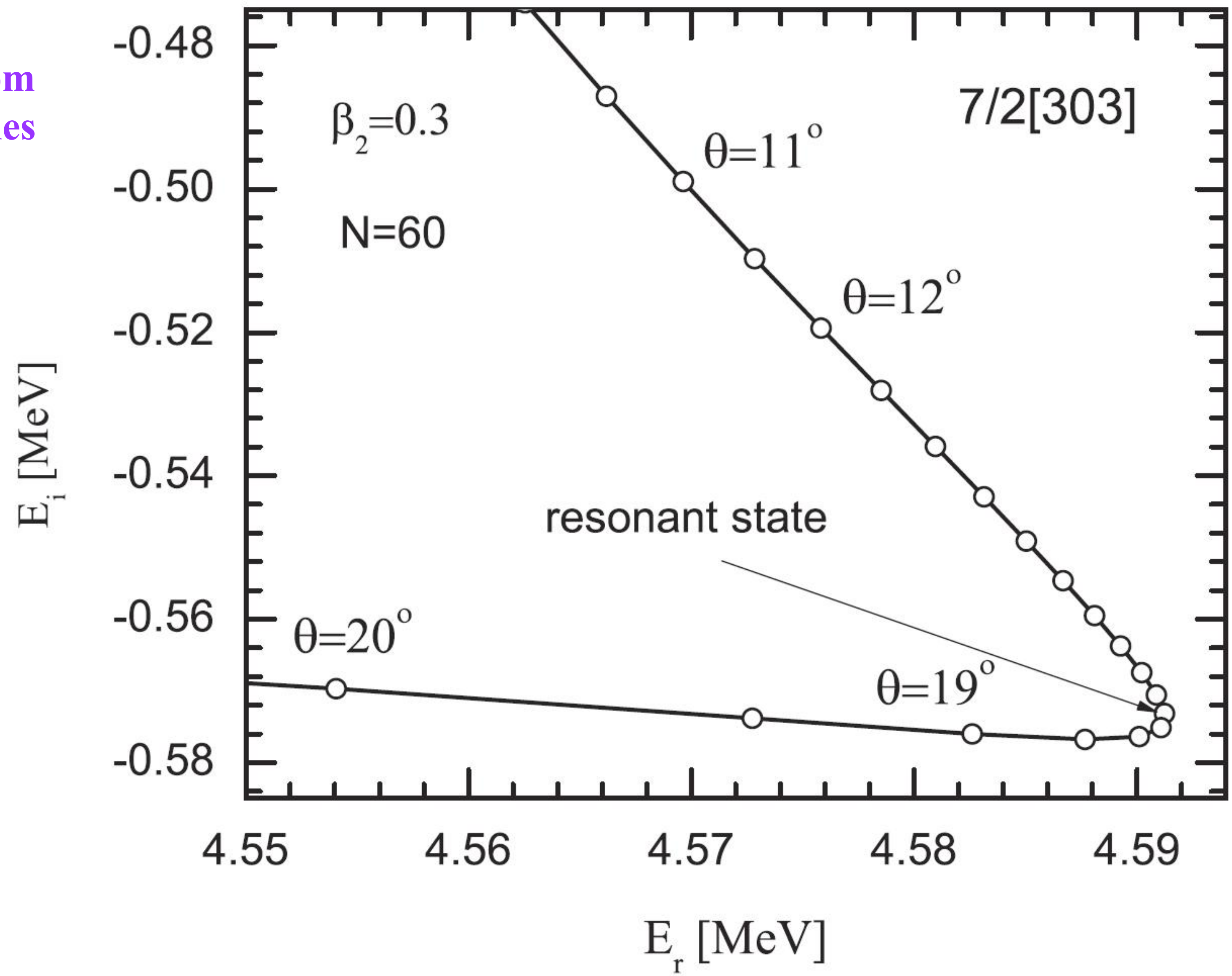

Comparison with the coupled channel method for the single-particle levels in ^{31}Ne

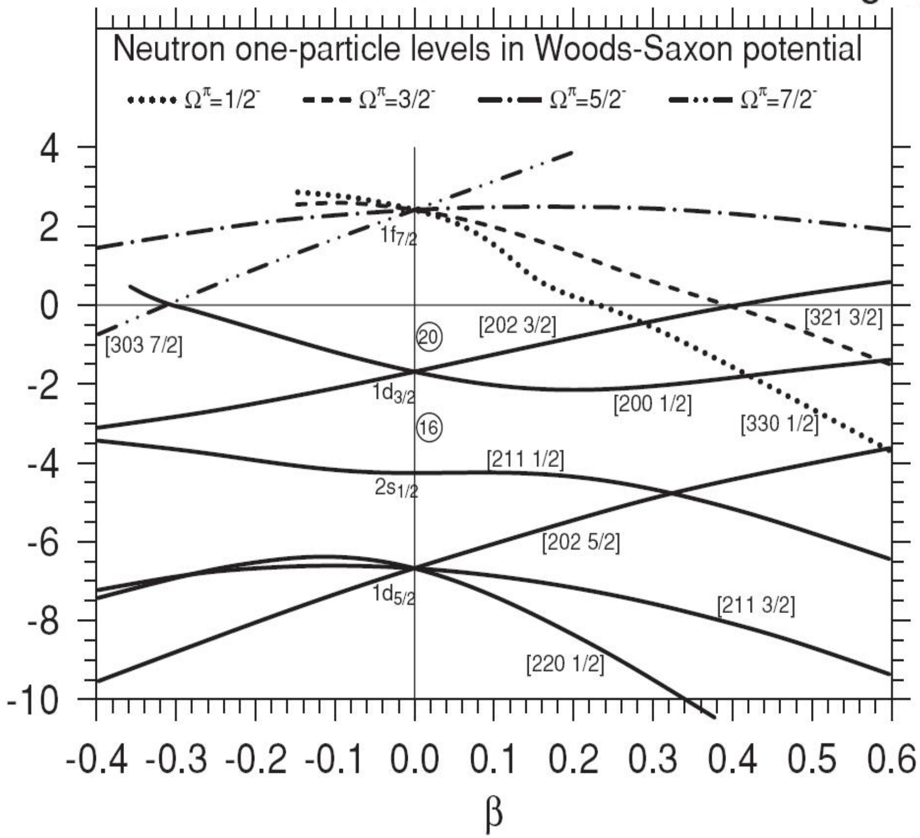

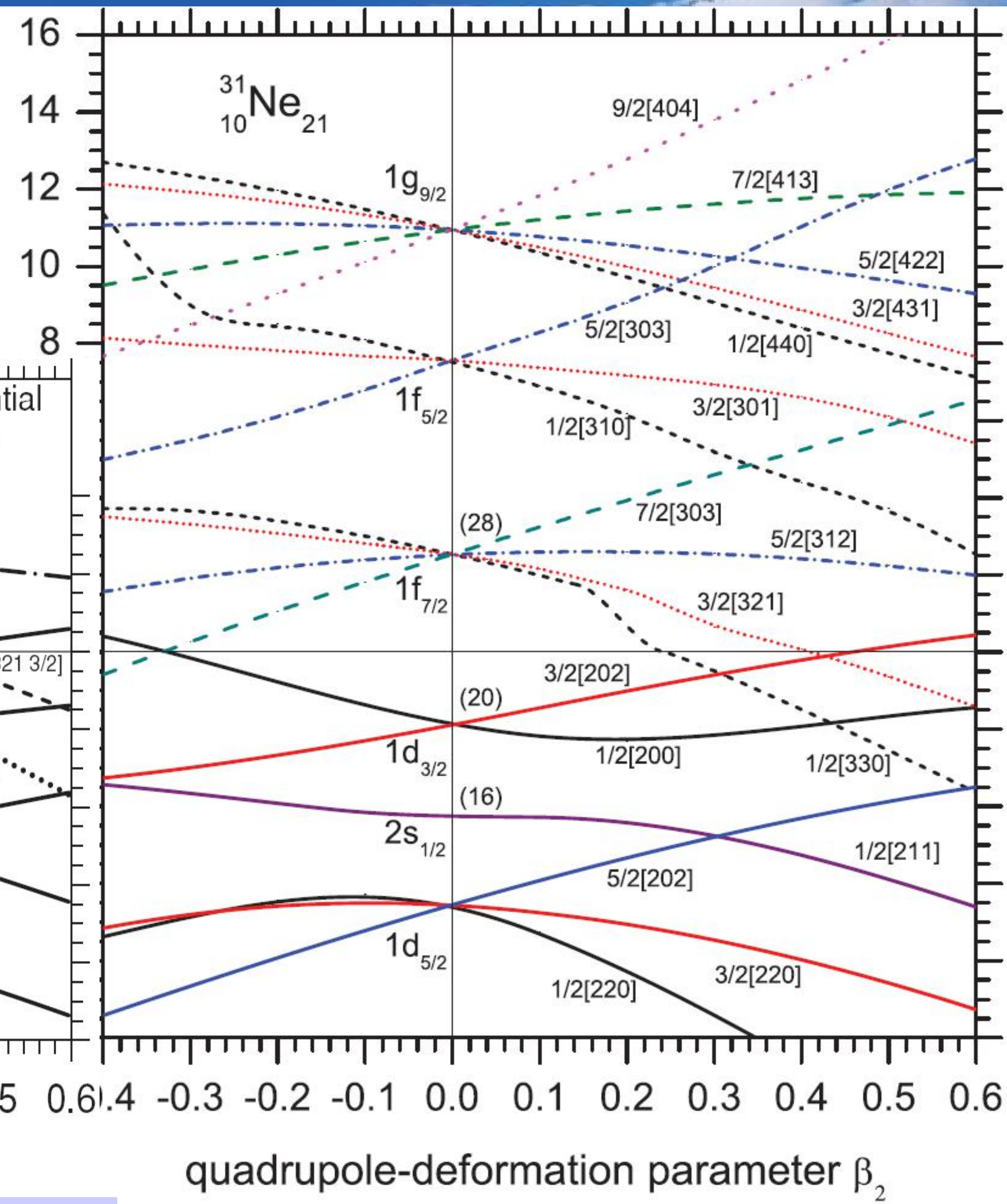

Hamamoto, PRC81,021304(R), (2010)

Liu, Guo, etal., PRC 86, 054312 (2012)

RMF-CSM for the resonances in deformed nuclei

The relativistic case

Shi, Liu, Niu, and Guo,
Phys.Rev.C 90, 034319 (2014).

$$H_\theta \psi_\theta(\vec{r}) = \varepsilon_\theta \psi_\theta(\vec{r})$$

The complex scaled Hamiltonian

$$H_\theta(\vec{r}) = \begin{pmatrix} A_\theta(\vec{r}) & B_\theta(\vec{r}) \\ B_\theta(\vec{r}) & C_\theta(\vec{r}) \end{pmatrix}$$

$$A_\theta(\vec{r}) = M + V(\vec{r}e^{i\theta}) + S(\vec{r}e^{i\theta}),$$

$$C_\theta(\vec{r}) = -M + V(\vec{r}e^{i\theta}) - S(\vec{r}e^{i\theta})$$

$$B_\theta(\vec{r}) = \begin{pmatrix} B_{11} & B_{12} \\ B_{21} & B_{22} \end{pmatrix}$$

$$B_{11} = -ie^{-i\theta}\left(\cos\vartheta\frac{\partial}{\partial r} - \frac{\sin\vartheta}{r}\frac{\partial}{\partial\vartheta}\right),$$

$$B_{12} = -ie^{-i\theta}e^{-i\varphi}\left(\sin\vartheta\frac{\partial}{\partial r} + \frac{\cos\vartheta}{r}\frac{\partial}{\partial\vartheta} - \frac{1}{r\sin\vartheta}i\frac{\partial}{\partial\varphi}\right)$$

$$B_{21} = -ie^{-i\theta}e^{i\varphi}\left(\sin\vartheta\frac{\partial}{\partial r} + \frac{\cos\vartheta}{r}\frac{\partial}{\partial\vartheta} + \frac{1}{r\sin\vartheta}i\frac{\partial}{\partial\varphi}\right),$$

$$B_{22} = ie^{-i\theta}\left(\cos\vartheta\frac{\partial}{\partial r} - \frac{\sin\vartheta}{r}\frac{\partial}{\partial\vartheta}\right).$$

$$f_\theta(\vec{r}) = \sum^{\alpha_{\max}} f_\alpha(\theta)\Phi_\alpha(\vec{r},s)$$

$$g_\theta(\vec{r}) = \sum_{\tilde{\alpha}=1}^{\tilde{\alpha}_{\max}} g_{\tilde{\alpha}}(\theta)\Phi_{\tilde{\alpha}}(\vec{r},s)$$

$$\Phi_\alpha(\vec{r},s) = R_{nl}(r)Y_{lm}(\vartheta,\varphi)\chi_{m_s}(s)$$

The Dirac matrix eq.

$$\sum^{\alpha_{\max}} A_{\alpha'\alpha} f_\alpha + \sum^{\tilde{\alpha}_{\max}} B_{\alpha'\tilde{\alpha}} g_{\tilde{\alpha}} = \varepsilon f_{\alpha'}$$

$$\sum_{\alpha=1}^{\alpha_{\max}} B_{\tilde{\alpha}'\alpha} f_\alpha + \sum_{\tilde{\alpha}=1}^{\tilde{\alpha}_{\max}} C_{\tilde{\alpha}'\tilde{\alpha}} g_{\tilde{\alpha}} = \varepsilon g_{\tilde{\alpha}'}$$

The single particle states in ^{31}Ne

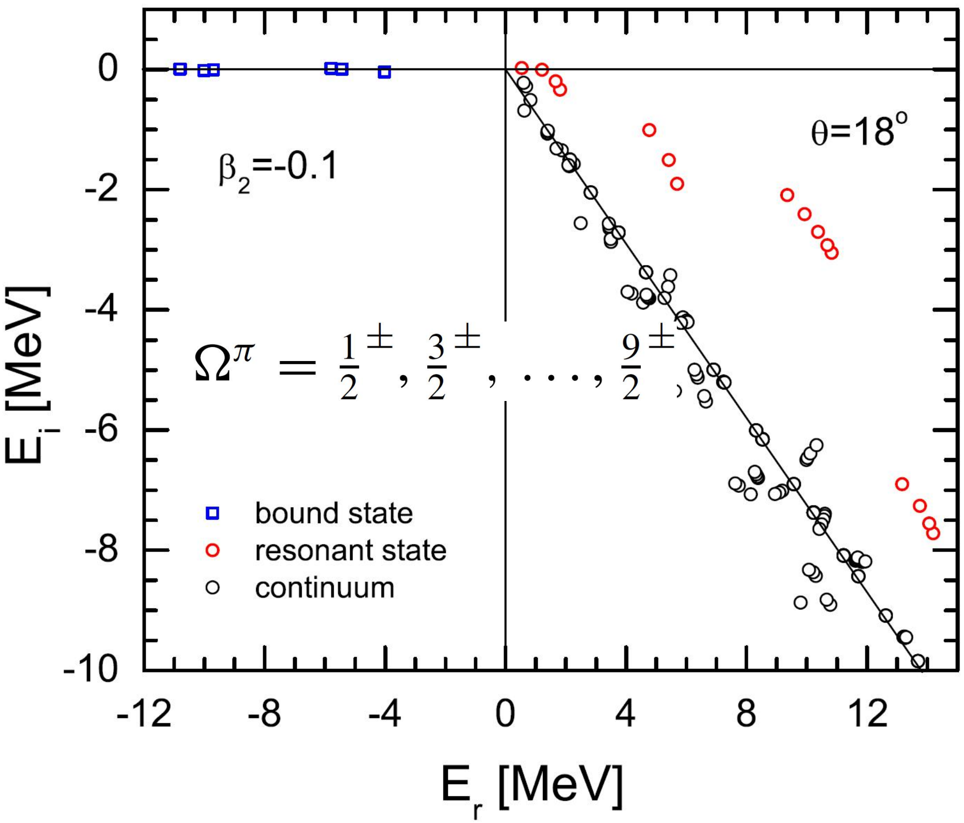

Shi, Liu, Niu, and Guo,
Phys.Rev.C 90, 034319 (2014).

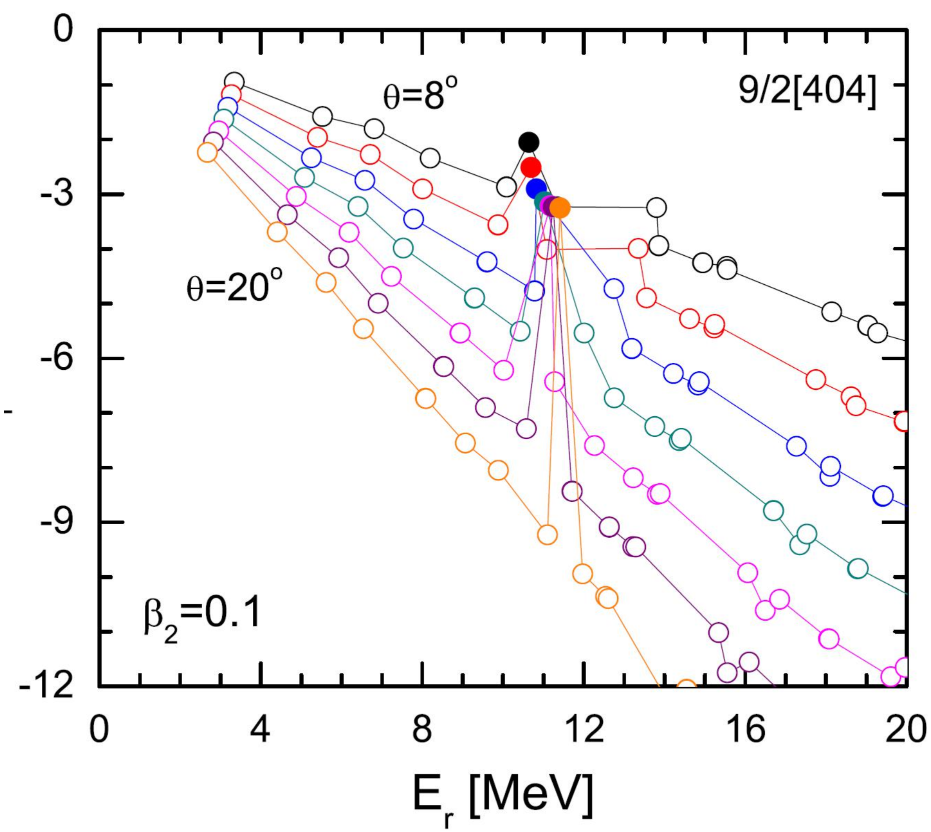

- The bound states, resonant states, and continuum are, respectively, labeled as open squares, color open circles, and open circles.
- The solid line rotating with θ marks the position of the continuum spectra.

The eigenvalues of H_θ with the deformation parameter β_2 = 0.0, 0.1, 0.2, and 0.3 in the calculations

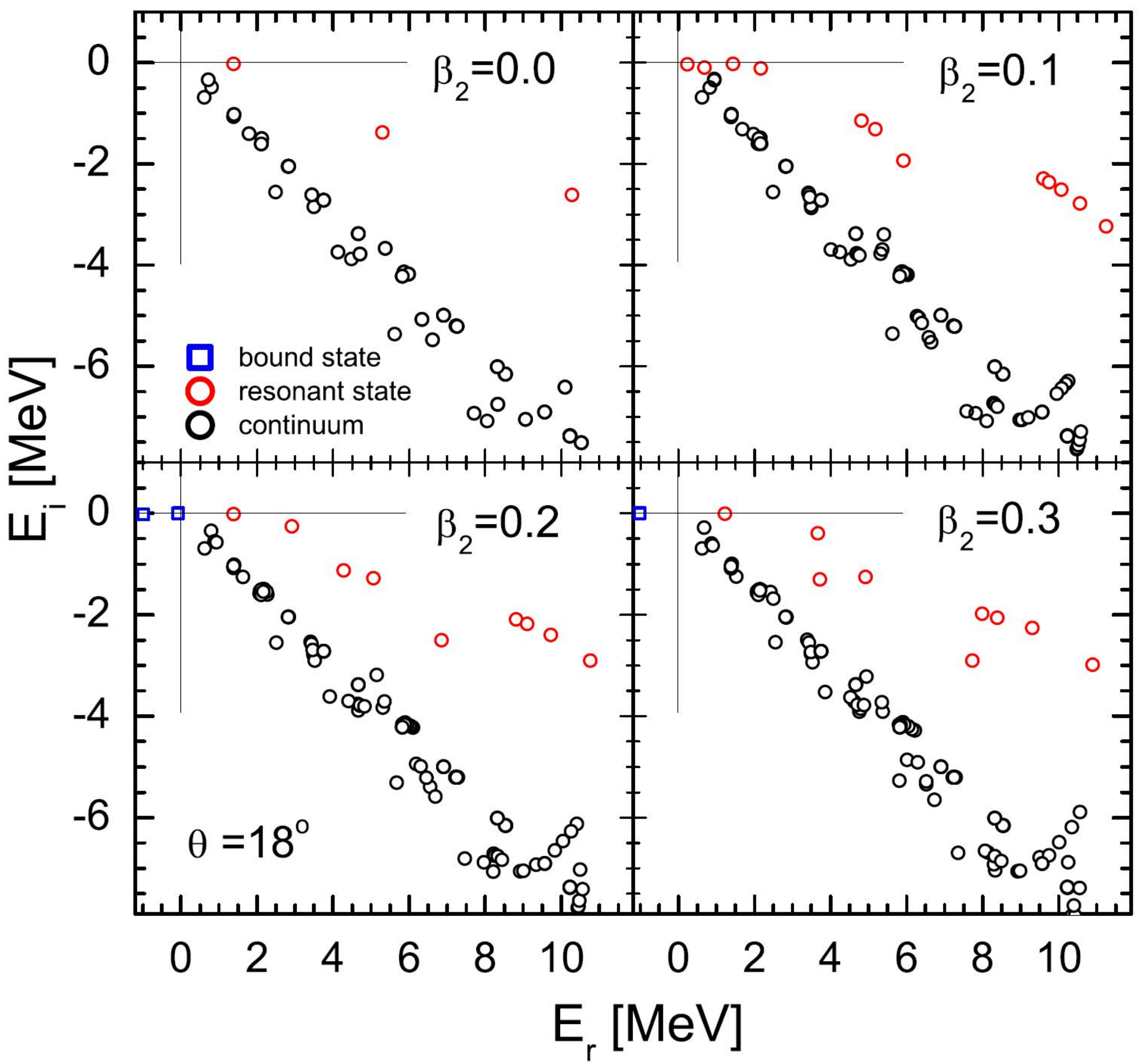

The single-particle levels in ^{31}Ne in the RMF-CSM calculations

Shi, Liu, Niu, and Guo, Phys.Rev.C 90, 034319 (2014).

- The single-particle levels for the bound states are in agreement with those obtained in the non-relativistic calculation with spin-orbit coupling by hand.
- The single-particle levels for the resonant states are also in agreement with those obtained by the coupling-channel method

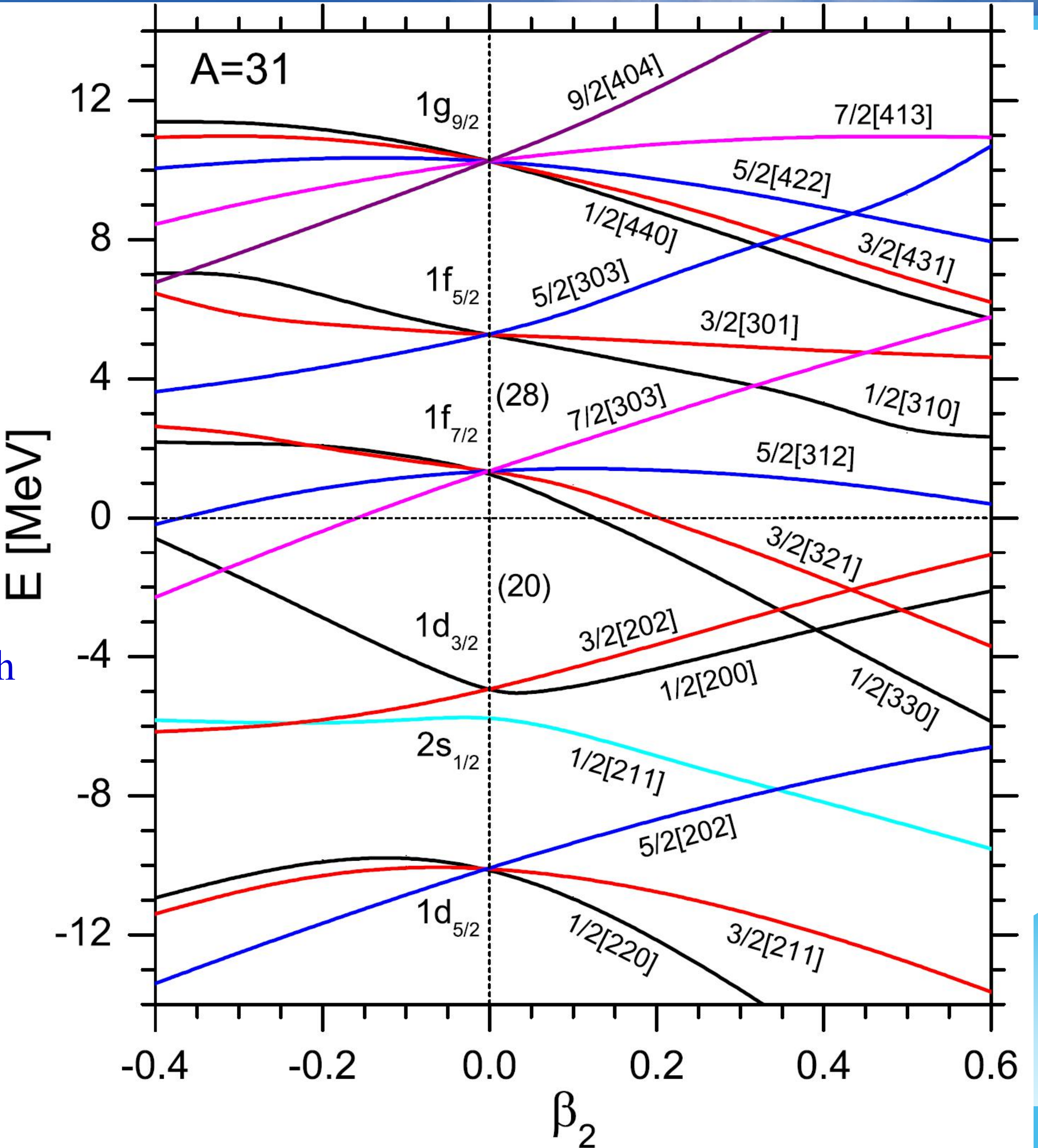

The RMF-CGF formalism

To make it more intuitive and easier to determine resonance parameters, we have developed a relativistic complex-scaled Green function method.

$$H = \boldsymbol{\alpha} \cdot \boldsymbol{p} + \beta(M + S) + V$$

$$H_\theta = U(\theta) H U(\theta)^{-1},$$

$$H_\theta \psi_\theta = \varepsilon_\theta \psi_\theta,$$

Shi, Guo, Liu, Niu, Heng, Phys.Rev.C 92, 054313 (2015).

Complex scaled Green function is defined as

$$G^\theta(\varepsilon, \mathbf{r}, \mathbf{r}') = \langle \mathbf{r} | \frac{1}{\varepsilon - H_\theta} | \mathbf{r}' \rangle$$

The level density of H_θ is defined as

$$\rho_\theta(\varepsilon) = -\frac{1}{\pi} \mathrm{Im} \int d\mathbf{r} \, \langle \mathbf{r} | \frac{1}{\varepsilon - H_\theta} | \mathbf{r} \rangle$$

The RMF-CGF formalism

The extended completeness relation:

$$\sum_b^{N_b} |\psi_b^\theta\rangle\langle\tilde{\psi}_b^\theta| + \sum_r^{N_r} |\psi_r^\theta\rangle\langle\tilde{\psi}_r^\theta| + \int d\varepsilon_c^\theta |\psi_c^\theta\rangle\langle\tilde{\psi}_c^\theta| = 1,$$

By using the extended completeness relation, the level density becomes

$$\rho_\theta(\varepsilon) = -\frac{1}{\pi}\mathrm{Im}\int d\mathbf{r}\left[\sum_b^{N_b} \frac{\psi_b^\theta(\mathbf{r})\tilde{\psi}_b^{\theta *}(\mathbf{r})}{\varepsilon - \varepsilon_b} + \sum_r^{N_r} \frac{\psi_r^\theta(\mathbf{r})\tilde{\psi}_r^{\theta *}(\mathbf{r})}{\varepsilon - \varepsilon_r^\theta} + \int d\varepsilon_c^\theta \frac{\psi_c^\theta(\mathbf{r})\tilde{\psi}_c^{\theta *}(\mathbf{r})}{\varepsilon - \varepsilon_c^\theta}\right],$$

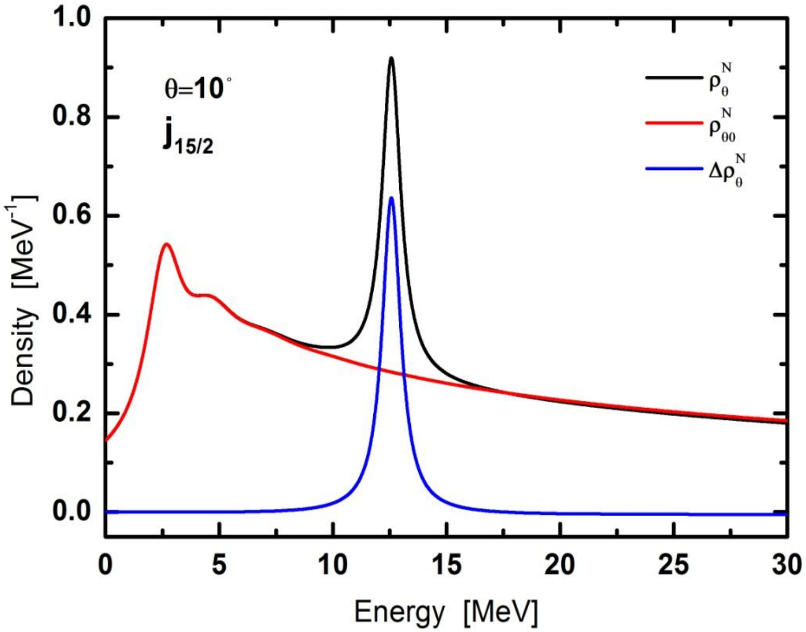

- The resonant state corresponds to the peak appearing in the density of energy level ρ(E).
- When θ is small, there exists oscillating phenomenon in ρ(E). With the increasing of θ, the oscillating disappears.
- When the background is removed off, the peak is more clear, which can be used accurately to determine the resonant parameters.

Shi, Guo, Liu, Niu, Heng, Phys.Rev.C 92, 054313 (2015).

The continuum level density is obtained by subtracting the background as

$$
\begin{aligned}
\Delta\rho(\varepsilon) &= \rho_\theta^N(\varepsilon) - \rho_\theta^{0N}(\varepsilon) \\
&= \sum_b^{N_b} \delta(\varepsilon - \varepsilon_b) + \frac{1}{\pi}\sum_r^{N_r} \frac{\Gamma_r/2}{(\varepsilon - E_r)^2 + \Gamma_r^2/4} \\
&\quad + \frac{1}{\pi}\sum_c^{N-N_b-N_r} \frac{\varepsilon_c^I}{\left(\varepsilon - \varepsilon_c^R\right)^2 + \varepsilon_c^{I^2}} \\
&\quad - \frac{1}{\pi}\sum_c^{N} \frac{\varepsilon_c^{0I}}{\left(\varepsilon - \varepsilon_c^{0R}\right)^2 + \varepsilon_c^{0I^2}},
\end{aligned}
$$

The resonant state corresponds to the peak appearing in the density of energy level ρ (ε).

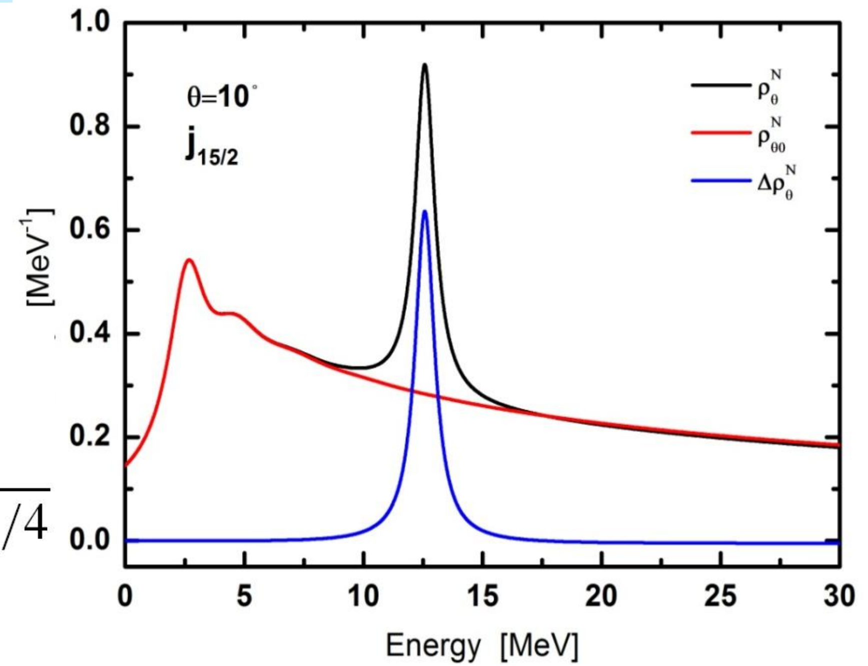

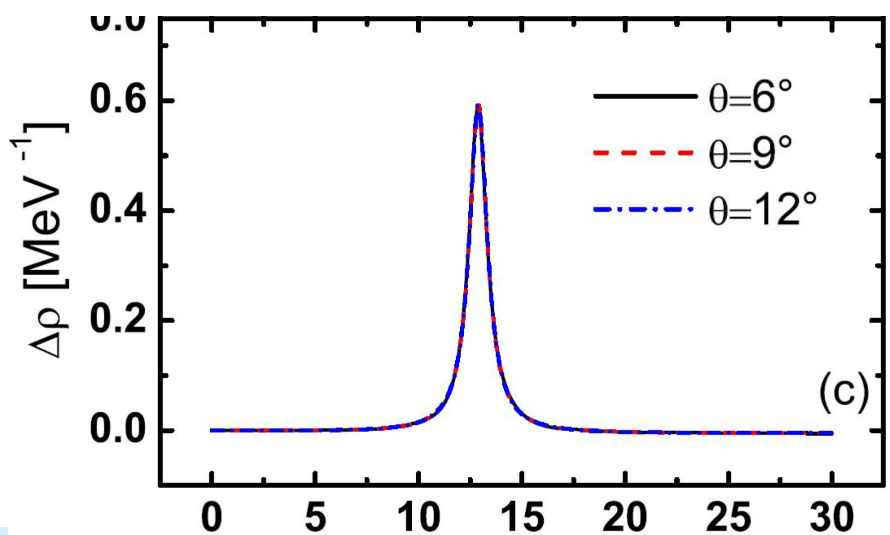

PHYSICAL REVIEW C **92**, 054313 (2015)

Relativistic extension of the complex scaled Green function method

Min Shi, Jian-You Guo,* Quan Liu, Zhong-Ming Niu, and Tai-Hua Heng
School of Physics and Material Science, Anhui University, Hefei 230601, People's Republic of China
(Received 29 August 2015; revised manuscript received 23 October 2015; published 17 November 2015)

PHYSICAL REVIEW C **94**, 024302 (2016)

Probing resonances in deformed nuclei by using the complex-scaled Green's function method

Xin-Xing Shi, Min Shi, Zhong-Ming Niu, Tai-Hua Heng, and Jian-You Guo*
School of Physics and Materials Science, Anhui University, Hefei 230601, People's Republic of China
(Received 29 May 2016; published 1 August 2016)

Resonance plays a key role in the formation of many physical phenomena. The complex-scaled Green's function method provides a powerful tool for exploring resonance. In this paper, we combine this method with the theory describing deformed nuclei with the formalism presented. Taking ^{45}S as an example, we elaborate numerical details and demonstrate how to determine the resonance parameters. The results are compared with those obtained by the complex scaling method and the coupled-channel method and satisfactory agreement is obtained. In particular, the present scheme focuses on the advantages of the complex scaling method and the Green's function method and is more suitable for the exploration of resonance.

There exist some shortcomings in CSM

- Need to introduce a unphysical parameter: complex rotation angle θ.
- CSM is only applicable to the dilation analytic potential.
- There is a singularity in the mean-field of nucleon movement when θ is very large. CSM is not applicable to very broad resonance in nuclei.

Complex momentum representation (CMR)

RMF-CMR method for spherical nuclei

Dirac equation in momentum representation

Liu, shi, Guo, etal., PRL117, 062502 (2016).

$$\int d\vec{k}' \langle \vec{k}|H|\vec{k}'\rangle \psi(\vec{k}') = \varepsilon \psi(\vec{k})$$

where $H = \vec{\alpha}\cdot\vec{p} + \beta(M+S) + V$

By assuming

$$\psi(\vec{k}) = \begin{pmatrix} f(k)\phi_{ljm_j}(\Omega_k) \\ g(k)\phi_{\tilde{l}jm_j}(\Omega_k) \end{pmatrix},$$

Dirac equation becomes

$$\begin{cases} Mf(k) - kg(k) + \int k'^2 dk' V_+(k,k') f(k') = \varepsilon f(k), \\ -kf(k) - Mg(k) + \int k'^2 dk' V_-(k,k') g(k') = \varepsilon g(k). \end{cases}$$

Here

$$V_+(k,k') = \frac{2}{\pi}\int r^2 dr\,[V(r)+S(r)]\, j_l(k'r)\, j_l(kr),$$

$$V_-(k,k') = \frac{2}{\pi}\int r^2 dr\,[V(r)-S(r)]\, j_{\tilde{l}}(k'r)\, j_{\tilde{l}}(kr).$$

Integral path in momentum space

Liu, shi, Guo, etal., PRL117, 062502 (2016).

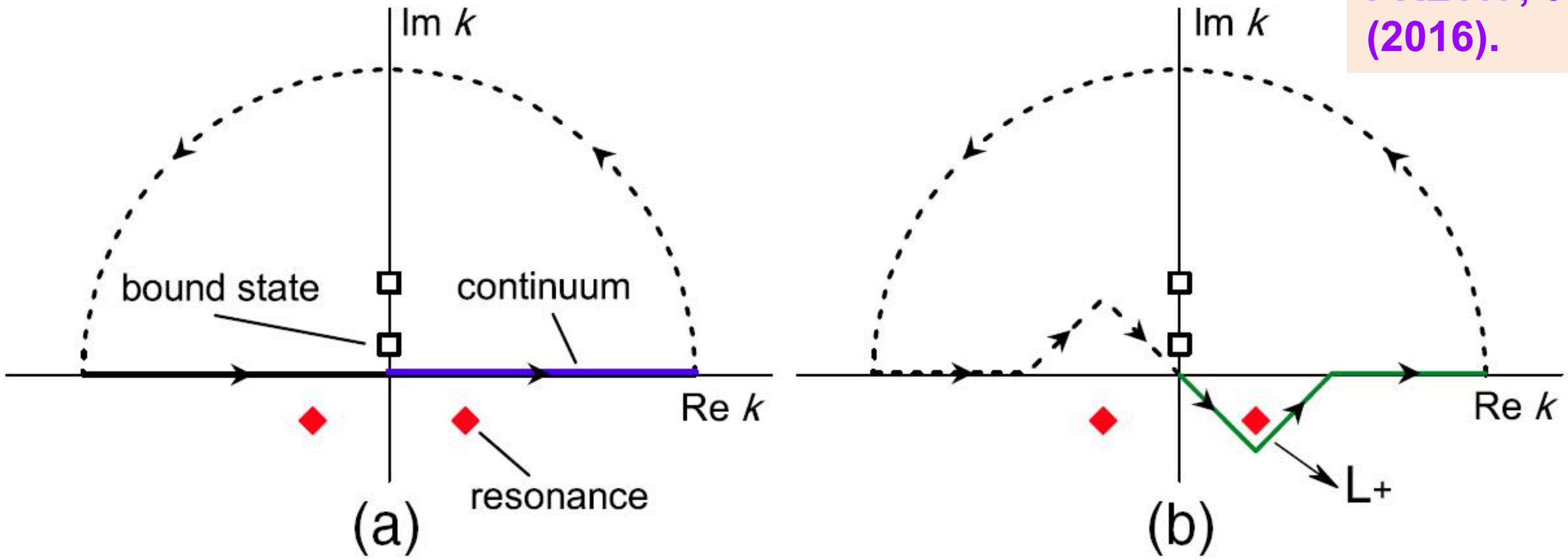

Wavefunction in coordinate space

$$\psi(\vec{r}) = \begin{pmatrix} f(r)\phi_{ljm_j}(\Omega_r) \\ g(r)\phi_{\tilde{l}jm_j}(\Omega_r) \end{pmatrix}$$

with

$$\begin{cases} f(r) = i^l \sqrt{\frac{2}{\pi}} \int k^2 dk\, j_l(kr)\, f(k), \\ g(r) = i^{\tilde{l}} \sqrt{\frac{2}{\pi}} \int k^2 dk\, j_{\tilde{l}}(kr)\, g(k). \end{cases}$$

Solution of Dirac equation in CMR

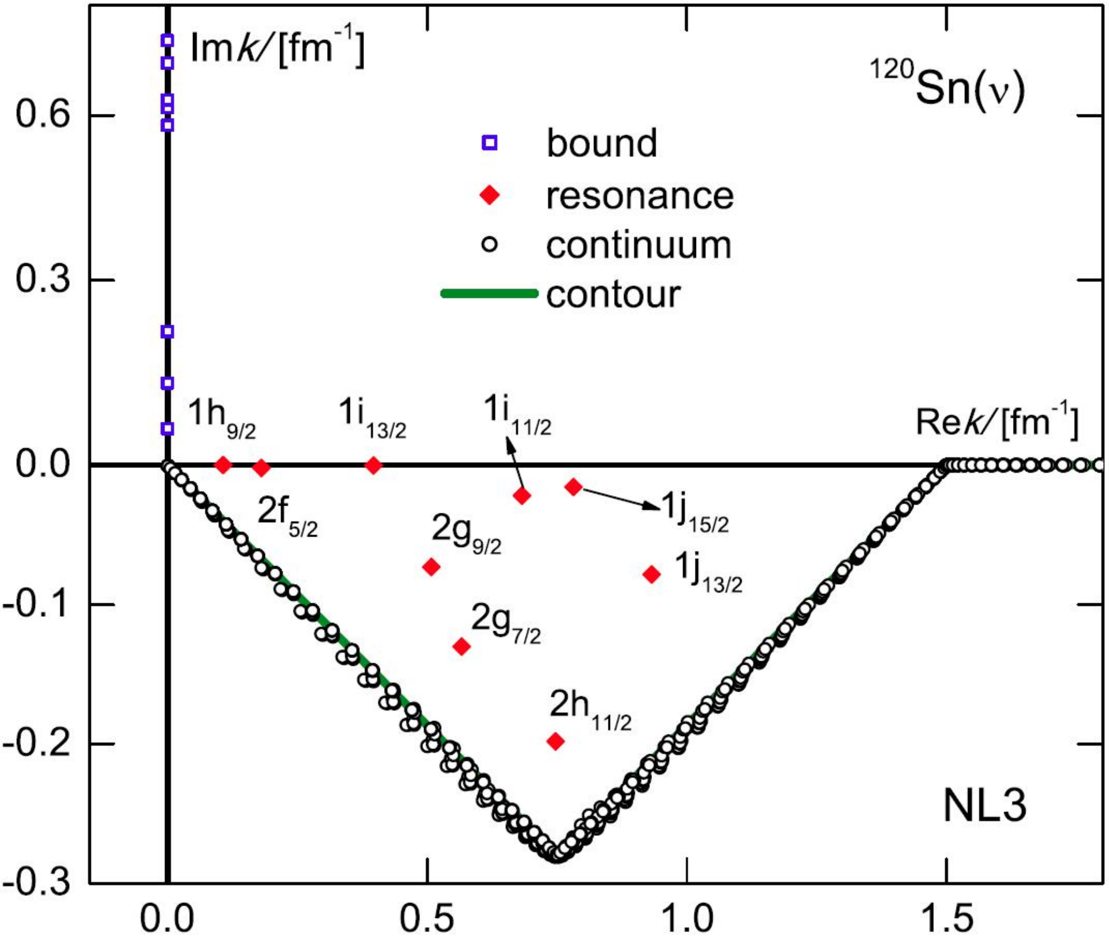

CMR advantages:

- CMR describes the bound states, resonant states, and continuum on an equal footing
- The bound states populate on the imaginary axis in the complex momentum plane
- The resonant states locate at the fourth quadrant
- The continuum follows the contour
- The bound states and resonant states are independent on the contour.

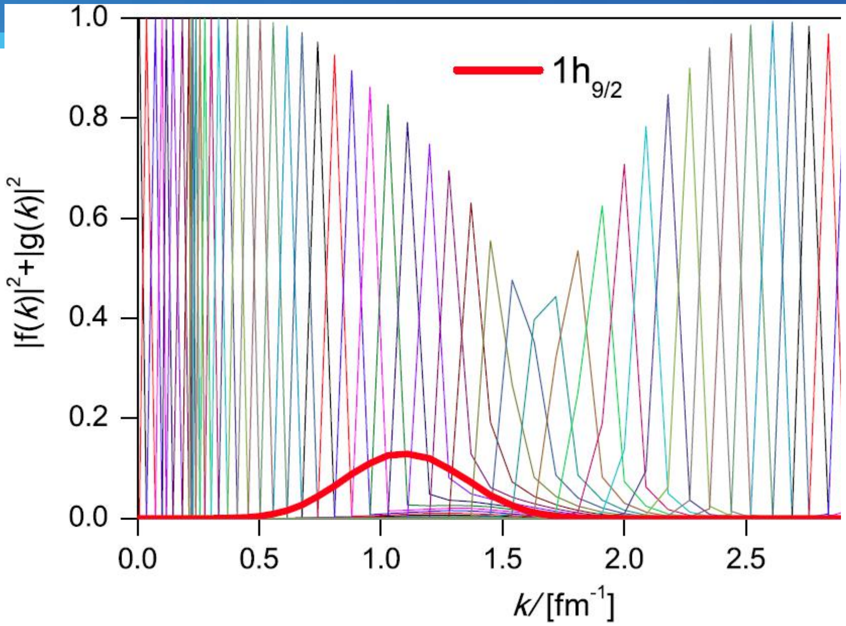

TABLE II. Energies and widths of single neutron resonant states for ^{120}Sn in the RMF-CMR calculations in comparison with the RMF-CSM, RMF-RSM, and RMF-ACCC calculations. Data are in units of MeV.

nl_j	RMF-CMR E_r, Γ	RMF-CSM E_r, Γ	RMF-RSM E_r, Γ	RMF-ACCC E_r, Γ
$2f_{5/2}$	0.678,0.031	0.670,0.020	0.674,0.030	0.685,0.023
$1i_{13/2}$	3.267,0.004	3.266,0.004	3.266,0.004	3.262,0.004
$1i_{11/2}$	9.607,1.219	9.597,1.212	9.559,1.205	9.60,1.11
$1j_{15/2}$	12.584,0.993	12.577,0.992	12.564,0.973	12.60,0.90

Wavefunction for the resonant state is expanded much wider than the free states which agrees the Heisenberg uncertainty principle: a less well defined momentum corresponds to a more well-defined position for bound and resonant states.

PRL **117,** 062502 (2016) PHYSICAL REVIEW LETTERS week ending 5 AUGUST 2016

Probing Resonances of the Dirac Equation with Complex Momentum Representation

Niu Li (李牛),[1] Min Shi (仕敏),[1] Jian-You Guo (郭建友),[1,*] Zhong-Ming Niu (牛中明),[1,†] and Haozhao Liang (梁豪兆)[2,3,‡]
[1]*School of Physics and Materials Science, Anhui University, Hefei 230601, People's Republic of China*
[2]*RIKEN Nishina Center, Wako 351-0198, Japan*
[3]*Department of Physics, Graduate School of Science, The University of Tokyo, Tokyo 113-0033, Japan*

RMF-CMR for deformed nuclei

The Dirac spinor is expanded as

$$\psi\left(\vec{k}\right) = \psi_{m_j}\left(\vec{k}\right) = \sum_{l'j'}\begin{pmatrix} f^{l'j'}(k)\phi_{l'j'm_j}(\Omega_k) \\ g^{l'j'}(k)\phi_{\tilde{l}'j'm_j}(\Omega_k) \end{pmatrix}, \left(\tilde{l}' = 2j' - l'\right)$$

Dirac equation in momentum representation

$$\begin{cases} Mf^{lj}(k) - kg^{lj}(k) + \sum\limits_{l'j'}\int k'^2 dk' V^+(l', j', p, q, l, j, m_j, k, k') f^{l'j'}(k') = \varepsilon f^{lj}(k), \\ -kf^{lj}(k) - Mg^{lj}(k) + \sum\limits_{l'j'}\int k'^2 dk' V^-(\tilde{l}', j', p, q, \tilde{l}, j, m_j, k, k') g^{l'j'}(k') = \varepsilon g^{lj}(k) \end{cases}$$

where

$$\begin{aligned} & V^+(l', j', p, q, l, j, m_j, k, k') \\ = \quad & (-)^l i^{l+l'}\frac{2}{\pi}\int r^2 dr\,[V(r) + S(r)]\, j_l(kr)\, j_{l'}(k'r) \sum_{m_s} \langle lm|\, Y_{pq}(\Omega_r)\left|l'm'\right\rangle \langle lm\tfrac{1}{2}m_s|jm_j\rangle\langle l'm'\tfrac{1}{2}m_s|j'm_j\rangle, \\ & V^-(\tilde{l}', j', p, q, \tilde{l}, j, m_j, k, k') \\ = \quad & (-)^{\tilde{l}} i^{\tilde{l}+\tilde{l}'}\frac{2}{\pi}\int r^2 dr\,[V(r) - S(r)]\, j_{\tilde{l}}(kr)\, j_{\tilde{l}'}(k'r) \sum_{m_s} \left\langle \tilde{l}\tilde{m}\right| Y_{pq}(\Omega_r)\left|\tilde{l}'\tilde{m}'\right\rangle \langle \tilde{l}\tilde{m}\tfrac{1}{2}m_s|jm_j\rangle\langle \tilde{l}'\tilde{m}'\tfrac{1}{2}m_s|j'm_j\rangle. \end{aligned}$$

Understanding of deformation halo in ^{37}Mg with RMF-CMR

The path independence of the calculation result for the single-particle spectra in ^{37}Mg

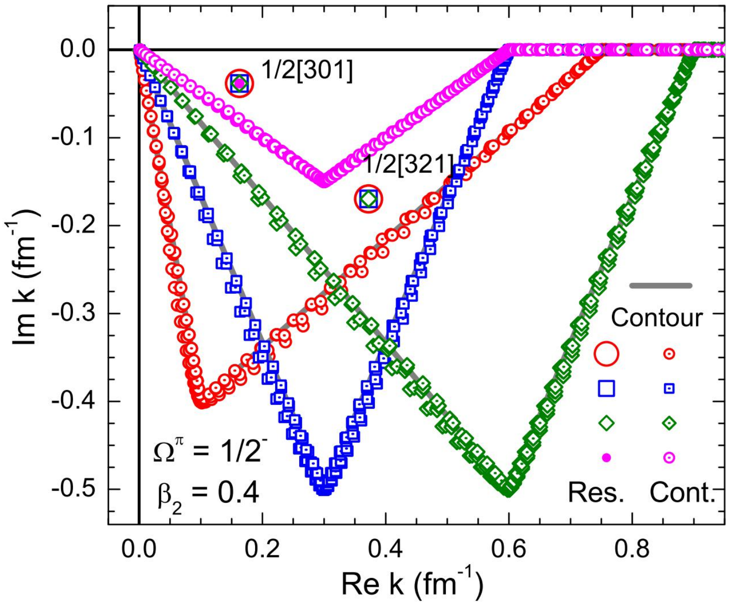

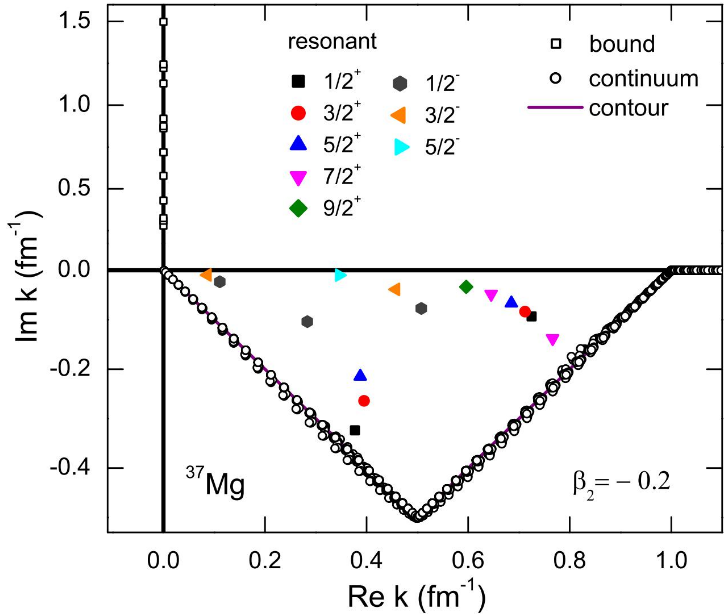

Fang etal, PRC 95, 024311 (2017)

Single-particle spectra in ^{37}Mg

Radial density distributions in the coordinate space for the bound states 1/2[110] and 1/2[310], and the resonant state 1/2[301] with $\beta_2 = 0.4$

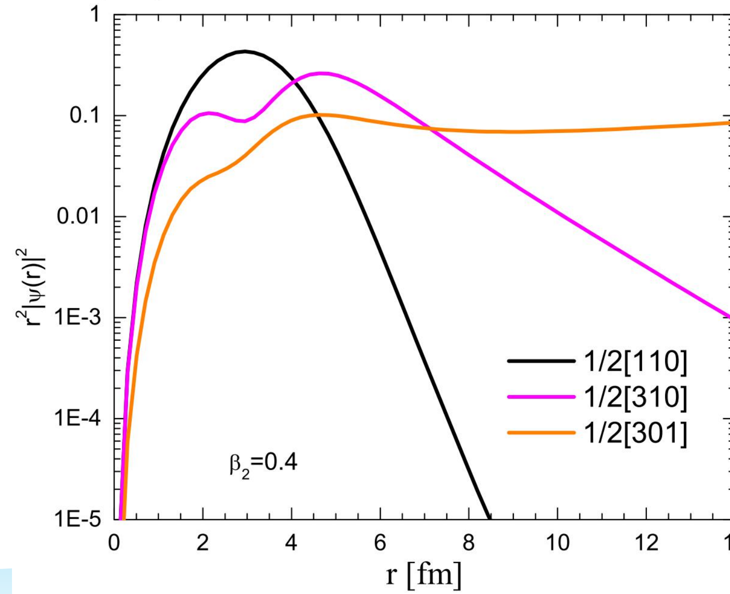

Explanation on halo in ^{31}Ne

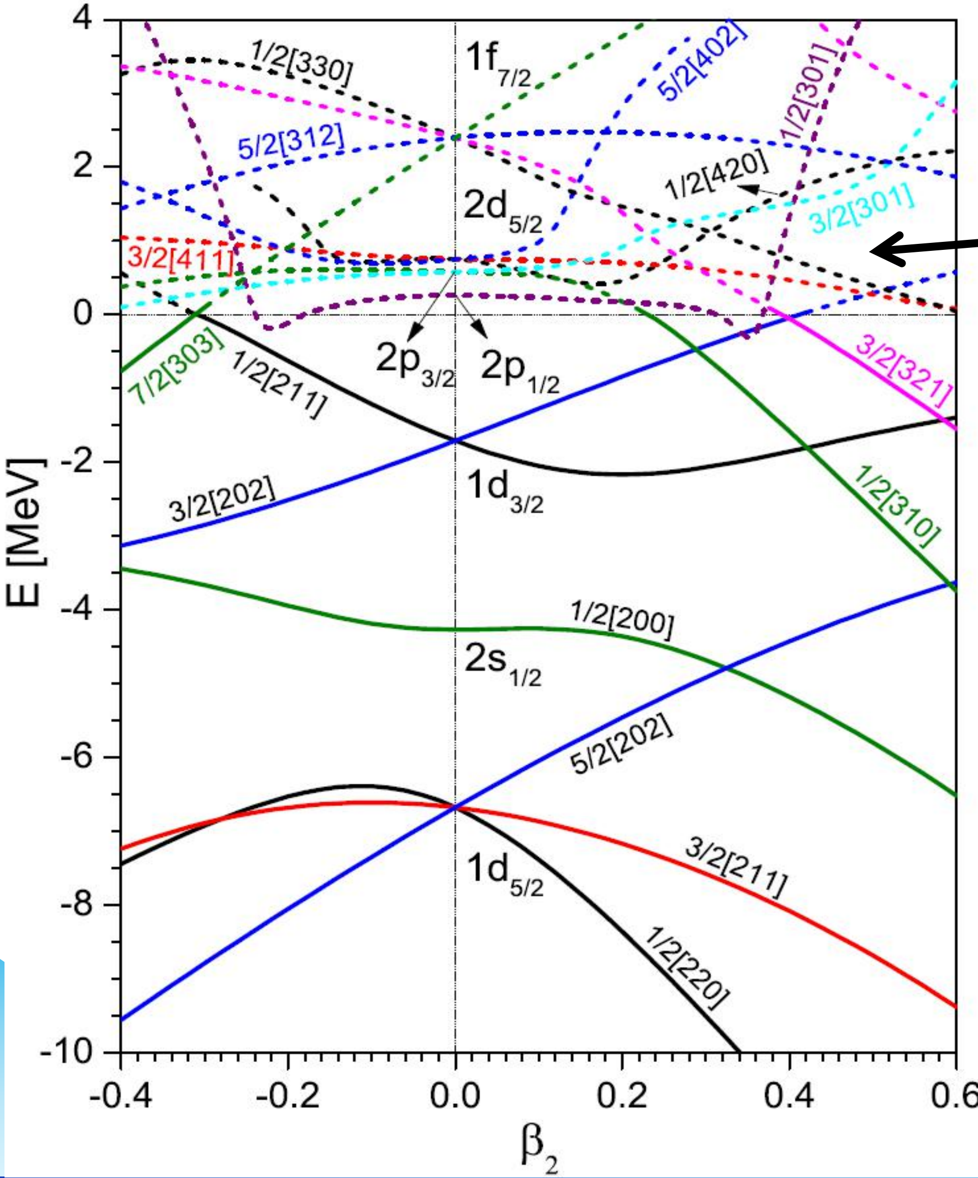

There appears the inversion in the levels for the resonant states

I.Hamamoto, PRC81, 021304(R) (2010).

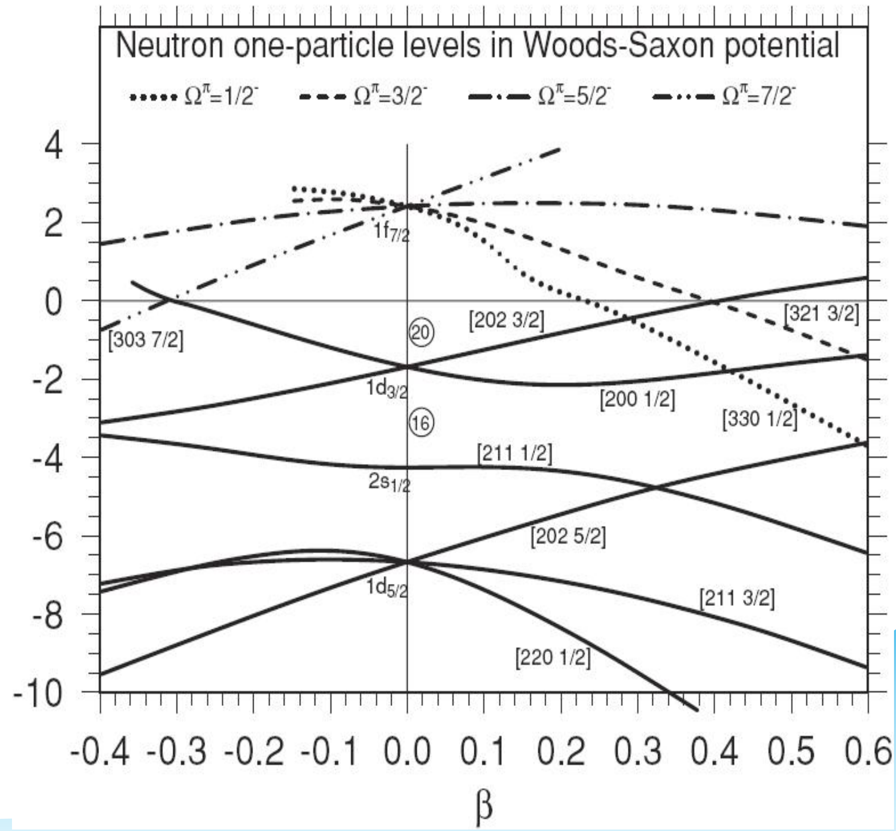

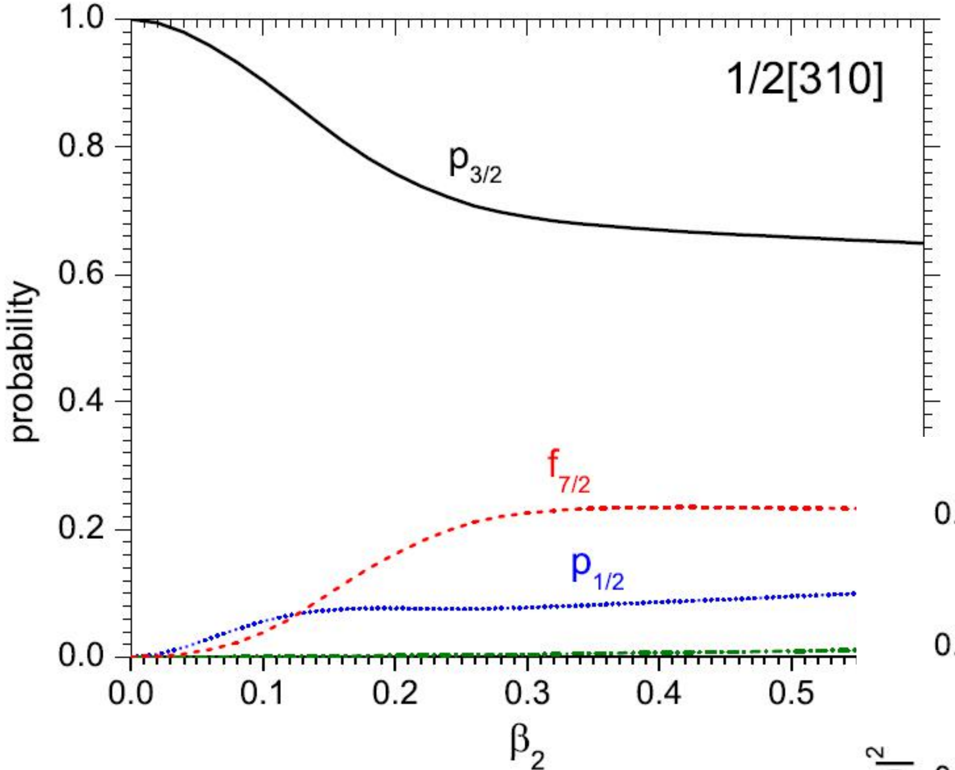

- Calculated probabilities of $p_{1/2}$, $p_{3/2}$, $f_{5/2}$, $f_{7/2}$, $h_{9/2}$, and $h_{11/2}$ components in the level 1/2[310]

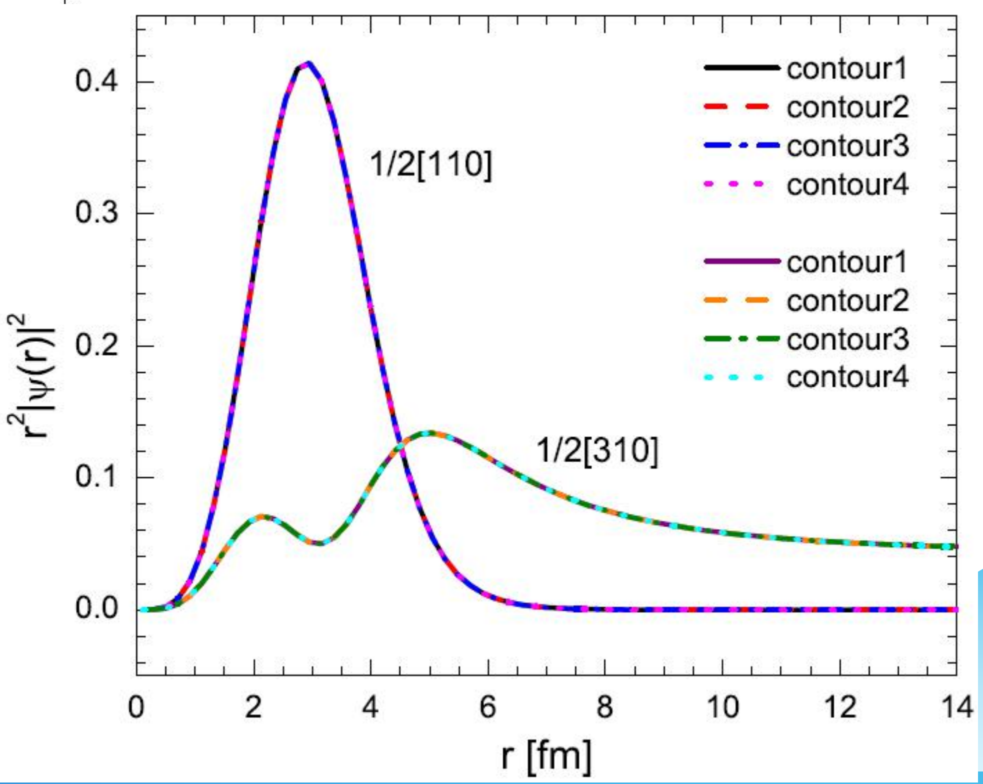

- Density distributions of resonant states with a long tail.

Explanation on halo in ^{19}C

Interpretation of halo in ^{19}C with complex momentum representation method

X.N.Cao, Q.Liu, J.Y.Guo, JPG 45, 085105 (2018)

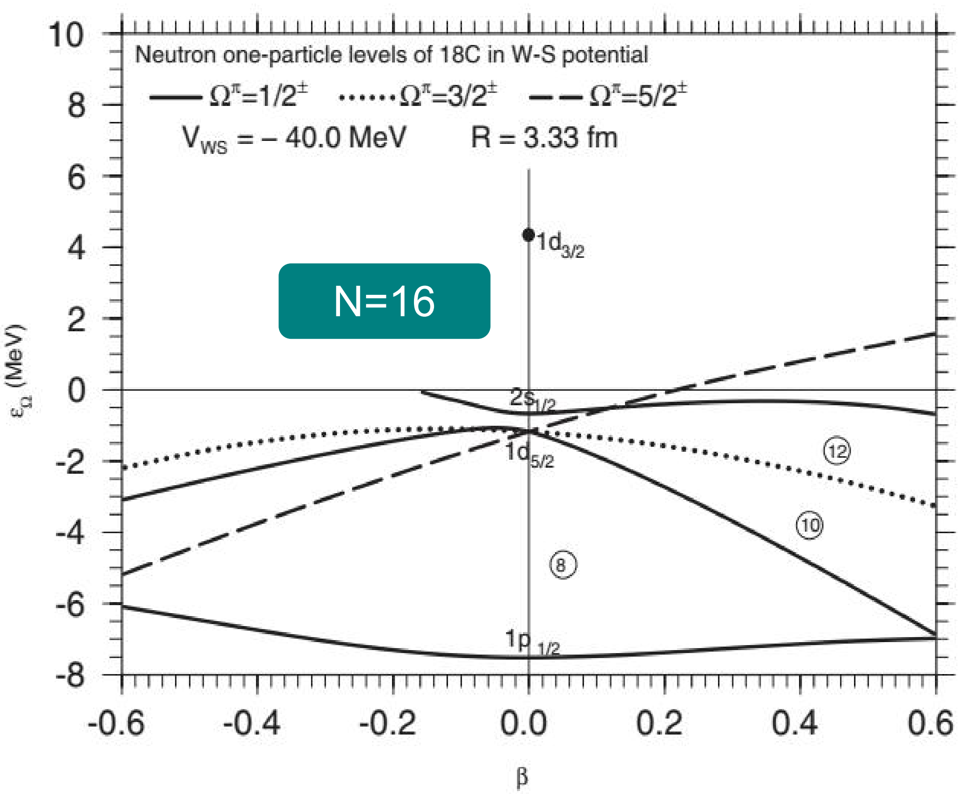

I. Hamamoto, PRC 85, 064329 (2012)

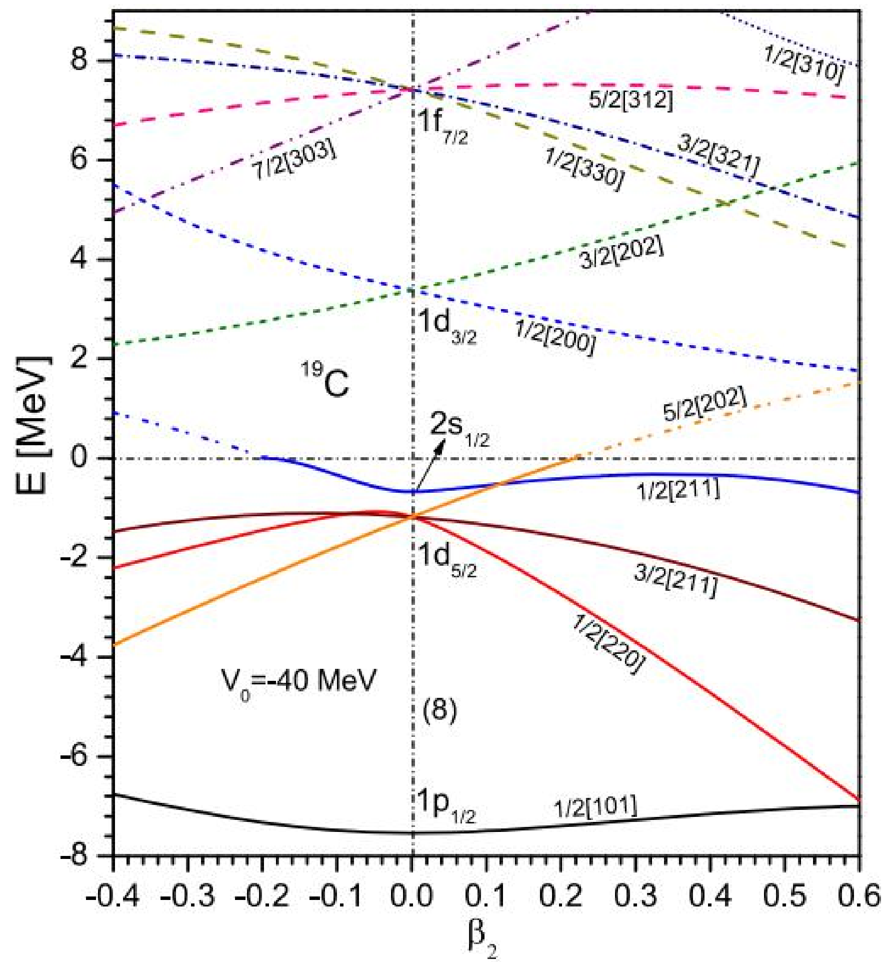

Interpretation of halo in ^{19}C with complex momentum representation method

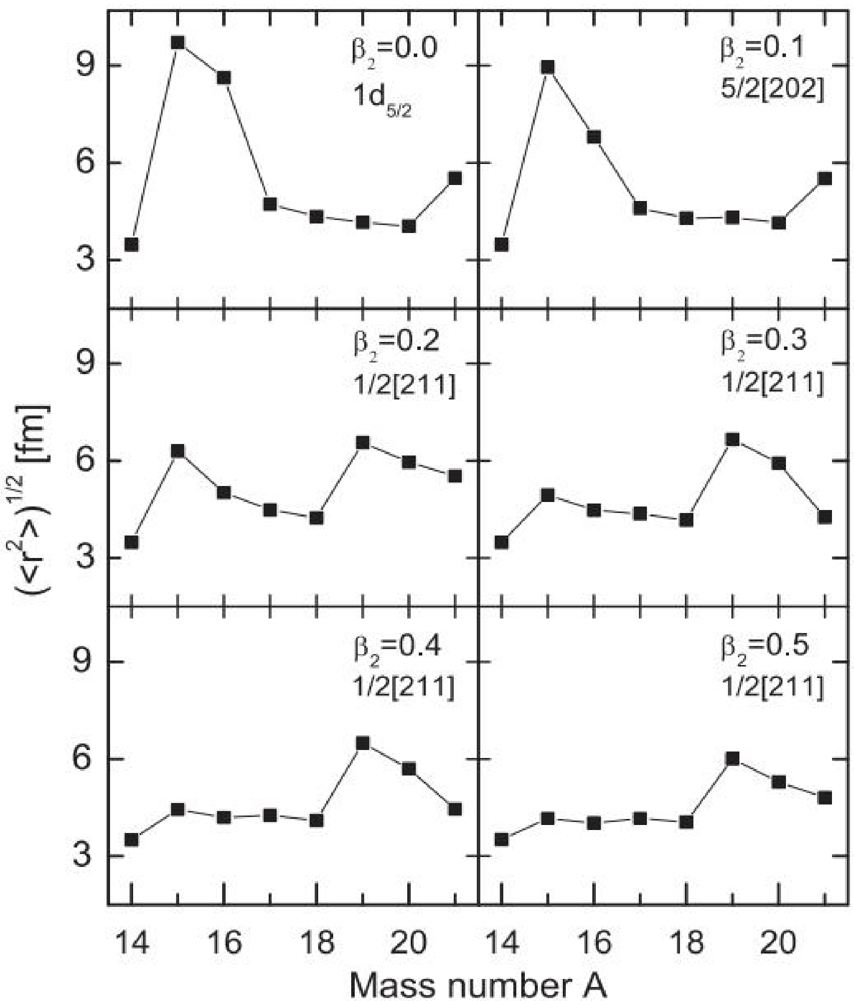

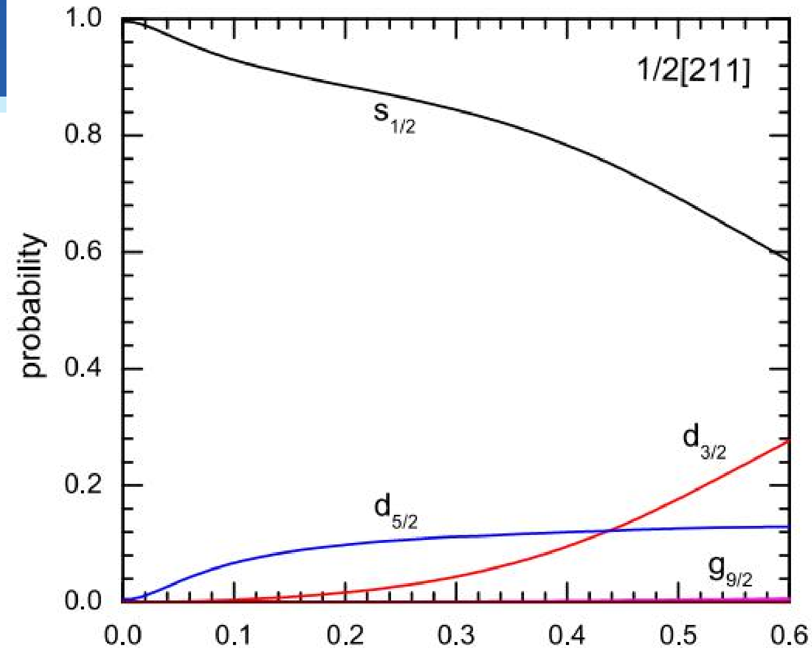

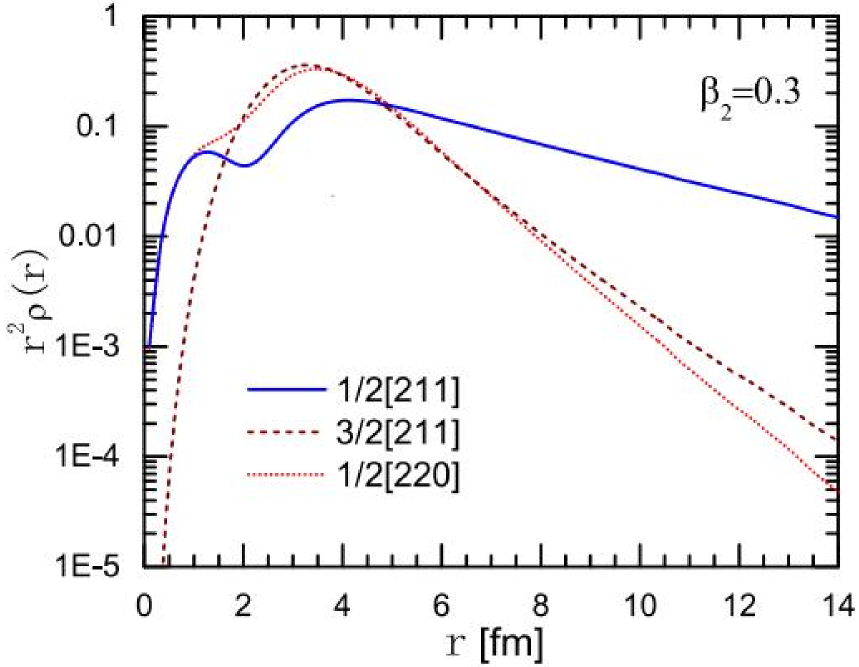

PHYSICAL REVIEW C **95**, 024311 (2017)

Probing resonances in the Dirac equation with quadrupole-deformed potentials with the complex momentum representation method

Zhi Fang,[1] Min Shi,[1,2] Jian-You Guo,[1,*] Zhong-Ming Niu,[1,3] Haozhao Liang,[2,3,4] and Shi-Sheng Zhang[5]
[1]*School of Physics and Materials Science, Anhui University, Hefei 230601, People's Republic of China*
[2]*RIKEN Nishina Center, Wako 351-0198, Japan*

PHYSICAL REVIEW C **95**, 064329 (2017)

Research on the halo in ^{31}Ne with the complex momentum representation method

Ya-Juan Tian, Quan Liu,[*] Tai-Hua Heng,[†] and Jian-You Guo[‡]
School of physics and materials science, Anhui University, Hefei 230601, People's Republic of China
(Received 14 April 2017; published 30 June 2017)

Interpretation of halo in ^{19}C with complex momentum representation method

Xue-Neng Cao, Quan Liu[1] and Jian-You Guo

IOP Publishing
J. Phys. G: Nucl. Part. Phys. **45** (2018) 085105 (15pp)

CMR for n-\alpha scattering

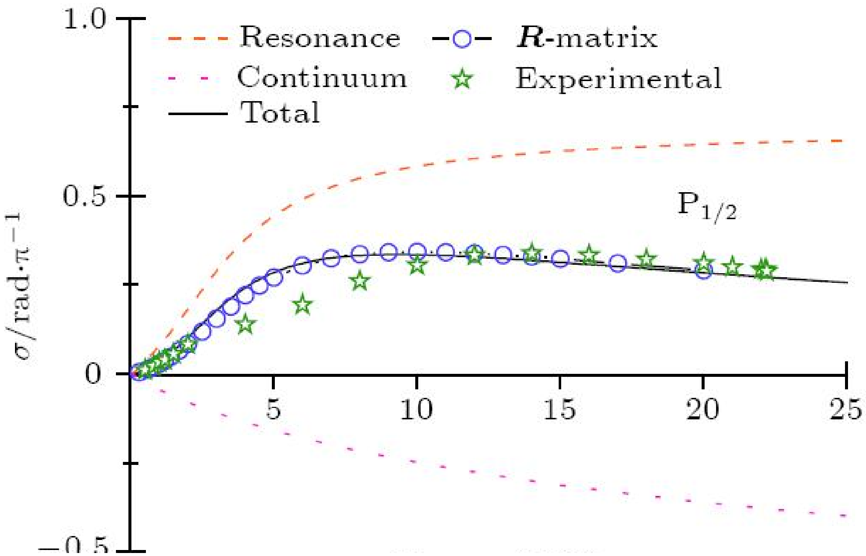

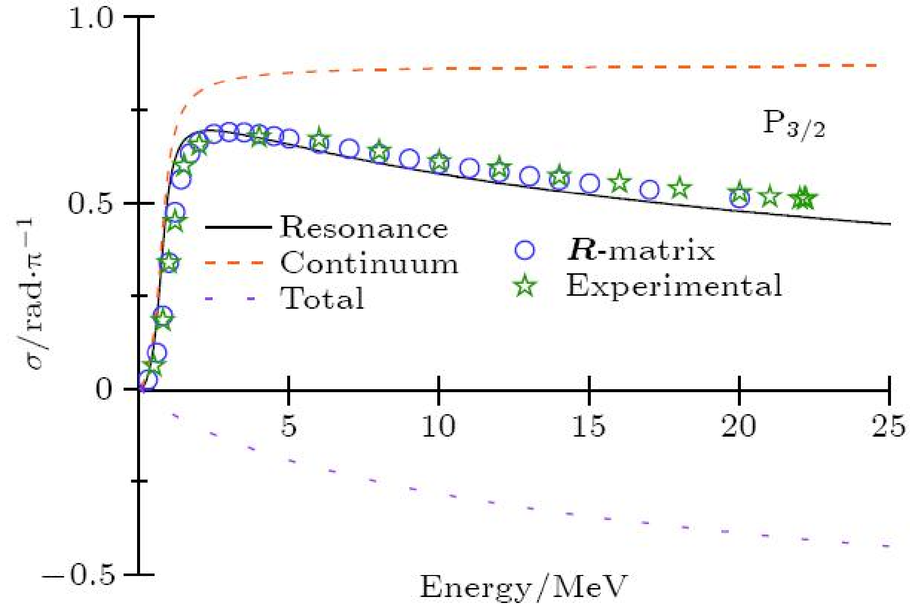

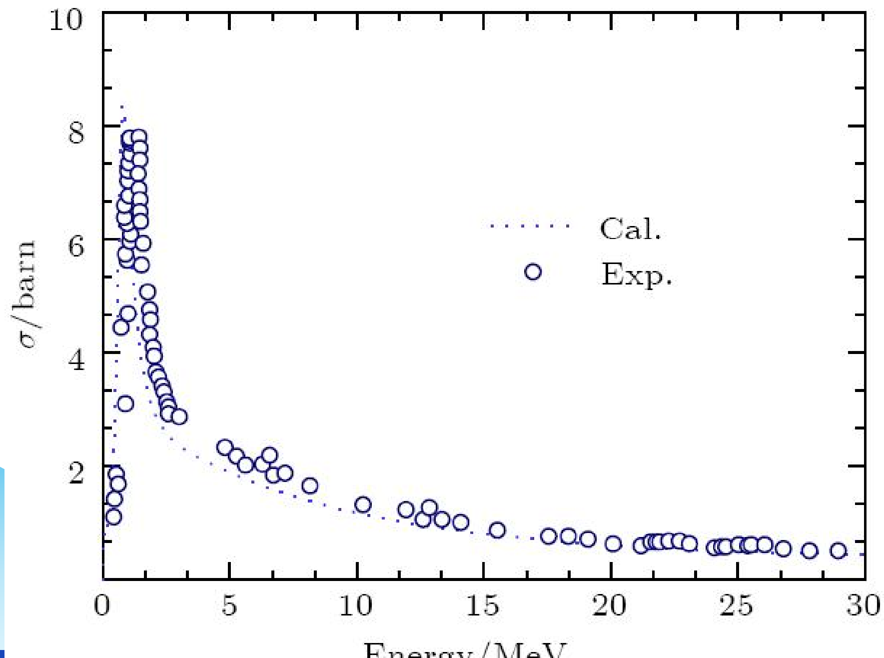

- CMR is used to study the elastic scattering of n-\alpha system, the continuum level density, phase shift, and cross section are obtained.
- The calculated results and experimental data are in good consistence.

Density distributions in ^{124}Zr

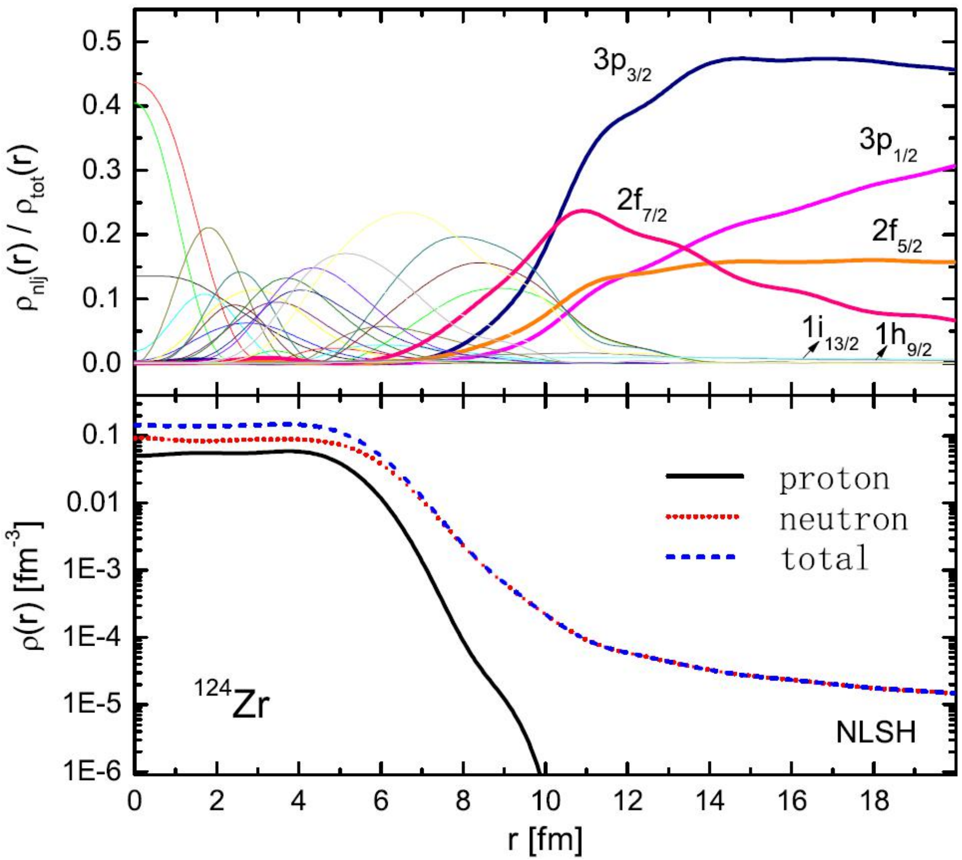

- **Density distributions in ^{124}Zr with a long tail.**
- The top panel displays the ratio of the neutron density of the single-particle levels to the total neutron density.
- The bottom panel displays the proton, neutron, and total matter densities marked by the black solid, red dot, and blue dashed lines, respectively

PHYSICAL REVIEW C **98**, 014316 (2018)

Resonant-continuum relativistic mean-field plus BCS in complex momentum representation

Ke-Meng Ding,[1] Min Shi,[2] Jian-You Guo,[1,*] Zhong-Ming Niu,[1,†] and Haozhao Liang[3,4]
[1] *School of Physics and Materials Science, Anhui University, Hefei 230601, China*
[2] *School of Mathematics and Physics, Anhui Jianzhu University, Hefei 230601, China*
[3] *RIKEN Nishina Center, Wako 351-0198, Japan*
[4] *Department of Physics, Graduate School of Science, The University of Tokyo, Tokyo 113-0033, Japan*

Pseudospin symmetry in resonant states

Pseudospin doublets

$$\begin{cases} n-1, l+2, j = l+3/2 \\ n, l, j = l+1/2 \end{cases}$$

Re-define the quantum numbers of states

$$\tilde{n} = n-1, \tilde{l} = l+1, j = \tilde{l} \pm 1/2$$

Here

$$\text{pseudo-orbit} \;:\; \tilde{l} = l+1$$
$$\text{pseudo-spin} \;:\; \tilde{s} = 1/2$$

Pseudospin doublets:

$$\left(\tilde{n}, \tilde{l}, j = \tilde{l} \pm 1/2\right)$$

Similar to the spin doublets

$$(n, l, j = l \pm 1/2)$$

Arima etal., PLB30, 517(1969);
Hecht etal., NPA137, 129 (1969)

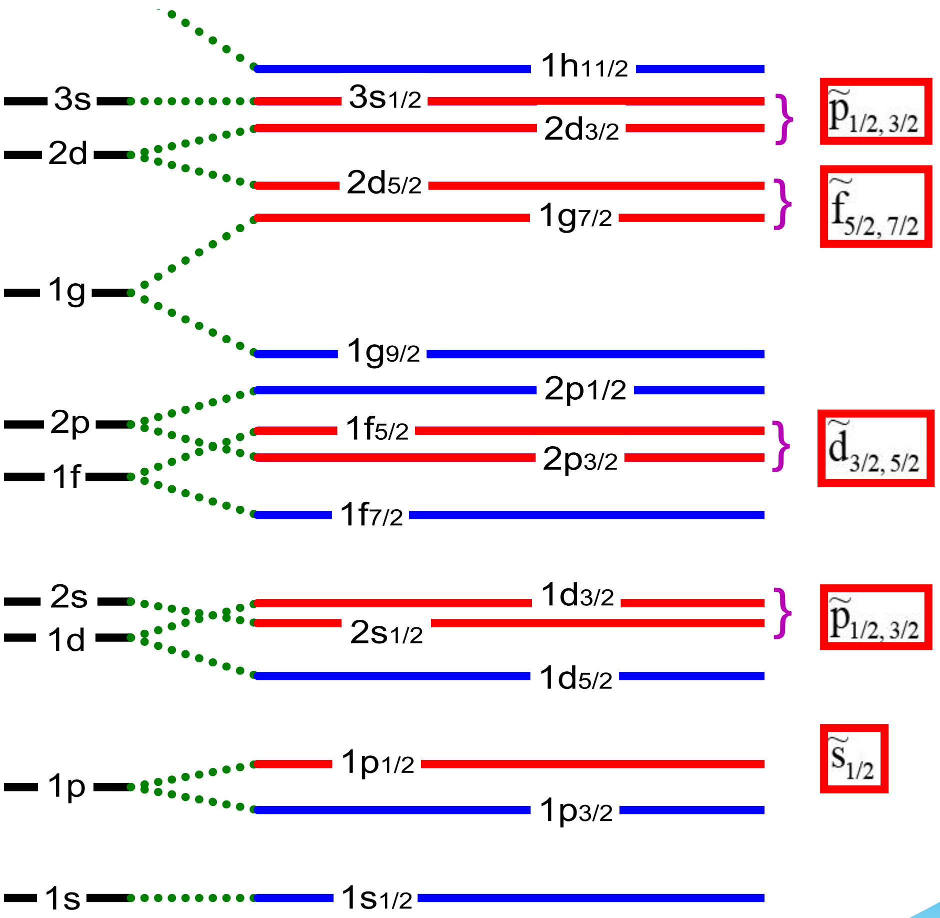

The splitting of both spin and pseudospin doublets play critical roles in the shell structure evolutions. It is a fundamental task to explore the origin of SS and PSS, as well as the mechanism of their breaking.

PHYSICAL REVIEW C **85**, 021302(R) (2012)

Exploration of relativistic symmetry by the similarity renormalization group

Jian-You Guo*
School of Physics and Material Science, Anhui University, Hefei 230039, People's Republic of China
(Received 30 August 2011; revised manuscript received 24 January 2012; published 14 February 2012)

PRL **112,** 062502 (2014) PHYSICAL REVIEW LETTERS week ending 14 FEBRUARY 2014

Probing the Symmetries of the Dirac Hamiltonian with Axially Deformed Scalar and Vector Potentials by Similarity Renormalization Group

Jian-You Guo,* Shou-Wan Chen, Zhong-Ming Niu, Dong-Peng Li, and Quan Liu
School of Physics and Material Science, Anhui University, Hefei 230601, People's Republic of China
(Received 31 August 2013; revised manuscript received 24 November 2013; published 11 February 2014)

Symmetry is an important and basic topic in physics. The similarity renormalization group theory provides a novel view to study the symmetries hidden in the Dirac Hamiltonian, especially for the deformed system. Based on the similarity renormalization group theory, the contributions from the nonrelativistic term, the spin-orbit term, the dynamical term, the relativistic modification of kinetic energy, and the Darwin term are self-consistently extracted from a general Dirac Hamiltonian and, hence, we get an accurate description for their dependence on the deformation. Taking an axially deformed nucleus as an example, we find that the self-consistent description of the nonrelativistic term, spin-orbit term, and dynamical term is crucial for understanding the relativistic symmetries and their breaking in a deformed nuclear system.

DOI: 10.1103/PhysRevLett.112.062502 PACS numbers: 21.10.Pc, 05.10.Cc, 21.10.Hw, 24.80.+y

Symmetry in resonant states in the RMF-CMR calculations

Physics Letters B 801 (2020) 135174

Contents lists available at ScienceDirect

Physics Letters B

www.elsevier.com/locate/physletb

Pseudospin and spin symmetries in single particle resonant states in Pb isotopes

Xin-Xing Shi (史新星)[a], Quan Liu (刘泉)[b,*], Jian-You Guo (郭建友)[b,*], Zhong-Zhou Ren (任中洲)[a,c]

[a] School of Physics, Nanjing University, Nanjing 210093, PR China
[b] School of Physics and Materials Science, Anhui University, Hefei 230601, PR China
[c] School of Physics Science and Engineering, Tongji University, Shanghai 200092, PR China

Ting-Ting Sun,etal., PRC 99, 034310 (2019)

Pseudospin symmetry in wavefunctions-bound

The upper components of Dirac spinors for the bound pseudospin doublet in 210Pb

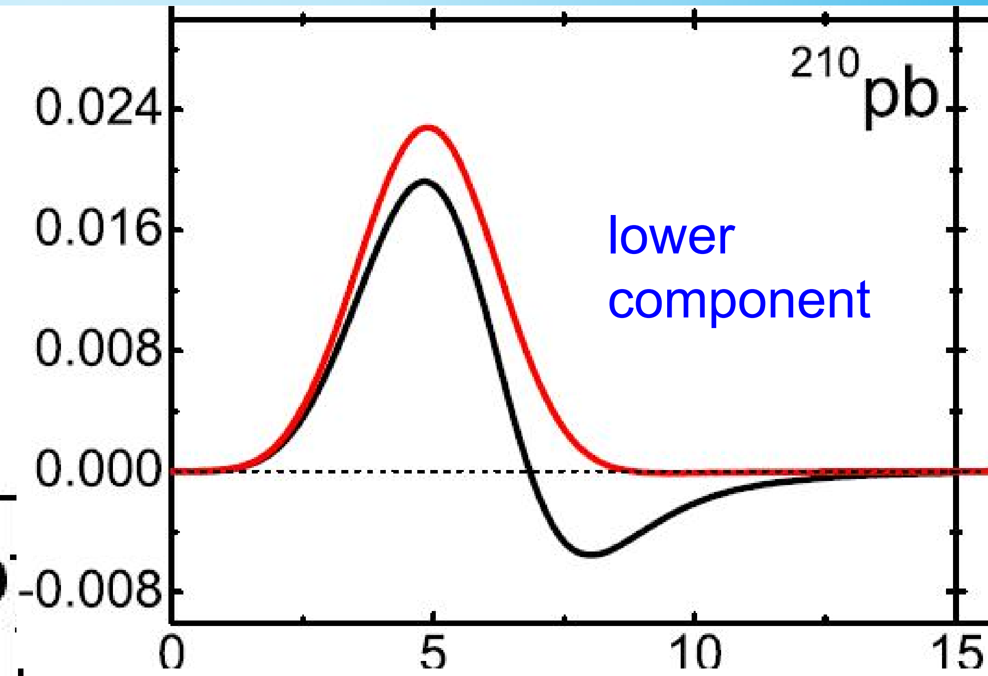

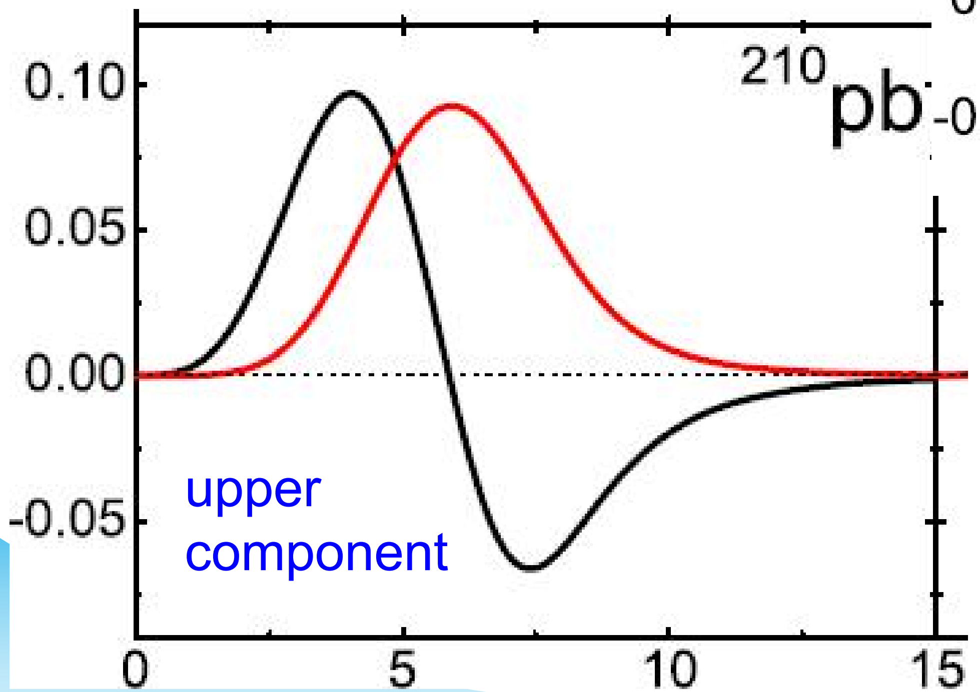

The lower components of Dirac spinors for the bound pseudospin doublet in 210Pb

Pseudospin symmetry in wavefunctions-resonant

The upper components of Dirac spinors for the resonant pseudospin doublet in 210Pb

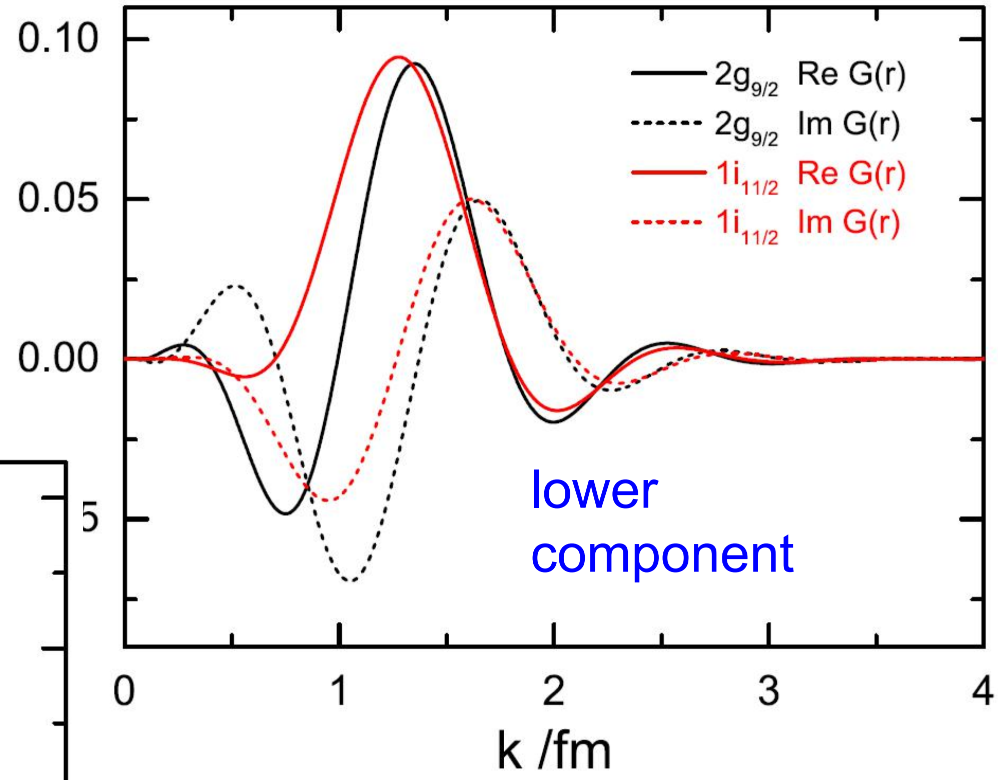

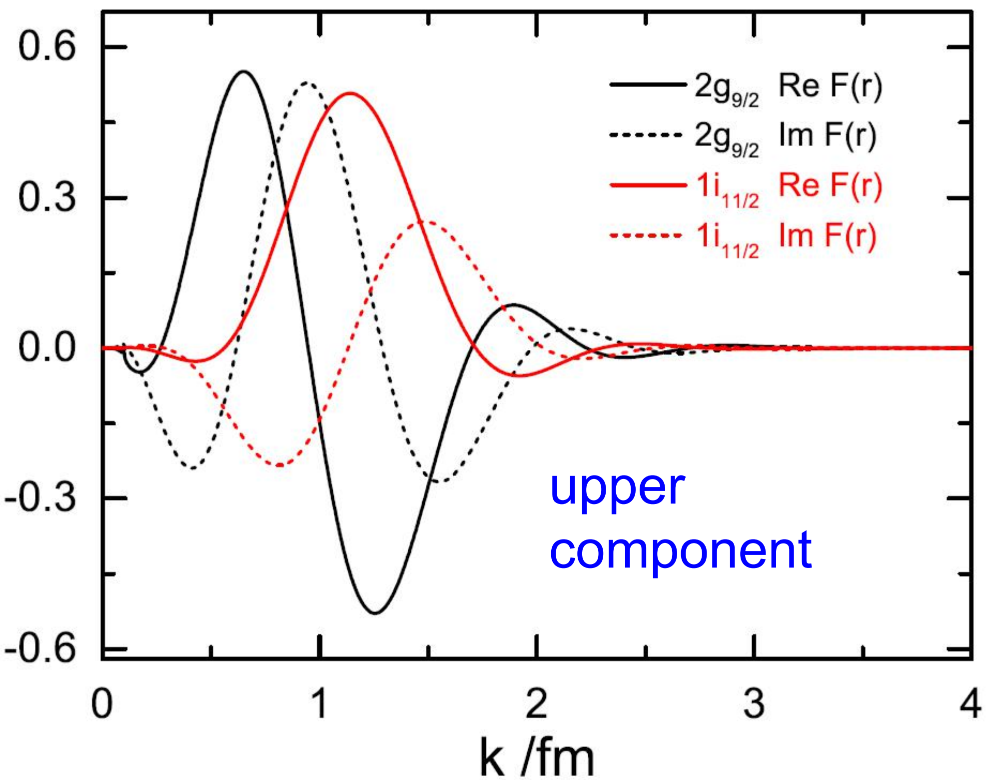

The lower components of Dirac spinors for the resonant pseudospin doublet in 210Pb

Summary

- Significance of resonant states is explained.
- Relativistic CSM,CGF, and CMR are introduced.
- Exploration of resonant states in nuclei is presented.

Perspective

- Development and perfection of theoretical formalism
- Prediction and explanation of novel phenomena in nuclei
- New observables related to resonant states

Thank you!